ENHANCED ISCHEMIA CLASSIFIER FOR ECG SIGNALS

A Thesis

Submitted by

Amit Kumar

(Registration No: 950904005)

for the degree of

Doctor of Philosophy

Under the Supervision of

Dr. Mandeep Singh

Associate Professor
Department of Electrical & Instrumentation Engineering
Thapar University, Patiala, INDIA -147004

Department of Electrical & Instrumentation Engineering
Thapar University, Patiala – 147 004

April 2015

DECLARATION

I hereby declare that the research work is being presented in this thesis entitled "**Enhanced Ischemia Classifier For ECG Signals**" submitted for the award of the degree of Doctor of Philosophy in the Department of Electrical and Instrumentation Engineering, Thapar University, Patiala is an authenticated record of my own research work carried out under the supervision of **Dr. Mandeep Singh**, Associate Professor, Department of Electrical and Instrumentation Engineering and refers other researcher's work are duly listed in the reference section.

The matter presented in this thesis has not previously been submitted in part or full to any other university or institution for the award of any degree in India or abroad.

Date: 23-10-2015

Amit Kumar
(950904005)

I certify that the above statement made by the student is correct to the best of my knowledge and belief.

Date: 23-10-2015

Dr. Mandeep Singh
Associate Professor
Department of Electrical &
Instrumentation Engineering,
Thapar University, Patiala, INDIA

CERTIFICATE

This is certified that the thesis entitled **"Enhanced Ischemia Classifier For ECG Signals"**, submitted by **Mr. Amit kumar**, in fulfillment of the requirement for the award of degree of **Doctor of Philosophy** in the Department of Electrical and Instrumentation Engineering, Thapar University, Patiala, is a record of candidate's own original and independent research work carried out by him under my supervision and guidance. The matter embodied in this thesis has not been submitted in part or full to any other university or institute for the award of any degree.

Date: 23-10-2015

Dr. Mandeep Singh
Associate Professor
Department of Electrical &
Instrumentation Engineering,
Thapar University, Patiala, INDIA

ACKNOWLEDGEMENT

I self-effacingly prostrate myself before the Almighty for HIS grace and plentiful blessings which enabled me to complete this research work successfully.

I am very thankful to **Dr. Prakash Gopalan**, Director, Thapar University, Patiala and **Dr. O. P. Pandey**, Dean of Research & Sponsored Projects, Thapar University, Patiala for providing facilities to complete this research work. I express my deep sense of gratitude towards, **Dr. Ravinder Agarwal**, Head, Department of Electrical and Instrumentation Engineering, Thapar University, Patiala.

I would like to express my thanks and indebtedness to my esteemed and worthy supervisor **Dr. Mandeep Singh**, Associate Professor, Department of Electrical and Instrumentation Engineering, Thapar University, Patiala for his effective supervision, deep involvement and continuous motivation throughout this research work. Most of the novel ideas and solutions found in this thesis are the result of our numerous discussions. His editorial comments were also invaluable for writing this thesis.

I would like to thank my doctoral committee: **Dr. Sanjay Kumar Jain,** Associate Professor, Department of Electrical and Instrumentation Engineering, **Dr. Kulbir Singh,** Associate Professor, Department of Electronics and Communication Engineering and **Dr. Sunil Kumar Singla,** Assistant Professor, Department of Electrical and Instrumentation Engineering, for their encouragement, constructive criticism and inspirations.

I am highly grateful to the management, administration, faculty and staff members of the **GIMT**, Kurukshetra, Haryana for providing support and facility to carry out this research work.

I am extremely grateful to my father, **Mr. Iqbal Manocha**, my mother, **Mrs. Sudesh Rani** and all other family members for their infinite love, affection and blessings. This journey would have been not so easy without the wonderful support of my wife **Mrs. Shilpa.** A special thanks to my daughters **Pariyagna and Mishika**, whose smiling faces always made me refreshing.

23/10/15

(**Amit Kumar**)

LIST OF PUBLICATIONS FROM PRESENT WORK

Papers in SCI Journals

- Amit Kumar, Mandeep Singh, "Optimal Selection of Wavelet Function and Decomposition Level for Removal of ECG Signal Artifacts", Journal of Medical Imaging and Health Informatics, vol. 5, No.1, pp 138-146, February 2015. IF: 0.623.
- Amit Kumar, Mandeep Singh, "Robust Multi-resolution Wavelet Analysis and Window Search Based Approach for Electrocardiogram Features Delineation", Journal of Medical Imaging and Health Informatics, Accepted Manuscript for Publication in Feb. 2016 issue. IF: 0.623.

Papers in Non-SCI Journals

- Amit Kumar, Mandeep Singh, An Overview of Ischemia Detection Techniques, International Journal of Science Engineering & Research, vol. 2, issue 11, November 2011, pp. 1-5.
- Amit Kumar, Mandeep Singh, Principles for QRS Detection: A Review, International Journal of Applied Engineering and Research, India, vol. 6, No. 5, 2011, pp. 763-769.

Papers in Conferences

- Amit Kumar Manocha, Mandeep Singh, "Automatic Delineation of ECG Characteristics Points using Window Search and Multi Resolution Wavelet Transform Approach" Proceeding of 4th International Conference on Emerging Trends in Engineering & Technology (IETET-2013), GIMT, Kurukshetra, Published in AEST-03, ACEEE, IDES, USA, pp755-761, October, 2013.
- Amit Kumar Manocha, Mandeep Singh, "An Improved Method for ECG Denoising Using Wavelet Transform", Proceedings of 2nd International Conference on Biomedical Engineering & Assistive Technologies, NIT Jalandhar, India, pp 247-251, 6-7 December, 2012.
- Amit Kumar Manocha, Mandeep Singh, "Application of Digital Signal Processing to ECG signal", National Conference, Trends in Instrumentation and Control Engineering, Thapar University, 29-30 October 2009, pp 23-32.

ABSTRACT

Myocardial ischemia (MI) is the most common type of coronary heart disease (CAD) and cause of the heart attacks. The ischemia is the result of the accumulation of cholesterol and plaque building narrows the lumen of the arteries of the heart, hence heart becomes starved of oxygen and the vital nutrients, it needs to pump properly. It usually leads to angina (chest pain), myocardial ischemia or sometimes Infraction. The non-invasive method, Electrocardiogram (ECG), is a universally adopted method for diagnosis of ischemia. The ECG is a procedure of recording of the electrical activity of the myocardial fibers of the heart over a period of time. The ECG has a characteristic morphology comprises of P wave, QRS complex and T wave. The ST segment deviations are produced by the flow of injury currents, generated by the voltage gradients between the ischemic and non-ischemic myocardium during the plateau and resting phases of the ventricular action potentials. This is manifested as elevated or depressed ST segments in the ECG. Elevated ST segments appear typically in transmural ischemia, while depressed ST segment appears subendocardial ischemia. During recording of ECG, artifacts are incorporated on the ECG. Commonly noticed artifacts include baseline wandering, power line interference and muscle tremors. Artifacts are extremely common, and knowledge of them and elimination is primarily required to prevent mis-diagnosis of ischemia. There are various ischemia detection methods available in the literature exhibiting certain disadvantages, like classifier trainings and the involvement of the complex calculations for decision. Hence, a simple, reliable and rugged method is required to address these disadvantages. Recent developments in signal processing methods, multi-resolution analysis, wavelet transform is found more suitable for ECG analysis, preprocessing and delineation technique. Using wavelet transform toolbox in MATLAB programming, we preprocessed the ECG records and then delineates the ECG characteristic points. The proposed method shows better performance than the existing methods. Simulated results show that the optimal value of the wavelet function for eliminating of artificially added artifacts as, db7 at 8^{th} decomposition level for baseline wander with percentage root mean square difference (PRD) of 0.1636%, coif2 at a 5th decomposition level for power line interference with PRD of 0.3980% and db7 at 8^{th} decomposition level for muscle tremor with PRD of 0.8959% in selected records of

European ST-T database. Moreover, it also addresses the issues of conventional methods. Similarly, for delineation process, the proposed method result shows 99.72% sensitivity (S_E), 99.78% positive predictivity (+P) for 10 records. Then detected ST segment has been classified as normal or ischemic based on proposed isoelectric energy function (IEEF), an alternate method to detect the elevation or depression of ST segment with respect to isoelectric reference. The proposed method is a mathematical function that detects these deviations in a rugged manner. The motivation behind developing this function is to go in for a simpler but reliable threshold based classification for detecting myocardial ischemia. The isoelectric energy threshold is used to classify ischemic beats from normal beats. The method is validated for 43,876 ST segments for one lead of annotated European ST-T database (EDB) records. The results show 98.12% average sensitivity, 98.16% average specificity, 98.36% average positive predictivity and 100% sensitivity for ischemic episodes detection process has been achieved for these records. These results are significantly better than those of existing methods cited in the literature. In addition, we have also proposed a simple classifier to classify the detected ischemia episode as transmural or subendocardial ischemia. Filtering and delineation has been performed in such a well-organized manner, which makes possible to attain significantly better results than the existing methods. The proposed method has following advantages. The method could provide an interpretation of the results. This is of great importance for a medical decision support for the patient in the critical care unit (CCU) without knowing past references. The developed method filters out the spurious beats in a record. Another advantage includes direct analysis based on isoelectric energy without involvement of any complicated algorithm.

TABLE OF CONTENTS

LIST OF FIGURES

LIST OF TABLES

LIST OF ABBREVIATIONS AND SYMBOLS

CVD	Cardiovascular DISEASE
CAD	Coronary artery disease
MI	Myocardial ischemia
VF	Ventricular fibrillation
VT	Ventricular tachycardia
PVC	Premature ventricular contractions
SVT	Supraventricular tachycardia
AF	Atrial fibrillation
AFL	Atrial flutter
WPW	Wolff parkinson white syndrome
SPC	Supra-ventricular premature contractions
EPS	Electrophysiology study
SCD	Sudden cardiac deaths
AV	Atrioventricular node
SA	Sinoatrial node
AP	Cardiac action potential
NSTEMI	Non-ST segment elevation myocardial infarction
STEMI	ST segment elevation myocardial infarction
ICU	Intensive care unit
CCU	Critical care unit
PCA	Principal component analysis
ANN	Artificial neural network
NLPCA	Nonlinear principal component analysis
ESC ST-T database	European ST-T database
SOM	Self organizing map
NN	Neural networks
SVM	Support vector machines

PDA	Personal digital assistants
LT-ST database	Long term ST-T database
IF	Imaging functions
ANFIS	Adaptive nueuro-fuzzy interface system
CCO	Critical care options
HMM	Hidden markov model
DWT	Discrete wavelet transform
KDE	Kernel density estimation
KNN	K-nearest neighbor
GMM	Gaussian mixture model
HFD	Higuchi fractal dimension
PTCA	Percutaneous coronary intervention
LAD	Left anterior descending artery
RCA	Right coronary artery
LCX	Left circumflex artery
EDB	European ST-T databases
IEEF	Isoelectric energy function
MRA	Multi-resolution analysis
CWT	Continuous wavelet transforms
DWT	Discrete wavelet transforms
FT	Fourier transform
STFT	Short time fourier transform
WT	Wavelet transform
IDWT	Inverse discrete wavelet transforms
GUI	Graphic user interface
BW	Baseline wandering
PLI	Power line interference
LDA	Linear discriminant analysis
ICA	Independent component analysis
PSD	Power spectral density

HOS	Higher order spectra
EMD	Empirical mode decomposition
IIR	Infinite impulse response filters
FIR	Finite impulse response filters
SVD	Singular value decomposition
CD	Detail coefficients
(CA)	Approximate coefficients
PRD	Percentage root mean square difference
RMSE	Root mean square error
SNR	Signal to noise ratio
S_E	Sensitivity
+P	Positive predictivity
S_P	Specificity
AICF	Adaptive impulse correlated filter
TSAF	Time sequence adaptive filters
SIF	Single input adaptive filter
CR	Compression ratio
DB	Daubechies
COIF	Coiflet
SYM	Symlet
IR	Isoelectric reference
SD	Standard deviation
CV	Coefficient of variation
ROI	Region of interest
IEE	Isoelectric energy
MCDA	Multi-criteria decision analysis
GA	Genetic algorithm
α	Artificial added constant to prevent IEEF acquiring infinite value
β	Threshold for classification of the beat

CHAPTER-1

INTRODUCTION AND LITERATURE SURVEY

1. Cardiovascular Diseases

Cardiovascular disease (CVD) is a class of disorders of the heart blood vessels. According to the definition of the World Health organization (WHO), CVD includes coronary artery disease (CAD), peripherihal arterial disease, congenital heart disease, cerebrovascular disease, rheumatic heart disease, deep vein thrombosis and pulmonary embolism [V.L. Roger et.al, 2012]. CVD is projected leading cause of deaths globally. Likely, 17.3 million people died, because of CVD in 2013, representing 31.5% of total global deaths. Expected deaths due to CVD will increase to 23.3 Million by 2030 [GDB, 2013]. Coronary artery disease and cerebral artery diseases are a major cause of deaths in industrialized countries, representing one third of global mortality. With the increasing sedentary lifestyle, more people are becoming prone to CVD [D. Singh et.al, 2012]. Important modulators of CVD are so called "modifiable risk factors, such as unhealthful diet, lack of exercise, consumption of snuff, alcohol, diabetes, raised lipids and stress. 'Non modifiable risk factors' comprise age and heredity. Improvement of CVD management is a primary task that requires advances in its diagnosis, treatment and prevention.

1.1 Coronary Artery Disease

Coronary artery disease (CAD) commonly acknowledged as 'atherosclerotic heart disease', is the most contributed type of heart disease and grounds of heart attacks. This disease is the result of plaque building and accumulation of cholesterol in the inner walls of the arteries of the heart (Figure 1.1). As it progresses, a smaller amount blood flows through the arteries; the heart muscle cannot receive sufficient blood and oxygen, which usually lead to chest pain (angina), myocardial ischemia (MI) or sometimes Infraction [P.K. Dash, 2002; J. Brownfield and M. Herbert, 2008]. Over the time, CAD usually deteriorates the heart muscles and contributes to the heart failure and arrhythmias [M. Gheorghiade et.al, 2006; E. Carmeliet, 1999; N. Luqman et.al, 2007; G.S. Wagner et.al,

2009]. Heart failure occurs, when the heart is not capable to efficiently pump blood to the body, whereas arrhythmia occurs when changes in the normal rhythm of the heart.

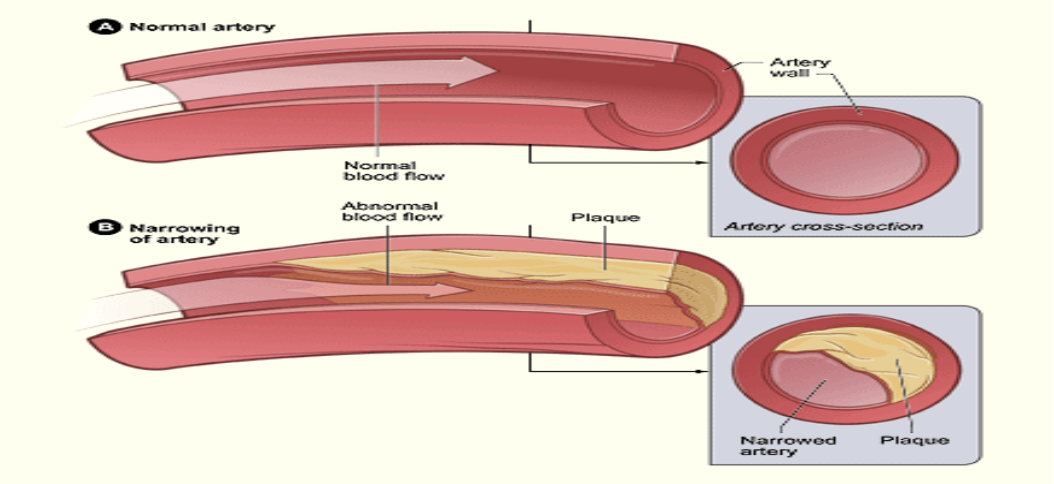

Figure 1.1 a) normal artery b) narrowing artery
[reproduced from http://www.nhlbi.nih.gov/health/health-topics/topics/atherosclerosis]

1.2 Cardiac Arrhythmia

An arrhythmia is a group of situations, in which the electrical activity of the heart becomes irregular. When the heartbeat is too faster than 100 beats per minute (bpm), is known as tachycardia, whereas, when the heartbeat is too slow, less than 60 beats per minute, is known as bradycardia. While, many arrhythmias are not life intimidating, but some arrhythmia may be a basis for the cardiac arrest. Arrhythmias have been divided into two different categories; supra-ventricular and ventricular. Supra-ventricular arrhythmias happen in the two upper chambers of the heart; while ventricular arrhythmias happen in the two lower chambers [D. R. Perez, 2013].

Ventricular Arrhythmias include ventricular fibrillation (VF), Ventricular tachycardia (VT) and premature ventricular contractions (PVCs)

Supra-ventricular Arrhythmias include supraventricular tachycardia (SVT), atrial fibrillation (AF), atrial flutter (AFL), Wolff Parkinson White syndrome (WPW) and supra-ventricular premature contractions (SPCs)

There are several factors that cause irregularities of the heartbeat. Certain types of heart disease, hemochromatosis and high blood pressure may also contribute to the generation of arrhythmias [M.T. Keating and M.C. Sanguinetti, 2001; E. Pueyo et.al, 2009]. In

addition, stress, snuff, caffeine, alcohol and some medical prescriptions for cough and catarrh may also affect. Arrhythmias can be diagnosed using various techniques, mainly ECG, Holter monitoring and Electrophysiology study (EPS). The most commonly used test to diagnose an arrhythmia is the non invasive method, i.e. standard electrocardiogram (ECG), which allows assessing the electrical potentials produced by the heart [M. Singh, 2010]. Often, the first step to treat the arrhythmia is the administration of anti arrhythmic drugs such as digitalis, beta blockers and calcium channel blockers. Other treatments include implantable devices, trans-catheter interventions and surgery in emergency cases. Further, sudden cardiac deaths (SCDs) are natural deaths. This typically covers cardiac causes, heralded by an unexpected loss of heart function within an hour, etc. It is mainly triggered by arrhythmias. It is estimated that 12.5% of deaths that occur naturally are sudden deaths and of these, 88% are of cardiac origin. In all cases of SCDs, 80% occur in patients with ischemic heart disease [R. Myerburg and A. Castellanos, 2001]. Both artery occlusion and reperfusion can cause arrhythmias leading to sudden death.

1.3 Myocardial Ischemia

Myocardial ischemia (MI) is the most contributed type of cardiac disease to the CAD. This is mainly caused by an inadequate blood and nutrient supply to the heart's cells and usually may lead to myocardial infarction. The development of plaque within the coronary artery (blocks 70% or more lumen of the vessel), cause symptoms of ischemia, such as decreased exercise tolerance and angina [C. R. Conti et.al; 2012, G Gupta, 2010]. This may be the first instance, where the subject starts the experience of suboptimal operation of the heart. Ischemia can turn into a chronic condition that can gradually deteriorate the heart. If the affected tissues recover the blood flow, Ischemia becomes reversible, or it may be irreversible resulting in death of tissues. Ischemia in myocardial muscle is a matter of clinical importance and is the subject of many dielectric investigations [F. S. Barnes, B. Greenebaum, 2006]. Ischemia contributes to heart attacks and strokes. It may also affect the intestines, resulting in abdominal pain, bloody stool and even intestinal rupture. Peripheral ischemia can be the reason for the loss of fingers, toes, etc. Further, Ischemia can occur with or without chest pain (angina) and other symptoms. Silent ischemia usually occurs with no symptoms, is caused by emotional,

mental stress, by exertion. Symptomatic ischemia is characterized by chest pain, known as angina pectoris. Angina pectoris is a process of severe chest pain due to myocardial ischemia [J. Garcia et.al, 2000]. It is very significant to recognize that, who experience angina may often describes the sensation as discomfort, heaviness and squeezing. The pain of angina tends to start under the breastbone; may also travel to the shoulder, arm, neck, jaw. [P. H. Stone, 2013; M. D. Thames, 2004]. The angina is of two types as follows:

Stable Angina appears when the heart is working harder and it needs more oxygen than the delivered through the narrowed arteries. Stable angina can be quickly relieved by resting or taking nitroglycerin.

Unstable Angina happens when blood flow to the heart is suddenly stopped due to blood clots made up in the coronary arteries. Unstable angina is a warning sign of heart attack. It may occur with light activity or even at rest. It does not go away by resting or by taking nitroglycerin.

1.3.1 Causes of Ischemia

There are a number of causes or risk factor [A. J. Grau et.al, 1994 and T. Huebner et.al, 2010] involved in the development of ischemia as follows:

- Compression of blood vessels
- Ventricular tachycardia
- Atherosclerosis
- Blood clots
- Tremendously low blood pressure
- Congenital heart defects
- Sickle cell anemia

1.3.2 Ischemia Symptoms

In most of the cases, chest pain (angina) is a common symptom for ischemia occurrence. However, ischemia may occur without any symptoms. Symptoms of cardiac ischemia [P.H. Stone, 2013] include:

- Chest pain, usually spread out to the shoulder, neck, back, arm and jaw

- Profuse sweat
- Less physical abilities
- Palpitations or irregular heart rhythms
- Shortness of breath
- Nausea with or without vomiting

1.4 Electrocardiogram (ECG)

The ECG is a process of interpretation of the electrical activity of the heart over a period of time. ECG presents the depolarization (activation) and reploarisation (relaxation) of the cardiac muscle [M. Singh, 2012]. These variations are normally acquired by leads and electrodes attached to the surface on specified position of the human body. The ECG recording provides a wealth of information about the heart function, allowing diagnosing a greater variety of cardiac alterations, which are further used for diagnosis of arrhythmias, ischemia, angina pectoris and changes in the size of the heart etc. [A. Gacek and W. Pedrycz, 2012]. The ECG is also used for diagnosis such as changes in the potassium and calcium ions, certain lung and thyroid problems in the human body.

1.4.1 Electrical System of the Heart

The heart has been divided into four chambers, the two lower chambers (ventricles) and the two upper chambers (atria). The ventricles are bigger than the atria and present a thicker wall because their pumping action is also higher. The wall of the left ventricle is thicker than the right ventricle, as it pumps blood to the whole body, whereas the right ventricle sends blood just to the pulmonary circuit. To make the cyclic contraction of the heart synchronous and ordered, there is an electrical conduction system consisting of specialized cardiac muscle fibers that allows the transmission of the electrical impulses and the stimulation of the atria and ventricular myocardium. Although the heart is innervated by the sympathetic nervous system, it beats even without this stimulus, as the conduction system is auto excitable. The conduction system consists of the atrioventricular (AV) node, the sinoatrial (SA) node, the bundle of Hiss to its right and left branches and the Purkinje fibers (Figure 1.2). The SA node performs the function of the natural pacemaker to the heart, having the property of automaticity, i.e., it

spontaneously generates electrical impulse that then spread to excite other cells of the myocardium [P. E. Mcsharry et.al, 2003]. The electrical stimulus passes to the atria coming from the SA node, activating the right atrium and then the left one. Once the impulse reaches the AV node, it is delayed to give time for the blood to pass from the atria to the ventricles before the valves that separate them get close. Subsequently, the AV node transmits the electrical stimulus across the right and left branches of the bundle of His until the stimulus reaches the ventricles and causes their contraction [E. J. Berbari, 2000]. In order to achieve a coordinated contraction of the ventricles, the electrical impulse must be transmitted quickly, which occurs through a number of conductive branches ending in the Purkinje network (Figure 1.2).

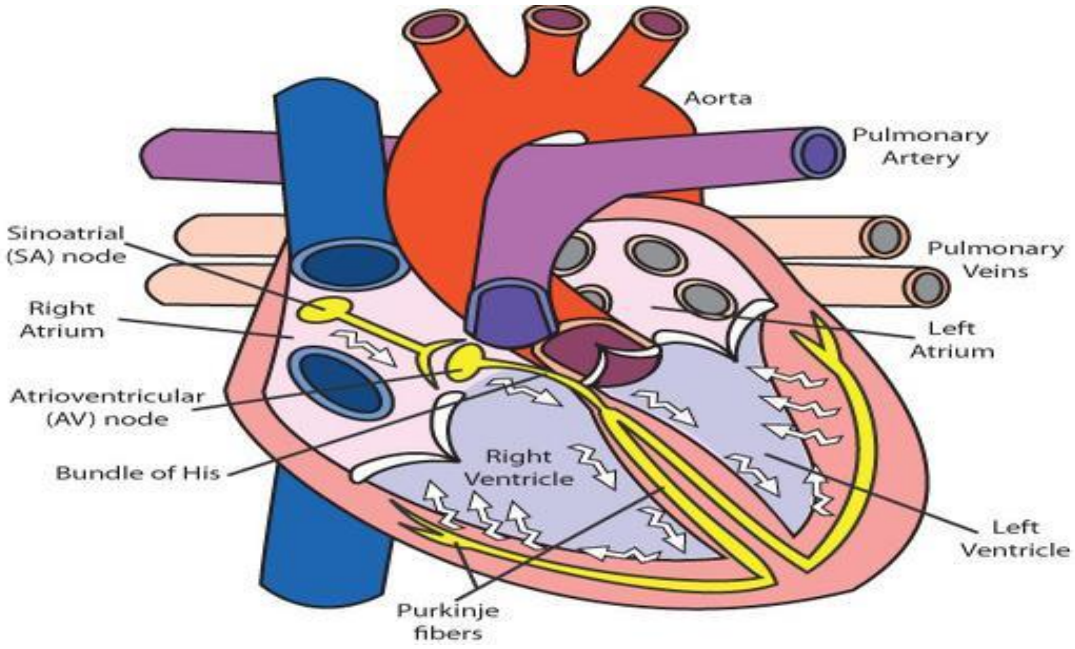

Figure 1.2: Electrical system of the heart
[reproduced from http://cdeastcprfirstaid.wikispaces.com]

1.4.2 Cardiac Action Potential

The cardiac action potential (AP) is a consistent trajectory of rising and falling corresponds to the potential difference of the interior and exterior cardiac cells [K.H.W.J. T. Tusscher and A.V. Panfilov, 2006; R. S. Khandpur, 1992]. The heart performs this function through a unique excitatory and contractile system. For instance, the unique excitatory system has positive increases in voltage across the cell's membrane potential, a

special property of depolarization without any external influence. This occurs between the end of one action potential and the beginning of the next one. The increase in membrane potential naturally permits the membrane potential to reach the threshold potential. At threshold, it fires the next action potential, known as pacemaker potential. Thus, the pacemaker potential drives the self generated rhythmic firing, is known as muscle auto-maticity. Further, the differentiation of the action potentials allows the different electrical characteristics of the various portions of the heart. The morphology of the AP varies from one cell to another, depending on their location. A general characteristic of the AP in the cardiac cells is its long duration, ranging between 150 and 300ms. This long duration has important functional consequences, as it allows the overlapping in time of the action potential (electrical phenomenon) with the contraction of the fiber (mechanical phenomenon). In all other cardiac fibers (ventricular and atrial) the AP presents the following phases, as shown in Figure 1.3.

- Phase 0 is the speedy depolarization phase with an initial fast upstroke due to the opening of the inward fast Na+ ions into the cell. The slope of this phase presents the maximum rate of potential change, known as dV/dt_{max}. This slope is proportional to the net ionic current in the heart muscle cells
- Phase 1 is the brief repolarisation phase. It occurs concurrently as the inactivation of the fast Na+ channels occurred. The transient net outward current due to the movement of K+ and Cl^- ions, causing the small downward deflection
- Phase 2 is also known as ‘plateau’ phase. In this phase, the duration of the action potentials of cardiac cells is prolonged. This phase is sustained because of balance between outward movement of K^+ through and inward movement of Ca^{2+} through L type calcium channels
- Phase 3 is fast repolarisation phase, mainly due to the massive outflow of K+ ions outside the cell and decrease in the inflow of Ca2+ ions, thus returning the cell to its resting state.
- Phase 4 is resting membrane potential. This is caused by the difference between conductance and ionic concentrations across the membrane of the cell. The normal resting membrane potential is about -85 to -95 mV in the ventricular myocardium

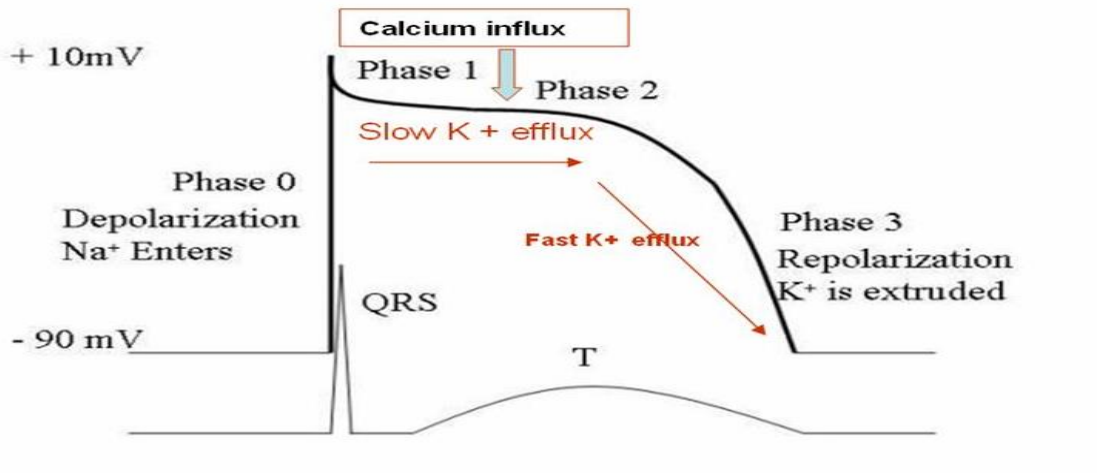

Figure 1.3: Standard model of a cardio-myocyte action potential
[reproduced from https://drsvenkatesan.wordpress.com]

1.4.3 Action Potential Propagation and Electrocardiogram Generation

The propagation of the electrical stimulus trough the myocardium results in the generation of action potentials (APs) at different intervals in time and space, which originate a variable electrical field on the body surface. The sum of those AP gradients along the entire cardiac cycle measured on the body surface is reflected in the ECG. Figure 1.4 shows the shape of different APs corresponding to different types of cardiac cells. Likewise, the final ECG signal obtained by the sum of all these APs at a particular placement of the body [W.F. Ganong et.al, 2005] is shown in the Figure 1.4.

1.4.4 Standard 12-Lead ECG System

A lead is a pair of electrodes positioned on the human body in designated anatomical locations to record of the electrical activity of the heart. Each lead has a negative (-) and positive (+) electrode. The standard 12-leads ECG system has three bipolar leads, three augmented unipolar leads and six chests (precordial) leads as shown in Figure 1.5 and mentioned in Table 1.1. Using 'lead selector' on the ECG machine, one is able to change the polarity of electrodes. This helps to get the various lead selections without actually moving the lead cables or electrodes [E. Frank, 1956; L. Cromwell, 2000]. The 12 lead systems are described as follows:

Bipolar leads records the potential difference between positive and negative poles.

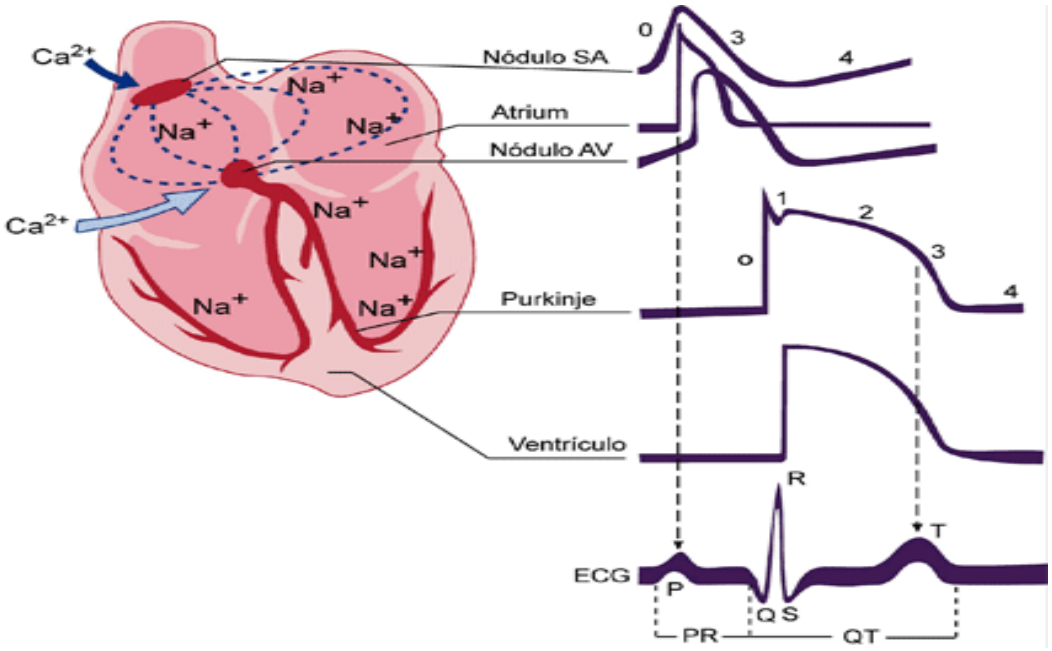

Figure 1.4: ECG Generations
[reproduced from W.F. Ganong et.al, 2005]

Unipolar leads records the electrical potential by means of a single exploring electrode.

Unipolar limb leads records potentials between aVR (right arm), aVL (left arm) and aVF (left leg)

Einthoven leads:

Lead III records potentials between the left arm and left leg

Lead II records potentials between the right arm and left leg

Lead I records potentials between the left and right arm

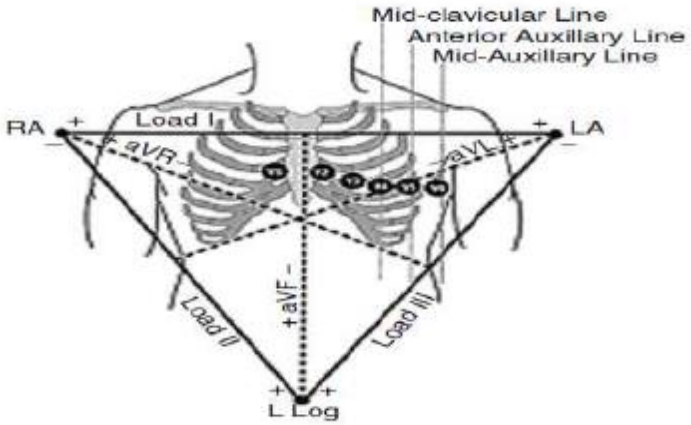

Figure 1.5: 12 lead ECG system
[reproduced from http://rtboardreview.com/public/equipment_room/ecg.htm]

Chest leads have

V6: in the midaxillary line

V5: on 5th rib, anterior axillary line

V4: 5th intercostal space in the midclavicular line

V3: between the 2nd and 4th electrodes

V2: 4th intercostal space, left Sternal edge

V1: 4th intercostal space, right Sternal edge

To diagnose of the heart rhythm it is adequate to use only a few electrodes, ten electrodes are characteristically is used for acquisition, when different waveform morphology information is required. In this case six leads are placed on the chest, and four on the extremities.

1.5 ECG Features

ECG wave can be analyzed for number of features. Each feature, individually or collectively is very useful for diagnosing the status of the heart. A typical ECG wave signal from lead II of a normal subject. The ECG has a typical morphology comprised of P wave, QRS complex and T wave. The normal ECG signal is having waves, complexes,

Table 1.1: Standard 12-lead ECG system

Standard leads	Limb Leads	Chest leads
Bipolar Leads	Unipolar Leads	Unipolar leads
Lead I Lead II Lead III	aVR aVL aVF	V1 V2 V3 V4 V5 V6

segments, and intervals recorded as the voltage on the vertical axis against the time on the horizontal axis. A single ECG waveform begins and ends at the isoelectric line. Two waveforms collectively are called a complex, whereas a segment is a flat, straight and isoelectric line. A waveform or complex connected to a segment is known as an interval. All ECG tracings above the isoelectric line are described as positive deflections, whereas,

below the isoelectric line are negative deflections [M. Singh, 2012; D. J. Bronzino, 2000]. A brief of ECG features [A. R Houghton, 2012] are described as follows.

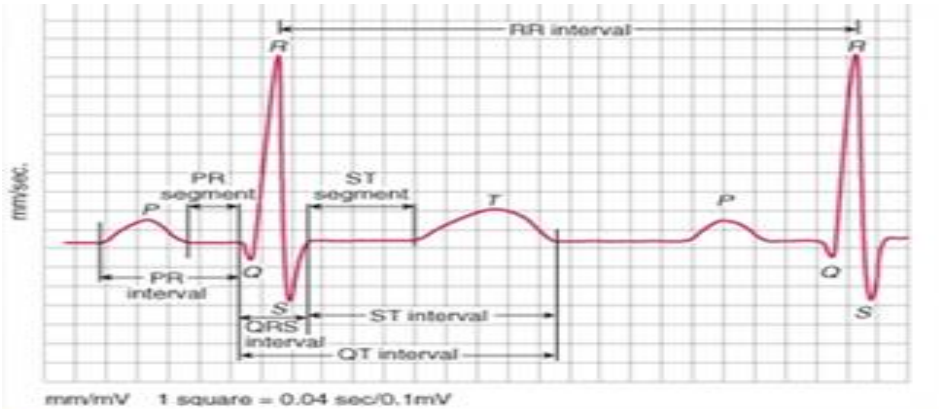

Figure 1.6: The human ECG signal over one cardiac cycle
[reproduced from http://www.datasci.com/solutions/cardiovascular/ecg-research]

P wave reflects the depolarization of the atria**.** During normal atrial depolarization, electrical vector is directed from the SA node towards the AV node and spreads from the right atrium to the left atrium. This turns into the P wave on the ECG. Its duration is around 80ms.

QRS complex reflects the rapid depolarization of the right and left ventricles. The ventricles have a large muscle mass compared to the atria, so the QRS complex usually has much larger amplitude than the P wave. A normal QRS complex has duration in between 80 to 100ms. Convention dictates that any combination of these waves can be referred as QRS complex.

T wave represents the reploarisation of the ventricles. The interval from the beginning of the QRS complex to the apex of the T wave, referred as the absolute refractory period. The last half of the T wave is referred to as the relative refractory period. The T wave is usually positive with duration of around 150-350ms.

RR interval represents the interval between an R wave and the next R wave; normal resting heart rate is between 60 and 100bpm. Its duration is 0.6 to 1.2 seconds.

PR interval is measured from the beginning of the P wave to the beginning of the QRS complex. The PR interval reflects the time of the electrical impulse takes to travel from the sinus node through the AV node and entering the ventricles. This is the best estimate of the AV node function. Its duration is around 120-200ms.

PR segment connects the P wave and the QRS complex. The impulse vector is from the AV node to the Bundle of His to the bundle branches and then to the Purkinje fibers. This electrical activity does not produce a contraction directly and is simply traveling down towards the ventricles. This shows up flat on the ECG and its duration is around 50-120ms.

J Point is the point at which the QRS complex finishes and the ST segment begin. It is used to measure the degree of ST elevation or depression.

ST segment connects the QRS complex and the T wave. The ST segment represents the period, when the ventricles are depolarized. The ST amplitude is measured as the deviation at the J point with respect to the isoelectric line (PQ or TP segment). From a clinical point of view, positive or negative deviations of the ST segment, larger than 1-2 mm, clear indicators of myocardial ischemia.

ST interval is measured from the J point to the end of the T wave. Its duration is around 320ms.

QT interval is measured from the beginning of the QRS complex to the end of the T wave. A prolonged QT interval is a risk factor for ventricular arrhythmia and sudden death. It varies with heart rate. For clinical relevance, it requires a correction, giving the QTc (QT interval/sqrt(R-R interval)). Its duration is up to 420 ms for heart rate of 60bpm.

1.6 Distinguishing Ischemia, Infraction and Necrosis

The ECG is a central tool used to establish the diagnosis of myocardial ischemia, infraction and necrosis. These occur commonly due to blockage of a coronary artery following the rupture of a vulnerable atherosclerotic plaque, an unstable collection of

lipids in the wall of an artery. It is the interruption of blood supply to part of the heart and causing some heart cells to die. The ischemia is representative of a shortage of oxygen to tissues, if left untreated for a sufficient period of time, can cause death of the heart tissues, i.e. infarction [G. Gupta, 2010, M.S. Sabatine, 2000]. Whereas, the necrotic area is electrically silent, means it is typically not depolarized. Abnormalities in the ST segment and T waves represent myocardial ischemia (sometime infarction) and may be followed by the formation of Q waves (necrosis) [E. B. Hanna and D. L. Glancy, 2011; A. Smrdel and F. Jager, 2011]. Necrosis is commonly represented by pathological Q waves. To differentiate Q waves from pathological significance from those, a different criterion has been established. However, the ECG may be normal or nonspecific in a patient with either ischemia or infarction. Also included in this research, specific ST segment (including elevation and depression) is evaluated for ischemia detection. It is also important to understand that ECG abnormalities are not the sole criteria for diagnosing ischemia, infraction and necrosis. ECG changes may be absent or nonspecific, and when present may be due to ischemia without infarction or to non ischemic disorders, such as acute pericarditis. Hence, ischemia, infarction and necrosis may be diagnosed by the appropriate combination of clinical and laboratory tests, in conjunction with the presence of characteristic ECG changes [K. Matsumura et.al, 1998].

1.7 ECG Manifestations of Myocardial Ischemia

The most important ECG change caused by myocardial ischemia includes ST deviation (elevation or depression) on the epicardium**.** This relates to a delay in conduction velocity due to accumulation of K+ in the ischemic zone in comparison to the normal zone. This causes a depolarization of the resting membrane potential and leads to ST deviation. The ST deviation has universally been used as an indicator of ischemic states of the myocardium during physical stress and silent ischemic episodes. The extents of sub-endocardial and related transmural potential gradients influence the measurement of ST deviation during ischemia [A. Goldberger, 1981; J. Park, 2012; A. Smrdel and F. Jager, 2011]. Elevation and depression of the ST segment with respect to isoelectric reference is the investigation of myocardial ischemia around the applied Lead. Elevated ST segments (episodes) appear usually in patients with transmural (sub-epicardial) ischemia, while

depressed ST segments (episodes) appear in patients with sub-endocardial ischemia, an example shown in Figure 1.7. Similarly, STEMI (ST segment elevation myocardial infarction), the coronary artery is completely blocked off by the blood clot, all the heart muscle affected starts to die. ECG changes are a characteristic elevation in the ST segment. Whereas, in NSTEMI (non-ST segment elevation myocardial infarction) is the least severe type. In NSTEMI, the blood clot only partly occludes the artery, only a portion of the heart muscle affected artery dies. In contrast to the more severe form of the heart attack (STEMI), the NSTEMI does not produce a characteristic elevation in the ST segment shows characteristic depression in the ST segment and T wave inversion. The ST segment elevation indicates that a relatively large amount of heart muscle damage, as the coronary artery is totally blocked [M.S. Sabatine, 2010].

1.8 Pictorial view of Ischemia

In most cases of normal ECG, the ST segment has the same electric potential as the isoelectric line i.e., TP segment. When myocardial ischemia is present, the electric potential of the ST segment is elevated or depressed with respect to the isoelectric line potential of the TP segment. The ST segment deviation is mainly due to injury current in myocardial cells [J. Park, 2012]. If the coronary artery blocked by plaque or blood clot, some myocytes is to be unresponsive to depolarization, or to repolarize earlier than adjacent myocytes, it causes ischemia. Elevated ST segments appear typically in patients with transmural ischemia, while depressed ST segments appear in patients with sub-endocardial ischemia [A. Goldberger, 1981]. The shaded region represents the area being affected by myocardial ischemia (transmural or sub-endocardial) has been shown in Figure 1.8.

1.9 Localization of the Ischemic Zone

ECG Changes are useful to locate ischemic regions through leads. The acute transmural ischemia of the anterior wall is reflected in ST segment elevation in one or several pre-cordial leads through V1-V6, and in lead-I and lead aVL. Ischemia of the inferior wall shows changes in leads-II, III and aVF. The ischemia in the posterior wall is detected

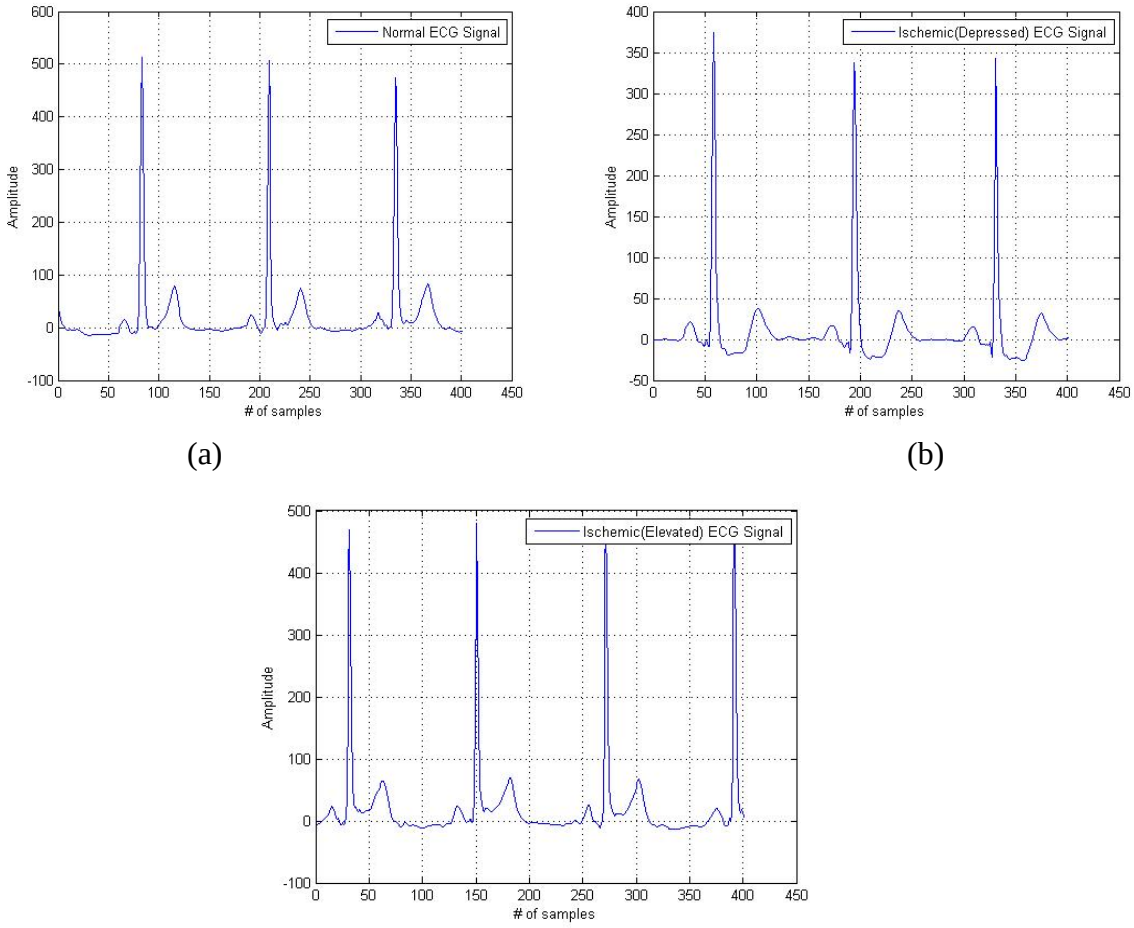

Figure 1.7: (a) Normal ECG (b) Subendocardial ischemic (depressed ST) ECG (c) Transmural ischemic (elevated ST) ECG

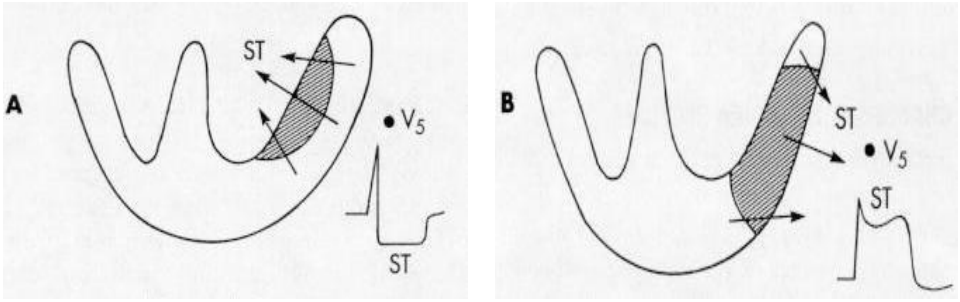

Figure 1.8: Pictorial view of ischemia a) Subendocardial ischemia b) Transmural ischemia
[reproduced from http://aiyisheng.org/Electrocardiograph.htm]

indirectly by reciprocal ST segment depression (subendocardial ischemia) in leads V1-V3 [Chia, 1998; A. S. Fauci et.al, 2008]. Prominent and reciprocal ST segment depression in these leads is also recorded in some infarcts of the inferior wall. Whereas right

ventricular ischemia frequently produces an ST segment elevation usually diagnosed in the right pre-cordial leads [S.A. Jones, 2005].

1.10 ECG Artifacts

ECG artifacts are turbulence on ECG tracings. As a result of artifacts, normal segments or components of the ECG get distorted. The word artifact is similar to artificial, frequently used to point to something that is not natural. In electrocardiography, an artifact is used to point to something that is not heart made. These may include electrical interference from electrical noise from elsewhere in the body, outside sources, poor contact of electrodes and malfunctioning of recording machine, etc. Artifacts are extremely common, and knowledge of them is necessary to prevent misinterpretation of an ischemia [C. M. Travieso, 2011; G. Clifford et.al, 2006; P. Coumel, O. Garfien, 1990].

1.10.1 Causes

During recording, artifacts can be generated by patient's motion or other attached electrical devices or implanted devices, like deep brain stimulator in the body. Shivering and tremors are best examples of motion induced artifacts. Simple movements, such as combing the hair or brushing can also cause ECG disturbances. Similarly, External sources of ECG artifacts include power line interference and radio frequency based medical devices. In operation theatres and in the intensive care unit (ICU), various equipments can affect ECG measurement system like, leads, electrodes, amplifiers and filters, etc. Common equipment, which can cause ECG artifacts, includes hemo-filtration machines, electrocautery, and transcutaneus nerve stimulator etc. [L. Schamroth, 2009; muvila, 2006; J. G. Webster, 2009]. Generated noise has been divided into three categories as described below:

1.10.1.1Noise Originating from Sources outside the Patient

a) Electrostatic sources
b) Radio frequency interference
c) Electromagnetic induction

1.10.1.2 Noise Originating from the Patient Electrode Contact

a) Mechanical movement of recording electrodes
b) Polarization of electrode distorts ECG

1.10.1.3 Noise Originating from the Patient

a) Muscle artifact
b) Electromyogram
c) Frequency overlapping
d) Signal enlargement than ECG
e) Muscular activity (especially shivering)

1.10.2 Artifact Characteristics

Artifacts on the ECG can distort individual or all components of ECG, i.e. P, QRS, T waves and PQ, TP and ST segments. Some time, these artifacts may mimic specific arrhythmia. It is important to recognize the artifact frequency and these artifacts changes from genuine changes to prevent mis-diagnosis. For example, if ST segments are affected by baseline wandering, either ST segment elevation or depression can be misinterpreted as myocardial ischemia.

1.10.2.1 Baseline Wandering

In baseline wandering, the isoelectric line (PQ or TP segment) changes position in the ECG as shown in Figure 1.9. The possible causes for the occurrence of this artifact include patient movement, cable moving during the recording, dirty lead wires or electrodes, loose electrodes may cause this artifact.

1.10.2.2 Power Line Interference

During, recording of ECG, If ECG machine is not properly grounded or not equipped with appropriate filter, a thick looking ECG line will appear in ECG tracings (figure 1.10). The alternating current (AC) is the common reason for this artifact. In the India, the electricity changes direction 50 times per second, i.e.50 Hz. However, many places in Europe, AC frequency is 50 Hz and in USA, AC frequency is 60 Hz.

Figure 1.9: Baseline wandering artifact
[reproduced from http://www.mauvila.com/ECG/ecg_artifact.htm]

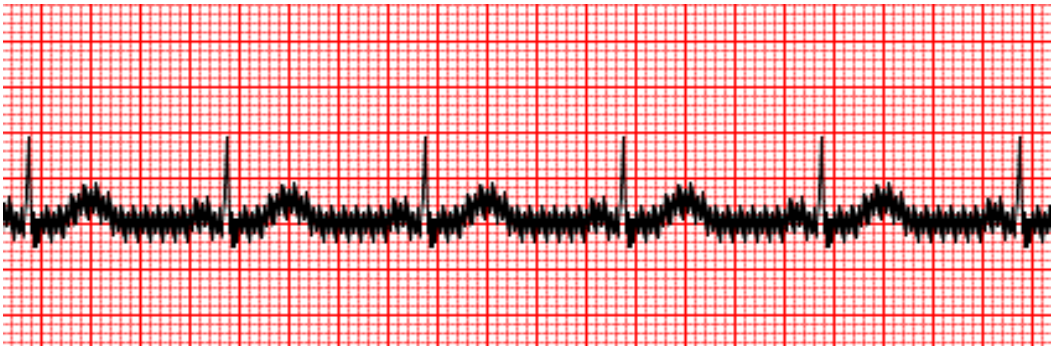

Figure 1.10: Power line interference artifact (AC interference)
[reproduced from http://www.mauvila.com/ECG/ecg_artifact.htm]

1.10.2.3 Muscle Tremor

The heart is not the only responsible organ to produce current organ in the human body. When human skeletal muscles experience tremors, the ECG is incorporated with apparently random activity. This artifact is low in amplitude and mimics the isoelectric line. Muscle tremors are normally a lot more subtle than that shown in Figure 1.11.

Figure 1.11: Muscle tremor artifact
[reproduced from http://www.mauvila.com/ECG/ecg_artifact.htm]

1.10.3 Artifacts Removal

The main goal of artifact removal or pre-processing is to formalize the accurate and efficient delineation of characteristic points in ECG signals, further used for detection of isoelectric reference and classification of the ST segment. Above mentioned artifacts are commonly noticed during recording. It is very significant to recognize the artifact frequencies and to discriminate these artifact changes from genuine changes to prevent mis-diagnosis. A number of methods have been designed till now, which may have linear or nonlinear structures for the elimination of baseline wander, power line interference and muscle tremors. These methods are broadly divided into four categories as, time based, frequency based, time-frequency based, and nonlinear methods. The advantages and disadvantages of above discussed methods can be studied in [R. J. Martis et.al, 2014]. Time-frequency based method, wavelet transform, in which higher scale contains lower frequency components, whereas lower scale contains higher frequency components of analyzing signals, known as multi-resolution analysis. Wavelet transform can provide discrimination between two different signals with the same spectrum magnitude. Hence, wavelet transform is found more appropriate for analysis of non-stationary ECG signal via wavelet coefficients thresholding [H. Y. Lin et.al, 2014]. After discarding of wavelet coefficients corresponding to artifact frequencies of original ECG signal have no destructive effects on the morphology of original ECG signal.

1.11 Available Methods for Ischemia Detection

There are numerous methods have been developed during last 15-20 years, a brief of these methodologies has been discussed below:

N. Maglaveras et.al presented an automated method based on a supervised neural network (NN) using adaptive back propagation for detection of ischemic episodes ensuing from ST segment depression and elevation. The advantages include, detection of ischemia was independent of the lead used and in case of critical care unit (CCU). It was found that the average sensitivity of 88.62% for recordings of the European ST-T database [N. Maglaveras et.al, 1998].

T. Stamkopolous, N. Maglaveras proposed a method for detection of ischemia based on the ST segment for Holter recordings using nonlinear principal component analysis (NLPCA) to classify detected ST segment in two classes as normal and abnormal. A classification rate of 80% for normal beats and 90% for the ischemic beats was achieved. The method exhibits superior performance as compared to principal component analysis (PCA) and neural network (NN) method [T. Stamkopolous, N. Maglaveras, 1998].

C. Papaloukas et.al proposed rule based algorithm for the finding of ischemic episodes in long duration ECGs. It includes four stages, noise handling, extraction of features; rule based beat classification and ischemic episode identification. The method was validated on the records of ESC ST-T database and obtaining sensitivity and positive predictive were 93.75% and 78.50% respectively. Advantages of this method include execution in real time and abilities to offer interpretations to decisions [C. Papaloukas, 2000].

S. Papadimitriou et.al presented self organizing map (sNet-SOM) supervising network imaging based method to exploit the computationally effective explanation for the ischemia detection. The method has potential frequency dependence ability to examine the immediate consequences of ischemia. The results indicate that differentiation between ischemic and normal myocardium on the basis of the cyclic variation of ultrasonic backscatter is feasible in the entire range from 3-8 MHz. The future work includes detection of the immediate consequences of ischemia in human subjects using clinical imaging systems [S. Papadimitriou et.al, 2001].

A. Cimponerin et.al presented a 2-D ventricular tissue model in order to investigate the determinants of ECG morphology during chronic and acute chronic ischemia. Aacidosis was induced by reducing Ca2+ and Na+ conductances, while Hyperkalenia was simulated by step changes in K+ out. Hypoxia was induced by its consequence on potassium activity. The results show that the restored normal ionic concentration created an isopotential ST segment, while an enlarged Q was still visible, despite irreversible uncoupling of the necrotic region. Future investigations of controversial mechanism of

tissue revascularization after infraction may identify the proper moments by applying newly promising methods [A. Cimponerin et.al, 2001].

C. Papaloukas et.al developed an automated method for the diagnosis of ischemic episodes in long duration ECG recordings of ESC ST-T database through artificial neural network (ANN) approach. The network was trained using a Bayesian method. The raw ECG signal containing the T wave and ST segment used as inputs to the beat classification system and the corresponding output was the classification of the beat. The dimensionality reduction of input to the network was produced through a principal component analysis (PCA). The network performance in beat classification provides 90% sensitivity and 90% specificity [C. Papaloukas et.al, 2002].

C. Papaloukas et.al presented a system for diagnosis of ischemia by using multi criteria decision analysis named HYSMID, consist of four stages viz. pre-processing, beat classification, window characterization and episode definition. The classification includes category prototypes and similarity in a fuzzy way. The genetic algorithm was also used for detection of parameter like, thresholds and weights for optimal values. HYSMID was validated for 10 records of European ST-T database, demonstrating with 91% sensitivity and 93% positive predictivity [C. Papaloukas et.al, 2003].

P. Ranjith et.al presented a method for detection of ischemic events using detected ECG characteristic points through wavelet transform technique. This method gives 92% sensitivity and 86% positive predictivity. The limitation was the computation time required was higher than other methods. The advantage includes easily extended to detect other abnormalities of the heart [P. Ranjith et.al, 2003].

H. Haraldssen et.al presented a method for the detection of acute myocardial infarction in 12-lead ECG using artificial neural networks (ANN). They tested 2238 ECG records of an emergency department of a Hospital. The obtained receiver operating characteristic (ROC) areas for ANN trained with Hermite functions, positive predictivity and sensitivity 83.4% and 84.3 % for P=0.4 respectively. Presented method has advantages of providing a decision support system for good advice for diagnosis [H. Haraldssen et.al, 2004].

T. Goletsis et.al proposed a method for cardiac beat classification algorithm for the detection of ischemic episodes using support vector machines (SVM) and wavelet transform after validation for records of European ST-T database. The method pre-processes the ECG recordings for QRS complex detection followed by the extraction of the ST segment. The next stage includes down sampling of extracting ST segment patterns and subtraction of down sampled pattern from normal template. The third stage includes, training for detection of ischemic beats using SVM. The results show sensitivity and positive predictivity of 92.13% and 90.34%, respectively [T. Goletsis et.al, 2004].

R.V. Andreao et.al proposed an ECG analysis system based on a Markovian approach for segmentation and online beat detection. Then precise localization of all beats, PQ & ST segments for ischemia detection for 48 records of European ST-T database was performed. The best average statistic results are 85% positive predictivity and 83% sensitivity. The future work covers robust analysis for rejection of noisy beats instead of treating them through noise reduction methods. Hence, some improvements in beat rejection are possible through the use of promising noise detection methods [R.V. Andreao et.al, 2004].

I. Niwas et.al (2005) proposed an expert system for an automatic classification of cardiac arrhythmias through ANN for significant improvement in the critical care unit (CCU) for subject monitoring. Feature sets include RR intervals, heartbeat intervals and spectral entropy of the ECG records of MIT-BIH Arrhythmia database. The proposed system is capable of classifying the normal beats from different arrhythmias. The overall accuracy of 99.02% was achieved for classification.

L. Dranca et.al investigates the technique for detection and classification of ischemia based on decision tree analysis in real time. The technique includes signal preprocessing for extraction of features from the ECG signal followed by detection and rejection of suspected as well as irrelevant ST segment events. The performance of technique includes sensitivity of 89.89% and positive predictivity of 70.03% for episodes over all

the records of LT-ST database. The proposed method advantage includes implementation on mobile devices such as personal digital assistants (PDAs) [L. Dranca et.al, 2006].

M. C. Maclachlan et.al presented a paper for determining the location and size of ischemia through the ECG inverse problem by measuring the ST segment shift. The posterior and anterior ischemia cases for both clean and noisy observation data were evaluated for the error in the center of mass not greater than 2%. For the anterior cases, an error in the area of the ischemic region of 31%–32%, while in the posterior case, 55% error in the area was observed for all noise levels. Future work includes the validation of this method for clinical observation data [M. C. Maclachlan et.al, 2006].

M. G. Tsipouras et.al presented an automated expert system using fuzzy theory for classification of ischemic and arrhythmic beats in ECG signals. The fuzzy stochastic global optimization procedure was performed for the modification of the model's parameters. The initial set of rules was decided by assigned expert cardiologists for a dataset of the MIT-BIH arrhythmia and European ST-T database. The presented system had an ability of interpreting the decisions, major advantage as compared to the black box approaches provided by neural networks [M. G. Tsipouras et.al, 2007].

J.Q. Xue introduced an algorithm based on reducing lead set using neural network models and binary tree classification model having automatic induced rules for ischemia detection. The study was tested on the ECGs of 1187 inferior MI patients, 993 anterior MI patients and 1987 non ischemic patients. The result shows that the reduced lead set to achieve 53% sensitivity for Inferior MI, while 54% for standard 12- lead set, and a specificity of 99% in both cases, without retaining. The sensitivity of the reduced lead set was 37%, for anterior MI, as compared to the 46% for standard 12 leads, without retaining. Reduced lead set achieves sensitivity of Anterior MI 56%, as compared to a standard 12 lead set of 57% and specificity of 98% for both lead sets, with retaining [J.Q. Xue, 2007].

C. Zizzo et.al proposed an ECG monitor capable of displaying changes in 3-D images of the heart for automated ST segment analysis and to assist the healthcare professional's for severity of acute ischemic changes. They describe two functions of the monitor, called ischemia detection and imaging functions (IF). Fifty doctors evaluate IF and the result shows an increase in their median proficiency from 50% to 100% to diagnose ischemia. The time to reach diagnosis was also dropped from 15 to 9 minutes for eight ECGs. After validation of European ST-T database records, sensitivity of 85% and positive predictivity of 93% was demonstrated [C. Zizzo et.al, 2008].

A. Gharaviri et.al presented a method using an adaptive Nueuro-fuzzy interface system (ANFIS) classification for the automatic finding of ischemic episodes. The algorithm performance was evaluated in terms of episode detection as well as beat by beat ischemia detection for European ST-T database records. The result shows average ischemia episode detection sensitivity of 88.62%. This method has advantages for use in ECG processing in case of critical care options (CCO). The resulting ANFIS was also capable of detecting ischemia used lead independent. The future work includes the use of the SVM classifier for the achievement of higher sensitivity [A. Gharaviri et.al, 2008].

E. Pueyo et.al proposed a method for quantifying ischemia using upward (IUS) and downward (IDS) slopes of the QRS complexes in ECG signals in the frequency band of 150- 250 Hz. The result shows that mean relative factors of change are much larger for IUS and IDS than for the high-frequency index and in addition, more robust measurements. The future work includes, the QRS slopes may be used for monitoring of ischemia in excess of time, separation of individuals with and without coronary artery disease needs for testing [E. Pueyo et.al, 2008].

T. S. Ruud introduced a new method for locating ischemic regions in the heart using ECG inverse problem through bi-domain equations. The proposed method examined the effects of ischemia on the electrical attributes of heart tissues by taking into account the ischemia as spherical. These tests indicate that the proposed algorithm might be

considered a promising supplement; it is fairly fast, simple and better able to distinguish cases of subendocardial ischemia [T. S. Ruud, 2009].

A. Minchole et.al proposed a method for diagnosis of myocardial ischemia in Holter recordings. The proposed method considered the mechanisms of ischemia that result in ST segment deviation in ECG, heart rate related episodes and body position changes for Long-Term ST Database. The method had reached an accuracy of 82.3%. The results in sensitivity of 76.8% and a specificity of 98.3% for distinguishing between transient episodes for ischemic and heart rate related, different ST signatures and or sudden step ST changes. Similarly, for classifying ischemia from heart rate related episodes, a sensitivity of 84.5% and specificity of 86.6% were reached and a sensitivity of 74.2% and obtained a specificity of 93.2% for separating ischemia from any other ST event [A. Minchole et.al, 2010].

S. Murgan and S. Radhakrishnan proposed an Ant-Miner algorithm based on data mining approach and association rule based classification for the detection of ischemic beats. The main advantage of this method includes higher accuracy with the facility to provide interpretation of the decisions made by the algorithm. The ischemic beat detection algorithm was tested on 10 records of European ST-T database and a sensitivity 92% and specificity 93% was demonstrated [S. Murgan and S. Radhakrishnan, 2010].

H. Rabbani et.al proposed entropy based methods comprising of wavelet sub-bands of ECG signals, including extracted ST segments. The method distinguishes between the ECG signal of healthy individuals and patients. The 40 patients exercise treadmill test was used, who had ischemic signs, diagnosed by a medical practitioner. Results show specificity and sensitivity of 95% and 94%, respectively. [H. Rabbani et.al, 2011]

A. Smrdel and F. Jager (2011) presented an algorithm for processing long AECG data, for transient ischemic heart disease. The 74 records of the Long Term ST database include both mixed ischemic episodes or no episodes and elevated or depressed ischemic episodes. The algorithm correctly classified records with Prinzmetal's angina 7 out of 8. The method correctly classified 47 out of 55 records for other coronary artery disease

excluding Prinzmetal's angina. Advantage of this include, suitability for processing long AECG data, correctly and efficiently classified the records according to as per annotations for ischemia [A. Smrdel and F. Jager, 2011].

X. Tang et.al presented a technique using hidden Markov model (HMM) of ECG signal for detection of ischemia for recordings of the Long Term ST database. The recorded ECG signals were firstly pre-processed to produce input sequences and then model training for detection of episode of local ischemia was held. The proposed technique provides a possible approach for the automatic, timely and rapid diagnosis of ischemia. Future work includes testing of methods to be used in portable medical diagnostic apparatus [X. Tanga et.al, 2012]

J. Park et.al proposed a method using support vector machine (SVM) and kernel density estimation (KDE) based classifier for training and testing of ischemic ST episodes. The 10 representative records of the European ST-T database were taken. Discrete wavelet transform (DWT) was used for baseline wandering removal and detection of QRS complexes. The normalized and signed sum from QRS offset, area between QRS offset and T peak points and slope from QRS onset to offset point was used for diagnosis of ischemia. Results indicate, sensitivity and specificity for KDE were 0.939 and 0.912, respectively, while sensitivity and specificity of SVM were 0.941 and 0.923, respectively [J. Park et.al, 2012].

S. Don et.al (2013) presented a 3-stage method for the classification of ECG beats through k-nearest neighbor (kNN) and Gaussian mixture model (GMM) classifiers. This includes filtering for baseline wandering followed by feature extraction using Higuchi's fractal dimension (HFD). Then k-NN and GMM were used as classifiers to classify ischemia and arrhythmia for a total of 30,000 ECG segments of European ST-T Ischemia and MIT-BIH Arrhythmia databases. An overall accuracy of 99% and 98.24% was demonstrated for k-NN and GMM, respectively, for 60% of the beats were used for training the classifier and the remaining 40%, for validation. [S. Don et.al**,** 2013]

V. Hellemond (2013) represents a new approach to find the total myocardial area at risk (MaR) during acute coronary occlusion for both ischemic and infracted ECGs by considering ST deviation and QRS abnormalities. Total 32 patients with acute inferior ST elevation myocardial infarction (STEMI) received Tc-Sestamibi before percutaneous coronary intervention (PTCA). The Aldrich score with SPECT ($r=0.17$, $p=0.36$) was used for ischemic components of the total MaR, an infracted component of the total MaR was estimated by the Selvester score with SPECT (for $r=0.55$, $p=0.001$) and for combined Aldrich and Selvester scores with SPECT improved ($r=0.58$, $p<0.001$) was estimated. Results show, there was no statistically significant difference between the MaR measured by SPECT (for $p=0.636$) and mean MaR estimated by the sum of Aldrich and Selvester scores [V. Hellemond, 2013].

P. Gomis and P. Caminal presented an approach to detect the acute myocardial ischemia using abnormal intra QRS at micro-volt level (μAIQP) based ECG index. The approach was assessing the changes of micro-volt amplitude intra QRS potentials induced during elective percutaneous coronary interventions (PCI) for 57 patients with balloon inflation periods ranging from 3.1 to 7.3 minutes. Results show that the mean μAIQP amplitude significantly decreased at the PCI event respect to baseline for each of the standard 12 leads. Decrease μAIQP in both the pre-cordial leads and the limb leads in Left anterior descending artery (LAD) occlusion, while affects the limb leads right coronary artery (RCA) and left circumflex artery (LCx) occlusions. Decreased in the precordial leads, R-wave amplitude increased during PCI in RCA and LCx groups in lead III, while the amplitude decreased in the LAD group in lead III. [P. Gomis and P. Caminal, 2014]

R. Correa et.al proposed a method for detection of ischemia using four vector-cardiographic ST-T parameters, including, T-wave vector magnitude area (aTVM), ST vector magnitude area (aSTVM), T-wave vector magnitude difference (TVD) and ST-T vector magnitude difference (ST-TVD). The comparison between the spatial ventricular gradient (SVG) and conventional ST-Change vector magnitude (STCVM) were also intended. The results indicate that several vector cardio-graphic parameters show

significant differences during and before starting PTCA for p-value of 0.05. The specificity 92.6% and sensitivity 90.5% were archived at the 5th minute of the PTCA for ST-TVD and STVM classifiers, respectively [R. Correa et.al, 2014].

1.12 Research Gaps

The various ischemia detection systems that have been proposed in literature so far, can be grouped in four categories. Each category is exhibiting certain disadvantages. The digital analysis techniques are the most common techniques used in medical signals. They are easy to implement and have real time performance in reaching a decision. The rule-based systems are simple to be implemented and their decision process resembles that of the medical experts. Fuzzy systems provide human-like reasoning and seem to have great potential in ischemia diagnosis by allowing the expression of doubtless concerning the validity of a rule. However, they still need further investigation in order to improve their diagnostic performance. The ANNs can usually detect ischemia more reliable than the other systems. Their main disadvantage is that they cannot provide an explanation for the diagnosis they provide. The support vector machine (SVM) and kernel density estimation (KDE) based classifier involved complex calculations for decisions. All the described systems should be further improved, especially in the ways that handle noisy recordings. The proper filtering must be utilized for elimination of noise in ECG recordings. Recent developments in digital signal processing methods may prove very effective in completely removing ECG noise and in the achievement of higher performance.

1.13 Objectives of Research Work

- To pre-process acquired ECG signal for removal of noises like baseline wanders, power line interference and muscle tremors.
- To detect various wave components of ECG leading to feature extraction required for ischemia detection.
- To develop an enhanced classifier for ischemia using an ST segment of ECG so as to achieve higher values for specificity and sensitivity than the existing values.
- To validate the results of the developed classifier using European ST-T database.

1.14 Proposed Methodology

Physio-bank is a well characterized digital recordings of physiologic signals and related sampled data used for validation of developed methods by the biomedical research community worldwide. The Physio-bank includes European ST-T databases (EDB) [A. Taddei, 1992] of normal, abnormal and multi rate biomedical signals from healthy subjects and patients. This database has been used for the present research work. The validation of results has been done as per the given clinical diagnosis of the European ST-T database for further enhancement of algorithms in terms of their positive predictivity, sensitivity as well as specificity. In order to achieve the first objective, we have taken records of annotated European ST-T Database. Using multi-resolution wavelet transform in MATLAB programming, we pre-processed the various ECG records for elimination of artifacts. We find out the optimal selection of wavelet function and decomposition level by recognizing the frequency of noises using correlation factor and PRD. To cover the second objective, again wavelet transform using window search based algorithms have been developed. This algorithm gives better results. The third objective has been covered to detect and classify normal, ischemic beats and episodes based on threshold decided by proposing mathematical function, named isoelectric energy function (IEEF). This also includes classification of subendocardial and transmural ischemia. Fourth objective is the validation of the results for annotated EDB. A schematic diagram of this research work has been presented in Figure 1.12.

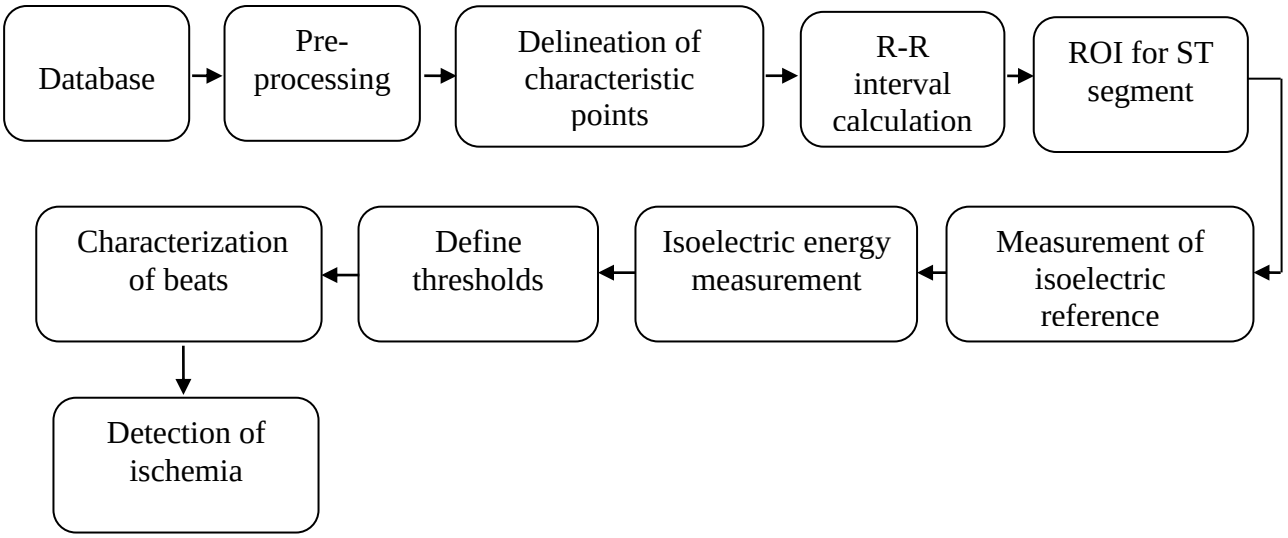

Figure 1.12: General schematic diagram for entire thesis

1.15 Organization of the Thesis

Entire thesis has been divided into six chapters. A summary of each of them is provided here.

Chapter 1 describes the significance of ECG monitoring and ischemia. Basic idea about the research problem, the origin of ischemia and detection methods is given in this chapter. It also includes, the methodology adopted to implement different proposed algorithms.

Chapter 2 describes the resources and methods which cover the description of the database and mathematical background of multi-resolution wavelet transform.

Chapter 3 discusses the methodology and detailed operating procedure for artifact elimination in ECG signals.

Chapter 4 presents a delineation technique for the characteristic points of ECG.

Chapter 5 focuses the validation of results for developed method, isoelectric energy function for detection and classification of ischemia for European ST-T database. Algorithms for beats characterization and ischemia classes have also been mentioned.

Chapter 6 summarizes all the major findings of the research work. Future prospective and scope in the field is also included in this chapter.

CHAPTER-2

RESOURCES AND METHODS

2.1 The European ST-T Database

The European ST-T Database (EDB) records are projected to be used for performance evaluation of the developed method for validation results. This database contains 90 ECG recordings, annotated beat by beat from 79 subjects. The subjects cover 8 women aged 55 to 71 and 70 men aged 30 to 84. Additional selection criteria were established to diagnose myocardial ischemia for each subject, including baseline ST segment displacement. The database has total 367 episodes corresponds to ST segment change. The durations of these episodes lie in the range of 30 seconds to several minutes. In addition, the peak displacements ranging from 100 μV to more than one mV have also been mentioned. Each record has the compact clinical reports document as header (.hea) files, which summarize medications, pathology, technical information and electrolyte imbalance. The header files also include information about the subject's age, sex, leads used for recording, medications, the recording equipment and the clinical findings. Each record contains two hours recording of two channels with 12-bit resolution over a nominal 20 mV input range and a sampling frequency of 250 samples per second. The sample values were re-scaled after digitization, in order to obtain a consistent scale of 200 ADC units per mV for all ECG signals. Each of the ECG signal files is 5,400,000 bytes long. In order to annotate each record beat by beat and for changes in ST segment, two independent cardiologists were appointed. Annotated ST segments identified their onsets, extremes, and the ends in both leads. After annotations made by two experts were compared, the disagreements were resolved by the Pisa software and final reference annotation record/files were prepared. These 90 records altogether, contain 802,866 annotations [A. Taddei, 1992]. The database contains records of two leads acquired from V_1, V_2, V_3, V_4, V_5 and MLI, MLIII positions. The present research work has been carried out on 43,876 ST segments from 10 representative records namely e0103, e0104, e0105, e0108, e0113, e0114, e0147, e0159, e0162, and e0206 recordings of this database. These records cover all almost all types of morphologies of ECG signals.

2.1.1 European Society of Cardiology's definition of Ischemic Episodes

Three expert cardiologists were appointed jointly; they defined a set of rules for the duration detection for the ST episodes during which the ECG signal exhibits significant ST segment displacement. To identify and annotate an ST episode, following criteria's [A. Taddei, 1992] were applied:

- ST segment deviations are measured relative to a reference waveform for each subject (usually selected from the first 30 seconds of each record). Measurements of ST segment deviation are taken 80 milliseconds after the J point if the heart rate does not exceed 120 bpm, and 60 milliseconds after the J point otherwise.
- ST episodes must contain an interval of at least 30 seconds during which the absolute value of the ST deviation is no less than 0.1 mV.
- The beginning of each ST episode is annotated. The beginning is located by searching backward from the time at which the absolute ST deviation first exceeds 0.1 mV. The search continues until a beat is found for which the absolute ST deviation is less than 0.05 mV, and for which the absolute ST deviation is less than 0.1 mV throughout the previous 30 seconds. An ST change annotation which indicates the beginning of the episode is placed immediately following this beat.
- The peak (i.e., the greatest deviation, positive or negative) of each ST episode is annotated. An ST change annotation is placed before the beat judged to exhibit the greatest ST deviation; this annotation contains a manual measurement of the peak ST deviation.
- The end of each ST episode is annotated. The end is located by searching forward from the time at which the absolute ST deviation last exceeds 0.1 mV. The search continues until a beat is found for which the absolute ST deviation is less than 0.05 mV, and for which the absolute ST deviation is less than 0.1 mV throughout the following 30 seconds. An ST change annotation which indicates the end of the episode is placed immediately before this beat.
- Each ST change annotation contains a text field which describes its significance. The text field contains characters which identify the episode type ('ST"), the signal number ('0' or '1'), and the direction of the deviation ('+' or '-'; extreme T deviations

are signified by '++' and '--'). The text field of an annotation which marks the beginning of an episode contains a '(' prefix. For an annotation which marks the end of an episode, there is a prefixed 'A' and an appended 3 or 4 digit decimal number which expresses the magnitude of the peak deviation in micro-volts. An annotation which marks the end of an episode has a ')' appended to the end of its text field. For example, an episode of ST depression in signal 0 with a peak (absolute) deviation of 200 micro-volts would be marked by three annotations, with text fields of '(ST0-', 'AST0-200', and 'ST0-)'.

2.2 Wavelet Transform

The Wavelet transform is a representation of a wavelet function [A. Graps, 1995]. The wavelet functions are scaled and translated version known as 'daughter wavelets' of a finite length signal, known as 'mother wavelet'. Through wavelet transform, a given continuous time signal is divided into different scale components, in which a range of frequency is assigned to each scale component. Each scale component can then be deliberated with a resolution, known as multi-resolution analysis (MRA). We define a mother wavelet function $\psi(t) \in L^2(R)$, limited in time domain, i.e., $\psi(t)$ has values in a certain range and zeros elsewhere [P.M. Louis and A. Rieder, 1997; C.L. Liu, 2010]. The mother wavelet has properties of zero-mean (Eqn. 2.1) and normalization (Eqn. 2.2).

$$\int_{-\infty}^{\infty} \psi(t)dt = 0 \qquad (2.1)$$

$$\int_{-\infty}^{\infty} \psi(t)\psi^{*}(t)dt = 1 = \left\|\psi(t)\right\|^{2} \qquad (2.2)$$

The dilation and translation properties (Eqn. 2.3) states that the mother wavelet can form a basis set denoted by

$$\psi_{s,u}(t) = \frac{1}{\sqrt{s}}\psi\left(\frac{t-u}{s}\right)\Bigg| \; u, s \in R \qquad (2.3)$$

Where 'u' is the translating and 's' is a scaling parameter holding property of greater than zero, because defining negative scaling is not possible. The multi-resolution wavelet

transform has a property of ortho-normal for obtained set$\left\{\psi_{u,s}(t)\right\}$. Theoretically, the continuous wavelet transform is the coefficient of the basis $\psi_{s,u}(t)$ as follows:

$$W f(s,u) = < f(t), \psi_{s,u} >$$

$$= \int_{-\infty}^{\infty} f(t)\, \psi^{*}_{s,u}(t)dt$$

$$= \int_{-\infty}^{\infty} f(t) \frac{1}{\sqrt{s}} \psi^{*}\left(\frac{t-u}{s}\right) dt \qquad (2.4)$$

One dimensional signal f(t) can be mapped in two dimensional coefficients using wavelet transform, Wf(s,u), mentioned in Eqn. 2.4. These two variables can be performed in the time as well as frequency analysis simultaneously. We can position a particular frequency (with s) at a certain time instant (with u).

$$f(t) = \frac{1}{C_{\psi}} \int_{0}^{\infty} \int_{-\infty}^{\infty} W f(s,u) \frac{1}{\sqrt{s}} \psi \left(\frac{t-u}{s}\right) du \frac{ds}{s^2} \qquad (2.5)$$

Where C_{ψ} is defined as

$$\int_{0}^{\infty} \frac{\left|\psi(w)\right|^2}{w} dw < \infty$$

ψ(w) is the Fourier transform of the ψ(t), mother wavelet, as mentioned in Eqn. 2.5. This equation is also acknowledged as admissibility condition. Wavelet transforms have two classifications, continuous wavelet transforms (CWTs) and discrete wavelet transforms (DWTs). It should be important to note that, both CWT and DWT are continuous time transforms. These can be used to represent continuous time signals. DWTs use a specific subset of translation & scale grid, whereas, CWTs work at every possible scale and translation grid. A signal, acquired from the different physical sources using electrode, transducer, cannot be analyzed directly to depict a useful conclusion. It desires to be processed in order to extract some important information from it. The acquired signal is usually transformed to different domains for better interpretation of the physical characteristics inherent in the signal. The original (acquired) signal can be reconstructed

back by taking its inverse transformation of decomposed signal without any loss of important clinical information. Some of the popular transform, or methods in signal processing include, Fourier analysis (FT), short time Fourier analysis (STFT), wavelet analysis (WT) etc. All of these methods map the signal into its own way. The advantages of one another over method can be analyzed in terms of its applicability for analyzing specific signal [R. Polikar, 2000]. WT have advantages over FT and STFT for accurately deconstructing and reconstructing finite, non-periodic as well as non-stationary signals.

2.2.1 One Stage Filtering: Detail & Approximations Coefficients

For analysis of ECG signals, the high and low frequency components are the most important part. In wavelet analysis, we usually talked about detail and approximation coefficients. The approximation coefficients are the high-scale, low-frequency components of the analyzing signal, whereas, detail coefficients are the low-scale, high-frequency components of analyzing signals. The filtering process [G. Strang and T. Nguyen, 1996; S.G. Mallat and S. Zhohgs, 1989; I. Daubechies, 1990], looks like, at its most basic level, as shown in Figure 2.1.

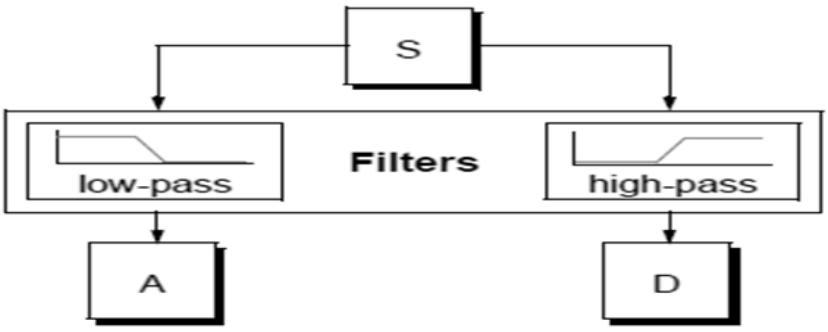

Figure 2.1: Approximations and details after signal filtering
[reproduced from http://in.mathworks.com/discrete-wavelet-transform.html]

The original signal, 'S' passes through two complementary filters, emerges two signals. Suppose, the original signal 'S' is having 1000 samples. After applying wavelet, the resulting signals, for a total of 2000, means each signal have 1000 samples. These signals 'A' and 'D' is interesting (Figure 2.2). There exists a more delicate way to carry out the decomposition of a given signal using wavelet transform. By taking care for the

computations, one can keep only one signal, in order to get the complete information of the decomposed signal. This process is known as down sampling. These produce two sequences called ‘cA’ and ‘cD’. The process of down-sampling (Figure 2.2) produces DWT coefficients. In order to gain a better admiration of this process, discrete wavelet transform decomposition for one stage has been performed.

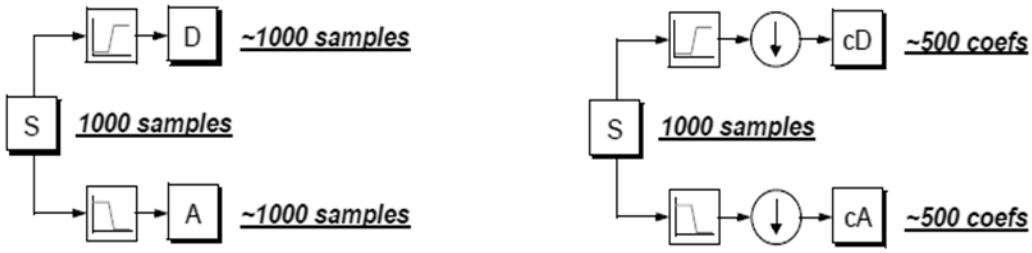

Figure 2.2: Effect of down-sampling
[reproduced from http://in.mathworks.com/discrete-wavelet-transform.html]

This signal is a pure sinusoid having high frequency noise. Figure 2.3 is presenting a schematic diagram wavelet decomposition process.

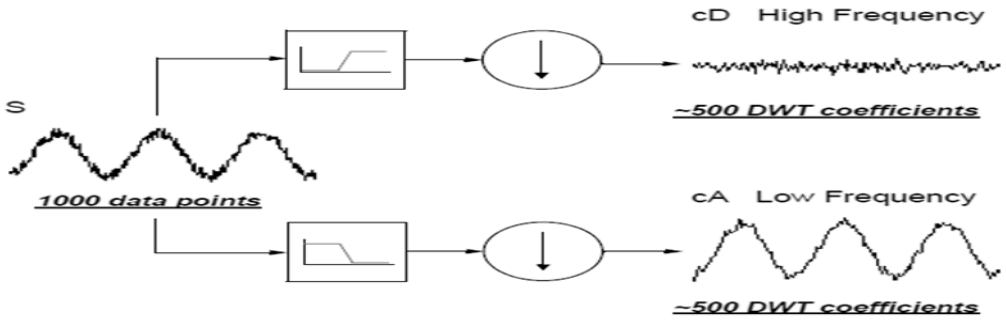

Figure 2.3: Wavelet decomposition for real signal
[reproduced from http://in.mathworks.com/discrete-wavelet-transform.html]

2.2.2 Multiple Level Decomposition

The decomposition process is generally iterated, in which successive approximations are decomposed in turn, up to required lower resolution components. This multiple decomposition is known as wavelet decomposition tree (Figure 2.4).

2.2.3 Number of Levels

The analysis process can be continued indefinitely, since this process is iterative. In theory, the decomposition process can be preceded, only until the individual details

consist of a single sample of analyzing signals. Whereas in practical cases, one select a suitable number of decomposition levels as per information required from the physiological signals.

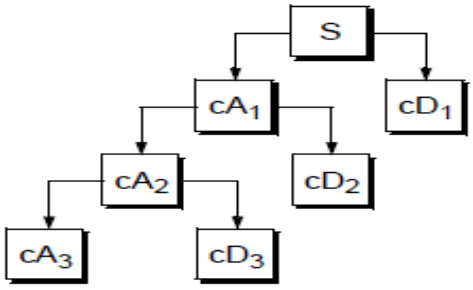

Figure 2.4: Multiple level decomposition
[reproduced from http://in.mathworks.com/discrete-wavelet-transform.html]

2.2.4 Wavelet Reconstruction

An analyzed signal is decomposed using discrete wavelet transform. This process is known as decomposition or analysis. The other half of the analysis involves how those decomposed signal components has been assembled back into the original signal, with a condition of not losing its clinical information. This process is known as reconstruction, or synthesis as shown in Figure 2.5. The inverse discrete wavelet transforms (IDWT) is mathematical manipulation that affects synthesis. To synthesize an original signal using Wavelet Toolbox™ software, one can easily reconstruct it from the approximate or detail coefficients, wavelet coefficients. In general, wavelet analysis involves down-sampling and filtering, whereas, wavelet reconstruction process covers up sampling and filtering.

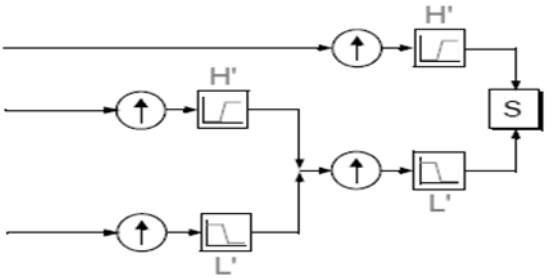

Figure 2.5: Wavelet reconstruction
[reproduced from http://in.mathworks.com/discrete-wavelet-transform.html]

Further, up-sampling may be called as a process of lengthening an original signal component by inserting zeros between the samples. An example of this process has been presented in Figure 2.6.

2.2.5 Reconstruction Filters

The decomposition (down-sampling) process, introduces a distortion in the original signal, known as aliasing. It should be careful for choosing filters for the reconstruction and decomposition phases, for cancellation of aliasing effect. The high and low pass

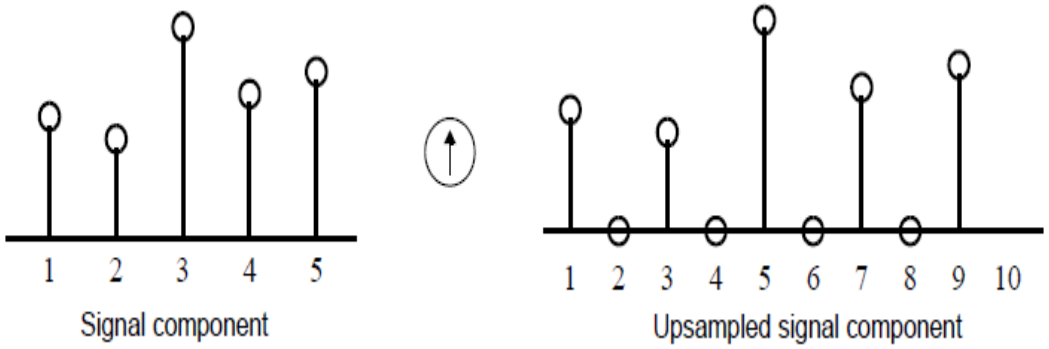

Figure 2.6: Up-sampling of signal
[reproduced from http://in.mathworks.com/discrete-wavelet-transform.html]

decomposition filters (H & L) and connected reconstruction filters (H' and L') construct a system, known as quadrature mirror filters (Figure 2.7).

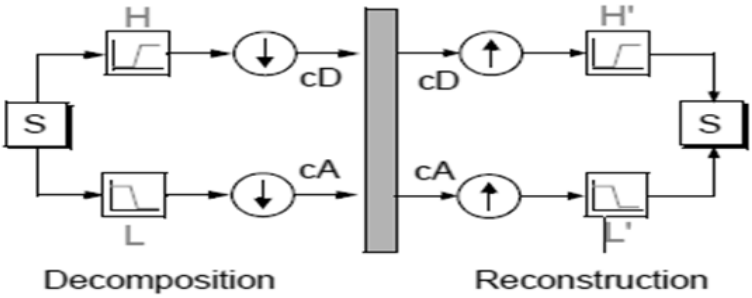

Figure 2.7: Quadrature mirror filters
[Reproduced from http://in.mathworks.com/wavelet-reconstruction.html]

2.2.6 Reconstructing Approximations and Details

The reconstruction of the original signal is possible through the high pass (approximations) coefficients and low pass filter coefficients (details), as shown in Figure 2.8. It is also possible to reconstruct the details and approximations themselves from their vectors coefficient. An example of this process is shown in Figure 2.9. The Figure is shows the reconstruction of the first level approximations (A1) from the cA1

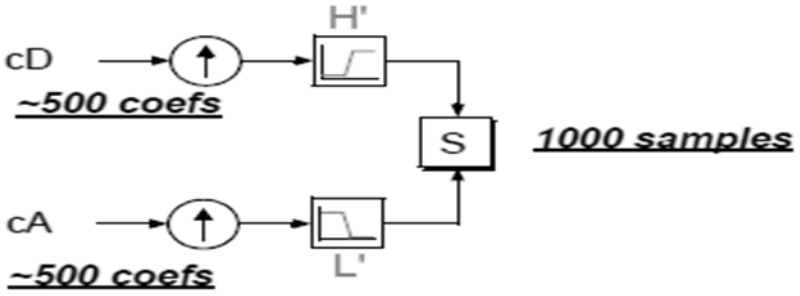

Figure 2.8: Reconstructing approximations and details
[Reproduced from http://in.mathworks.com/wavelet-reconstruction.html]

(approximation coefficient vector). For cD1 (detail coefficients) feed in a vector of zeros in place of.

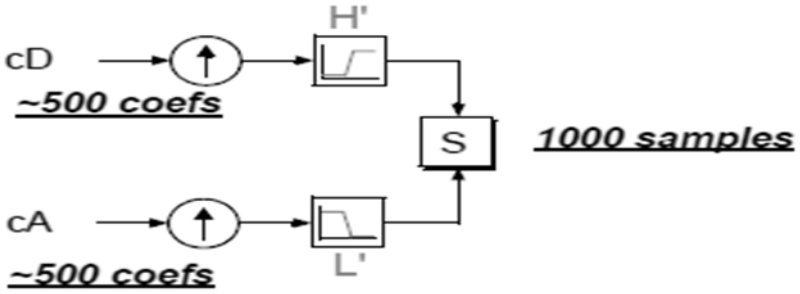

Figure 2.9: Reconstructing approximations and details with details being zero's
[Reproduced from http://in.mathworks.com/wavelet-reconstruction.html]

We combine the original signal by cA1 and cD1 to obtain the original signal S (Figure 2.10), as mentioned in Eqn. 2.6.

$$A_1 + D_1 = S \qquad (2.6)$$

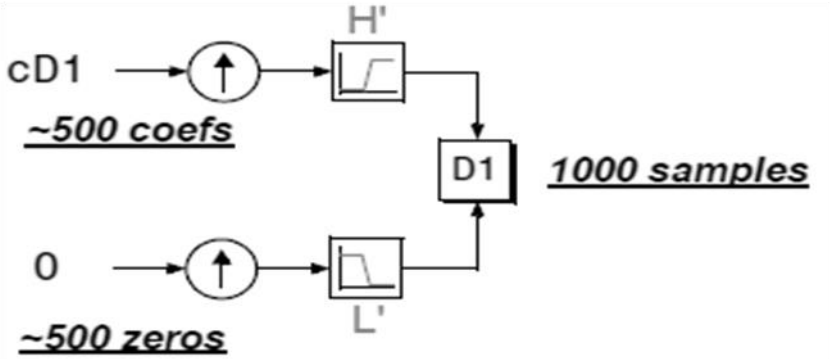

Figure 2.10: Reconstructing approximations and details with approximations being zero's
[Reproduced from http://in.mathworks.com/wavelet-reconstruction.html]

It is important to note that the coefficient vectors ‘cD1’ and ‘cA1’ directly, as these were produced by down-sampling. It is necessary to reconstruct the details and approximations first before combining them. In this extension, the technique of multilevel analysis, find that similar interaction hold for all the constituents of the reconstructed signal. An example of this process is shown in Figure 2.11.

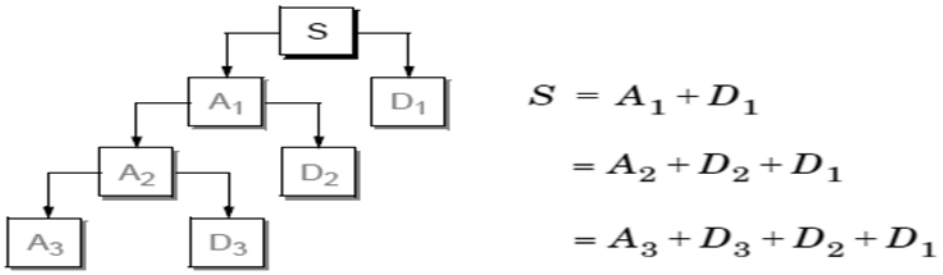

Figure 2.11: Reconstructed signal components
[Reproduced from http://in.mathworks.com/wavelet-reconstruction.html]

2.2.7 Multi-step Decomposition and Reconstruction

A multi-step decomposition and reconstruction (analysis and synthesis) process has been represented in the Figure 2.12. This process involves two steps, to get the wavelet coefficients thorough breaking up of an original signal, and reassembling back of the original signal from the obtained coefficients.

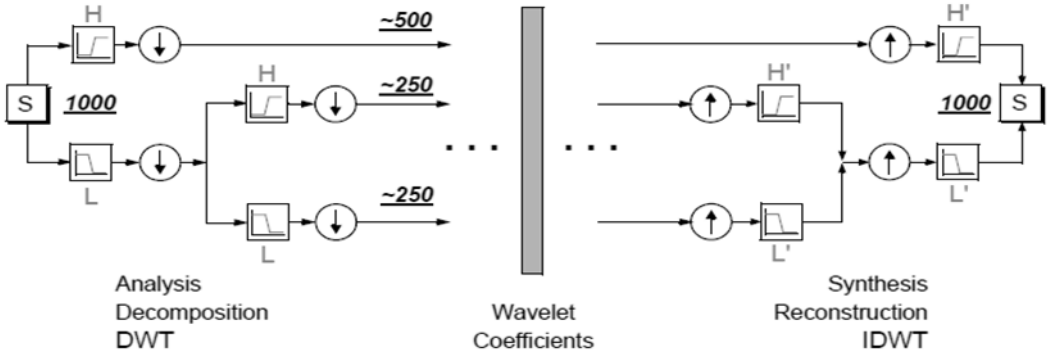

Figure 2.12: Multistep analysis-synthesis process
[Reproduced from http://in.mathworks.com/wavelet-reconstruction.html]

The wavelet analysis is performed to obtain coefficients have numerous applications, de-noising being foremost among them.

2.2.8 Frequency and Scale

Wavelet analysis, the different scales have different frequency ranges. As the wavelet is more stretched, the longer the portion of the original signal and thus the coarser the signal features being deliberate by the wavelet coefficients [I. Daubechies, 1990].

Thus, there is a relation between the frequency and wavelet scales, exposed by the wavelet analysis as

- High scale s => Stretched wavelet => slowly changing, coarse features => Low frequency ω.
- Low scale s => compressed wavelet => rapidly changing details => High frequency ω.

2.3 Discrete Wavelet Transform

Determining wavelet coefficients at each scale is a fair hard work. It generates a terrible lot of data. It turns out, that if one chooses scales and positions based on powers of two, so called dyadic scales and positions, then the analysis will be much more efficient and accurate. This analysis is possible through the discrete wavelet transform (DWT). This is an efficient method to implement this scheme using filters. This method was developed by 'Mallat' in 1988 [S. G. Mallat, 1989]. The 'Mallat algorithm' is a standard scheme in the signal processing society, as a two channel sub-band coder [C. L. Liu, 2010]. This is very practical filtering algorithm yields a fast wavelet transforms. The scaling and wavelet functions are specified by Haar, Daubechies etc. for which, the basis function is known. We can approximate a discrete signal (Eqn. 2.7).

$$f[n] = \frac{1}{\sqrt{M}} \sum_k W_\emptyset[j_0, k] \emptyset_{j_{o,k}}[n] + \frac{1}{\sqrt{M}} \sum_{j=j_0}^{\infty} \sum_k W_\psi [j, k] \psi_{j,k}[n] \qquad (2.7)$$

Here $f[n], \emptyset_{j0,k}[n]$ and $\psi_{j,k}[n]$ are discrete functions defined in [0, M-1], totally M points. As, the sets are orthogonal to each other, we can simply take the inner product to obtain the wavelet coefficients

$$W_\emptyset[j_0, k] = \frac{1}{M} \sum_n f[n] \emptyset_{j_{0,k}}[n] \qquad (2.8)$$

$$W_{\psi}[j,k] = \frac{1}{\sqrt{M}}\sum_{n} f[n]\psi_{j,k}[n] \quad j \geq j_0 \tag{2.9}$$

2.4 Fast Wavelet Transform

Generally, if wavelet function and scaling is known, its coefficients can be easily obtained as defined in Eqn. 2.8 and 2.9. One can find a different way to find the wavelet coefficients without knowing the scaling and the dilation function [C. L. Liu, 2010]. The calculation time can be reduced.

$$\begin{aligned} \emptyset_{j,k}[n] &= 2^{\frac{j}{2}}\,\emptyset\left[2^j n - k\right] \\ &= \textstyle\sum_{n'} h_{\emptyset}[n']\sqrt{2}\,\emptyset[2\left(2^j n - k\right) - n'] \end{aligned} \tag{2.10}$$

Let $n' = m - 2k$, we have

$$\emptyset_{j,k}[n] = \sum_{m} h_{\emptyset}[m-2k]\sqrt{2}\emptyset\left[2^{j+1}n - m\right] \tag{2.11}$$

If, we combine above Eqns. 2.10, 2.11 with Eqn. 2.8, it becomes,

$$\begin{aligned} W_{\emptyset}[j,k] &= \frac{1}{\sqrt{M}}\sum_{n} f[n]\emptyset_{j,k}[n] \\ &= \frac{1}{\sqrt{M}}\sum_{n} f[n]2^{\frac{j}{2}}\emptyset[2^j n - k] \\ &= \frac{1}{\sqrt{M}}\sum_{n} f[n]2^{\frac{j}{2}}\sum_{m} h_{\emptyset}[m-2k]\sqrt{2}\emptyset[2^{j+1}n - m] \\ &= \sum_{m} h_{\emptyset}[m-2k]\left(\frac{1}{\sqrt{M}}\sum_{n} f[n]2^{\frac{j+1}{2}}\emptyset[2^{j+1}n - m]\right. \\ &= \sum_{m} h_{\emptyset}[m-2k]W_{\emptyset}[j+1,m] \qquad (2.12) \\ &= h_{\emptyset}[-n] * W_{\emptyset}[j+1,n]|n = 2k, k \geq 0 \qquad (2.13) \end{aligned}$$

Similarly, for detail coefficients (Eqn. 2.14), it is

$$W_{\psi}[j,k] = h_{\psi}[-n] * W_{\emptyset}[j+1,n]n = 2k, k \geq 0\Big| n = 2k, k \geq 0 \tag{2.14}$$

For discrete time signals, the original signal or data can be viewed as approximation coefficients with order J. i.e., f[n] = W[J, n] as presented by Eqn. 2.12 and 2.13. The next level of approximation and detail can be obtained. This algorithm is 'fast' because one can find the coefficient level by level rather than directly using Eqn. 2.8 and 2.9 [C.L. Liu, 2010].

2.5 Comparison between Fourier Transform, Short Time Fourier Transform and Wavelet Transform based Analysis

Fourier Transform based Analysis

Signal analysts already have in their discarding an impressive armory of tools. Possibly, the most well known technique of these is Fourier analysis as shown in Figure 2.13. This method breaks down an original signal into ingredient sinusoids of different frequencies. The Fourier analysis is a mathematical method for transforming the original signal to frequency based from time based [R. Polikar, 2000] (Eqn. 2.15).

$$H(\omega) = \int_{-\infty}^{\infty} f(t) e^{-\omega t}\, dt \qquad (2.15)$$

Where H(ω) is the Fourier transform of a signal f(t).

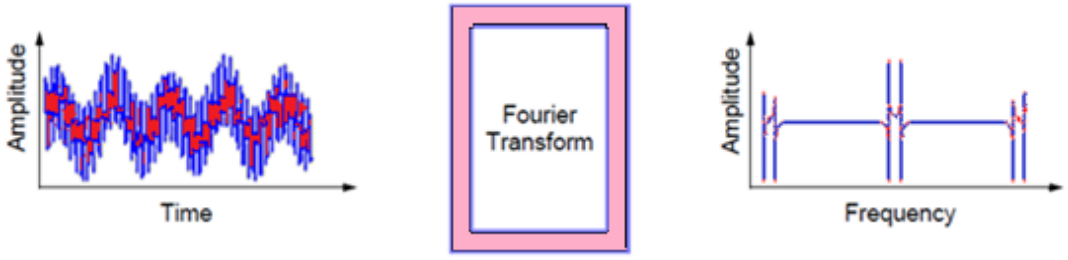

Figure 2.13: Fourier transform
[reproduced from http://in.mathworks.com/discrete-wavelet-transform.html]

For numerous signals, Fourier analysis is tremendously helpful because the signal's frequency content is of immense significance. Fourier analysis has a serious hitch, time information is lost when transforming to the frequency domain. Another hitch include, it is impracticable to notify a particular event took place. This hitch is not very important for a stationary signal. However, the most physiological interesting signals hold frequent

non-stationary or transitory characteristics include abrupt changes, drift, trends, beginnings and ends of events. These individualities are usually the most important part of the physiological signals; hence Fourier analysis is not appropriate for detecting them.

Short Time Fourier Transform based Analysis

In an effort to correct above mentioned deficiency, Dennis Gabor tailored the Fourier transform, to analyze only a small section of the signal at a time, called windowing the signal as shown in Figure 2.14. This adaptation is known as Short Time Fourier Transform (STFT) as mentioned in Eqn. 2.16. It maps an original signal into a 2-dimensional signal, which is a function of frequency as well as time. STFT employs a frequency-time depiction 'H(ωτ)'of the continuous time signal 'f(t)', Eqn. 2.16.

$$H(\omega,\tau) = \int f(t)g*(t-\tau)e^{-\omega t}dt \qquad (2.16)$$

Where g(t-τ) is a window function.

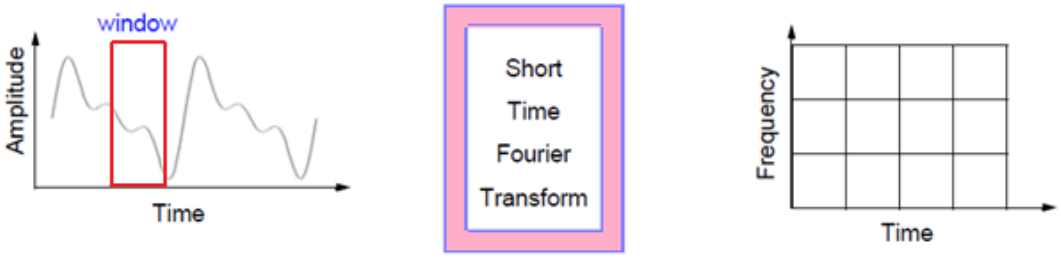

Figure 2.14: Short time Fourier transform
[reproduced from http://in.mathworks.com/discrete-wavelet-transform.html]

The STFT represents a sort of concession between the frequency and time based view of a signal. It provides information in short, at what frequencies and when a signal event occurs. Though, one can only get this information with limited precision, as precision is decided by the size of the window. On the other hand, the STFT concession between frequency and time information can be useful. The disadvantage of STFT include, once a meticulous size of the time window has been chosen, the time window will remain same for all frequencies. A lot of signals need a more flexible approach, where the variation of the size of the window is primarily required to find more accurate either frequency or time or both based information at a time.

Wavelet Transform based Analysis

Wavelet analysis represents the next logical step to STFT analysis. This analysis involves a windowing technique with variable sized regions. It allows the use of long time intervals where one wishes shorter regions, whereas one wishes high-frequency information or more precise low-frequency information as shown in Figure 2.15.

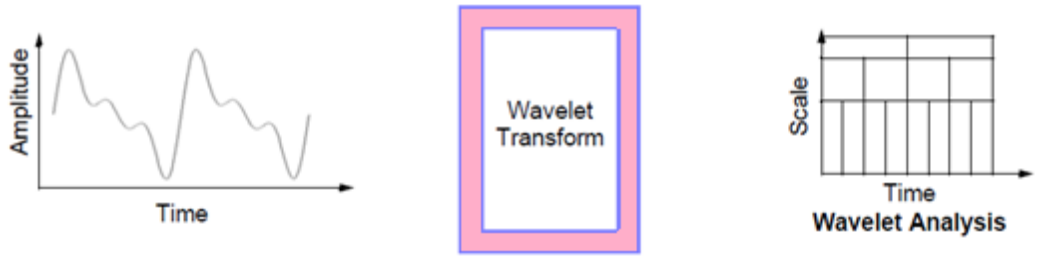

Figure 2.15: Wavelet transform
[reproduced form http://dsp.stackexchange.com/wavelet-transform]

Here's what this looks similar to in contrast with the frequency-based, time-based and STFT views of an original signal:

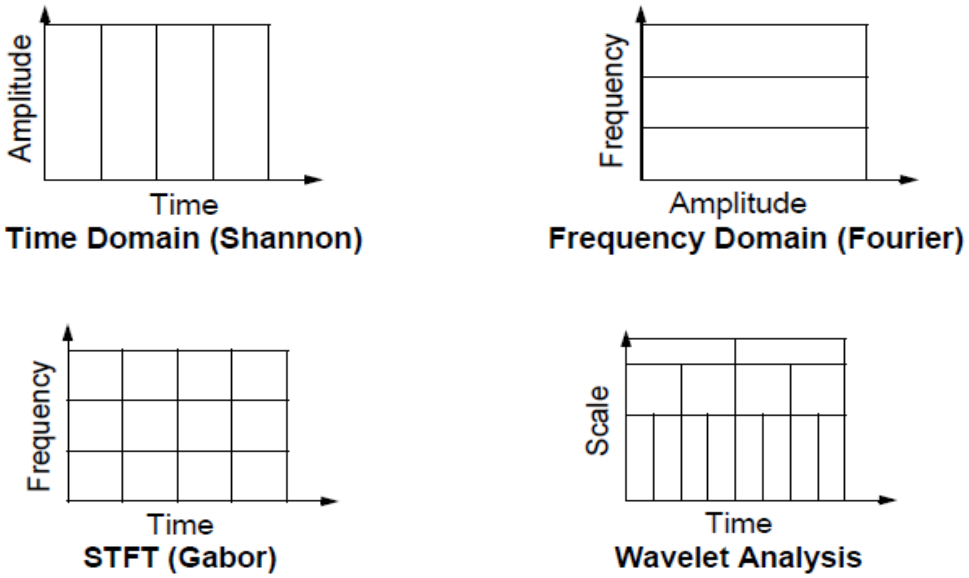

Figure 2.16: Time, frequency domain, STFT vs. wavelet transforms based analysis
[reproduced form http://dsp.stackexchange.com/wavelet-transform]

Here, a noticeable point about the wavelet analysis is that, it does not use a frequency-time region, but somewhat a scale-time region. This analysis is capable of enlightening aspects of other than signal analysis methods. This analysis is used detection of

breakdown points, discontinuities in higher derivatives, trends and self similarity. In addition, wavelet analysis can de-noise a signal without significant degradation as compared in Figure 2.16.

2.6 Properties of Wavelet Transform

Various properties of wavelet transform are described below [J. Kovacevic and W. Sweldens, 2010]:

- Regularity
- The window for a function is the smallest time set outside, for which function is identically zero
- Orthogonal filters escort to the orthogonal wavelet basis functions; means, the resultant wavelet transform is energy preserving
- The symmetry of the wavelet filters. Among orthogonal, the Haar wavelet is the only symmetric wavelet. For bi-orthogonal wavelets, both scaling and wavelet functions are either symmetric or anti-symmetric
- Approximation of the order of the polynomial is determined by number of vanishing moments
- Support of the wavelet in frequency, time and rate of decay, the accompanying perfect reconstruction filters have linear phase
- Number of vanishing moments, wavelets with increasing numbers of vanishing moments result in sparse representations for a large class of signals
- Iterative algorithms for wavelet construction converge faster and the existence of a scaling function

2.7 Wavelet Families

Following families have been defined in five categories, are the basic types of mother wavelets:

- Crude wavelets: Gaussian, Morlet, Mexican hat
- Infinitely irregular wavelets: Meyer, Dmeyer
- Orthogonal & Compactly supported wavelets: Daubechies, Symlet, Coiflets

- Bi-orthogonal & Compactly supported wavelet pairs: Bi-orthogonal, Reverse bi-orthogonal
- Complex wavelets: Complex Morlet, Complex Shannon, Complex Gaussian, Complex frequency B-spline

Corresponding properties of these wavelets [R. Janani, 2014, I. Daubechies, 1988] are as follows:

- Haar

Compactly supported orthogonal, symmetry, scaling function, orthogonal analysis, bi-orthogonal analysis, exact reconstruction, continuous and discrete time transform, fast algorithm, explicit expression, FIR filters

- Daubechies

Arbitrary regularity, compactly supported orthogonal, asymmetry, arbitrary number of vanishing moments, orthogonal analysis, bi-orthogonal analysis, FIR filters, continuous and discrete time transformation, exact reconstruction, fast algorithm, scaling function

- Coiflets

Compactly supported orthogonal, near symmetry, number of vanishing moments, Arbitrary regularity, vanishing moments for scaling function, orthogonal analysis, bi-orthogonal analysis, scaling function, exact reconstruction, FIR filters, fast algorithm, continuous and discrete time transformation

- Bi-orthogonal

Compactly supported bi-orthogonal, symmetry, Arbitrary regularity, arbitrary number of vanishing moments, bi-orthogonal analysis, exact reconstruction, scaling function, FIR filters, continuous and discrete time transformation

- Reverse Bi-orthogonal

Arbitrary regularity, symmetry, arbitrary number of vanishing moments, compactly supported bi-orthogonal, existence of the scaling function, exact reconstruction, FIR filters, bi-orthogonal analysis, continuous and discrete transform, fast algorithm

2.8 The MATLAB Environment

The MATLAB stands for Matrix Laboratory. It is a fourth-generation programming

language and having multi-paradigm numerical computing environment. The MATLAB is developed by the Math-Works, USA. It allows matrix manipulations, implementation of algorithms, plotting of data, visualization, creation of graphical user interfaces, and interfacing with other languages written programs. MATLAB includes a family of application oriented solutions, called toolboxes. One of its most strengths involve is that it allows building its own re-usable functions. Customized programs and functions can be easily created in MATLAB code. Biomedical engineers use MATLAB to develop algorithms as well as in research and designing of medical devices. This software has a large number of advantages over the other conventional means of numerical computing as mentioned:

- Data structures require minimal attention
- Arrays need not be declared before first use
- It allows easy and quick coding in a very high level language
- An interactive interface allows easy debugging and rapid experimentation
- MATLAB M-files are completely portable across a wide range of platforms
- High quality graphic and visualization facilities are possible
- Toolboxes can be added to extend the system

2.8.1 Wavelet Toolbox

Wavelet Toolbox software [M. Misiti, 2012] is an enormous method to perform with wavelets. This toolbox, together with the power of MATLAB® software, really allows one to write powerful and complex applications, in a very short span of time. The Graphic User Interface (GUI) is intuitive and user friendly. It provides an excellent interface to explore the various aspects and applications of wavelets; it takes away the tedium of typing and remembering the various function calls. Wavelet Toolbox™ software is a collection of functions built on the MATLAB® technical computing environment. It provides tools for the analysis and synthesis of signals and images, using wavelets within the framework of MATLAB. The Wavelet Toolbox software provides two categories of tools:

- Graphical interactive tools

- Command-line functions

The main features of the MATLAB Wavelet toolbox contain

- Continuous wavelet transforms (CWT)
- Discrete wavelet transforms (DWT) in 1D and 2D
- Multi-resolution decomposition and analysis of signals
- Wavelet packets, implemented as MATLAB objects
- 1D and 2D wavelet packet transforms
- User-extensible selection of wavelet basis functions
- Soft and hard thresholding based de-noising

CHAPTER-3

ARTIFACTS REMOVAL IN ECG SIGNALS

3. Introduction

As discussed in chapter 1, ECG signal is recorded by placing electrodes on the skin at the specified positions of the human body. During recording of ECG, the artifacts (anything other than muscular activity of heart), also get incorporated in the ECG. The most common artifacts are baseline wandering (BW), power line Interference (PLI) and muscle tremors. These artifacts have an adverse effect on ECG and make the accurate delineation of characteristic waves more difficult, as baseline wander overlaps the ST segment of ECG; muscle tremors mimic the iso-electric line and power line interference distorts all segments of ECG. A practised cardiologist may simply diagnose the heart functions by a single just look at the ECG waves, even in the presence of these artifacts. The goal of artifacts removal in the ECG (known as pre-processing), is to facilitate easy and accurate delineation of the characteristic waves of ECG signal through developed algorithms. Accurate delineation play a pivotal role in many medical applications, like detection of QRS complex, classification of ectopic beats, analysis of asymptomatic arrhythmia, diagnosis of myocardial ischemia, heart rate variability and ECG signal data compression etc. During last few years, a lot of researches have been reported in literature for elimination of the artifacts, these include filters [U. M. Chaskar et.al, 2009], wavelet based de-noising [G. Kaushik, 2012; T. Gandhi et.al, 2011], neural network based [M. E. Cohen, 2006], nonlinear signal processing [U. R. Acharya, 2013] based analysis, linear prediction based [J. Makhoul, 1975], principal component analysis (PCA) based [R. Duda et.al, 2001], linear discriminant analysis (LDA) based [R. Duda et.al, 2001], independent component analysis (ICA) [E. Oja et.al, 2001; M. Sheoran et.al, 2014], Fourier transform [D .L. Fugel, 2009], power spectral density (PSD) based [J. G. Proakis, 1992], higher order spectra (HOS) based [R. J. Martis et.al, 2011; C. L. Nikias and J. M. Mendel, 1993], Empirical mode decomposition (EMD) based [S. Pal and M. Mitra, 2012]. Each method exhibits own advantages and disadvantages. Like, digital infinite impulse response (IIR) filters have been used for the removal of noises from ECG

signals [S. C. Mahesh, 2008]. The design of IIR filter is quite easy and even higher order IIR filters performance is also good, but due to the drawback of long filtering time, it requires more memory and is not suitable for filtering of highly non-linear, physiological ECG signal. Adaptive filtering technique [S. M. M. Martens et.al, 2006; F.C. Chang et.al, 2007; D. Dobromir et.al, 2008] is also used for elimination of power line interference. This method is more suitable for elimination of this noise due to its smaller residual errors and faster response [S.G. Tareen, 2008]. However, this method requires the reference signal information for the efficient filtering. Notch filters [M.S. Chavan et.al, 2008] and finite impulse response (FIR) filters [V. J. A. Alste et.al, 1985; C.B. Mbachu, 2011] are popular and effective techniques for de-noising ECG signals for PLI. Unfortunately, these filtering algorithms have not given remarkable results. Another technique, averaging filter [M.R. Rangaraj, 2002] is also adopted for the artifacts removal, but it requires a huge number of time frames. Researchers have implemented independent component analysis (ICA) for removal of these noises in ECG signals [M. P. S. Chawla et.al, 2008; H. Taigang et.al, 2006; A.K. Barros et.al, 1998]. But, ICA does not permit the prior information of processed signals for competent filtering. Advanced techniques like empirical mode decomposition [Z. Zhidong and M. Chan, 2008], neural networks [J. Mateo et.al, 2008], PCA [M.P.S. Chawla, 2011] and wavelet transform [M. Kania et.al, 2007] have also been implemented for PLI. For muscle tremor removal in ECG, wavelets [A. D. Ivan, 2008; P. Augustyniak, 2006; B.S. Raghavendra et.al, 2012; A. Graps, 1995], singular value decomposition (SVD) filters [J. S. Paul et.al, 2000] have been studied. In the same way, for correction of baseline wanders, the linear filtering [I. Markovsky et.al, 2012] is adopted in the frequency range of 0.5 Hz to 1 Hz. This method is having ringing effect, commonly known as Gibbs phenomenon. For correction of this concern, the polynomial fitting, commonly known as cubic spline filtering was introduced [J. R. Laguna et.al, 1992]. Many other methods include, time varying digital filters [L. Sornmo, 1993], digital filters [H. Norbert, 2006], Projection pursuit gradient ascent algorithm [U. Zahoor and A.O. Farooq, 2009], wavelet transforms [K. Daqrouq, 2005; H. Nagendra et.al, 2011; E.B. Lin et.al, 2013; O. Sayadi and M.B. Shamsollahi, 2007], empirical mode decomposition (EMD) [K.M. Chang and S.H. Liu, 2010], hybrid

algorithm of wavelet and genetic algorithm [E.S. El-Dahshan, 2011] have been implemented. A comparison of algorithms for removal of baseline wanders can be studied in reviews [F.A. Afsar, 2009]. Though PCA, ICA and NN methods are used for extraction of artifacts in ECG signals by the band selection, these methods are having the problem of sensitivity to small changes in either the original signal or in the artifact, unless the basis-functions are trained on ECG signal. This is very important to know the artifacts and its frequency incorporated in recorded ECG signal. Hence, in order to resolve the above listed limitations of various methods for the removal of artifacts from ECG, time-frequency analysis based, wavelet transform is being preferred. There are several types of wavelet functions available in MATLAB to de-noise the ECG signals. The wavelet transform independently generates the detail coefficients (CD) and approximate coefficients (CA) [A. K. Manocha and M. Singh, 2013] as shown in Figure 3.1. The selections of appropriate wavelet function and thresholding methods play an imperative role in ECG signal de-noising. Different researchers have used the different performance analysis methods for the evaluation of their developed algorithms, like, kurtosis [L. N. Sharma et.al, 2013], standard deviation, percentage root mean square difference (PRD), sensitivity, positive predictivity, signal to noise ratio (SNR), root mean square error (RMSE) and distortion measurement [M. Singh et.al, 2010; M. Singh et.al, 2010; H. Nagendra et.al, 2011].

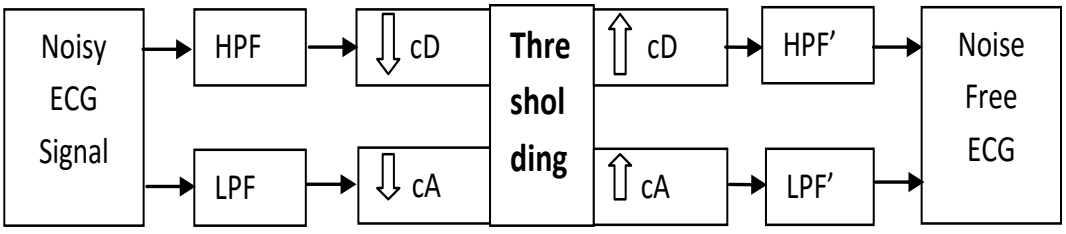

Figure 3.1: Wavelet decomposition & reconstruction process

3.1 Wavelet Thresholding

It is an estimation method that exploits the capabilities for de-noising of any type of artifact in acquiring non-stationary ECG signal. Thresholding is categorized into two types, i.e. hard and soft thresholding as shown in Figure 3.2. According to Eqn. 3.1, hard thresholding is more sensitive to small changes in the signal and is unstable as it tends to

have larger variance. On the other hand, soft thresholding involves larger bias due to shrinkage of large wavelet coefficients after decomposition. The soft thresholding is found, additional stable than that of hard thresholding, as mentioned in Eqn. 3.2. Hard thresholding makes all coefficients equal to zero for X_{dh} smaller than threshold value T and soft thresholding makes coefficient value for X_{ds} smaller than threshold value T to be zero and T is subtracted from the signal greater than T [M. Misiti et.al, 2013].

$$X_{dh} = \begin{cases} 0, & x < T \\ x, & x > T \end{cases} \tag{3.1}$$

$$X_{ds} = \begin{cases} x - T & x > T \\ 0 & x \leq T \\ x + T & x < -T \end{cases} \tag{3.2}$$

Many researchers have proved that, the soft thresholding method provides better results for de-noising the ECG signals [D.L. Donoho, 1995].

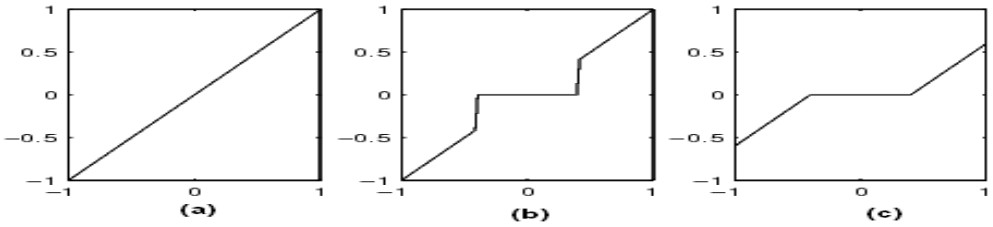

Figure 3.2: a) Original signal b) hard thresholded signal c) soft thresholded signal
[reproduced from http://in.mathworks.com/help/wavelet/ref/wthresh.html]

3.2 Methodology for Artifacts Removal in ECG Signals

Let S(n) be the original ECG signal without artifact and A(n) be the artificially generated artifact added to the original ECG signal. The signal received is represented by, SA(n) in Eqn. 3.3.

$$SA(n) = S(n) + A(n) \tag{3.3}$$

The purpose for de-noising is to extract S(n) from SA(n), while preserving the diagnostic information like amplitudes and frequency components of various segments of ECG. Artificially generated artifacts A(n) added to the original ECG signal. The properties of wavelet transforms have been employed to recover the original signal from the noisy

signal; First step is the selection of an appropriate wavelet is very important known as analysis. Second step includes the decomposition of a noisy signal using wavelet function. After decomposition, the vectors of decomposed signal are obtained as detail and approximate (smooth) coefficients. The approximate coefficients are resultant of the high-scale, low-frequency vectors of the decomposed signal, while detail coefficients are presenting the high-frequency, low-scale vectors. The approximated coefficients serve as input for the next iteration. This process is carried out until the desired level is achieved. The third step is the thresholding, which quantizes the wavelet generated coefficients performed for detail or approximate coefficients. The use of hard or soft thresholding depends upon the type of artifacts, and the last step is the reconstruction of signal of same decomposition level by applying the inverse wavelet transform. The reconstruction capability has been decided on percentage root square difference (PRD) and cross correlation criterion. This means, decomposed and reconstructed signal must have the lowest value of PRD and the close cross correlation. The flow chart for an algorithm for the optimal selection of wavelet function and decomposition level for removal of artificially added artifacts (de-noising) has been presented in Figure 3.3.

3.2.1 Removal of Baseline Wandering

For baseline wandering algorithm, we have taken 15,000 samples of ECG record (e0125) of European ST-T database of 250 Hz sampling frequency (x-axis is having no. of samples of record and y-axis is having voltage level in mV) in order to illustrate in a better manner. The baseline wandering is categorized as; D.C. components affecting the iso-electrical line of ECG signal and baseline drifting, a low frequency noise in the range of 0.5-1 Hz. For normalization, median of samples [A. K. Manocha et.al, 2012] has been taken and subtracted from original ECG signal, it is called basic (noise free) signal. Then sine wave (artificial baseline) of approx. 01 Hz is added to the noise free signal in order to illustrate ECG signal contaminated with baseline wanders. The decomposition by different wavelet transforms at different scales is performed, after that threshold (discarding of approximation coefficients to zero) is applied. The reconstruction takes place by a particular wavelet at the same decomposition level. A particular wavelet

function for which the reconstructed ECG signal is having close correlation of original ECG signal as well as having the lowest value of PRD is considered suitable for the

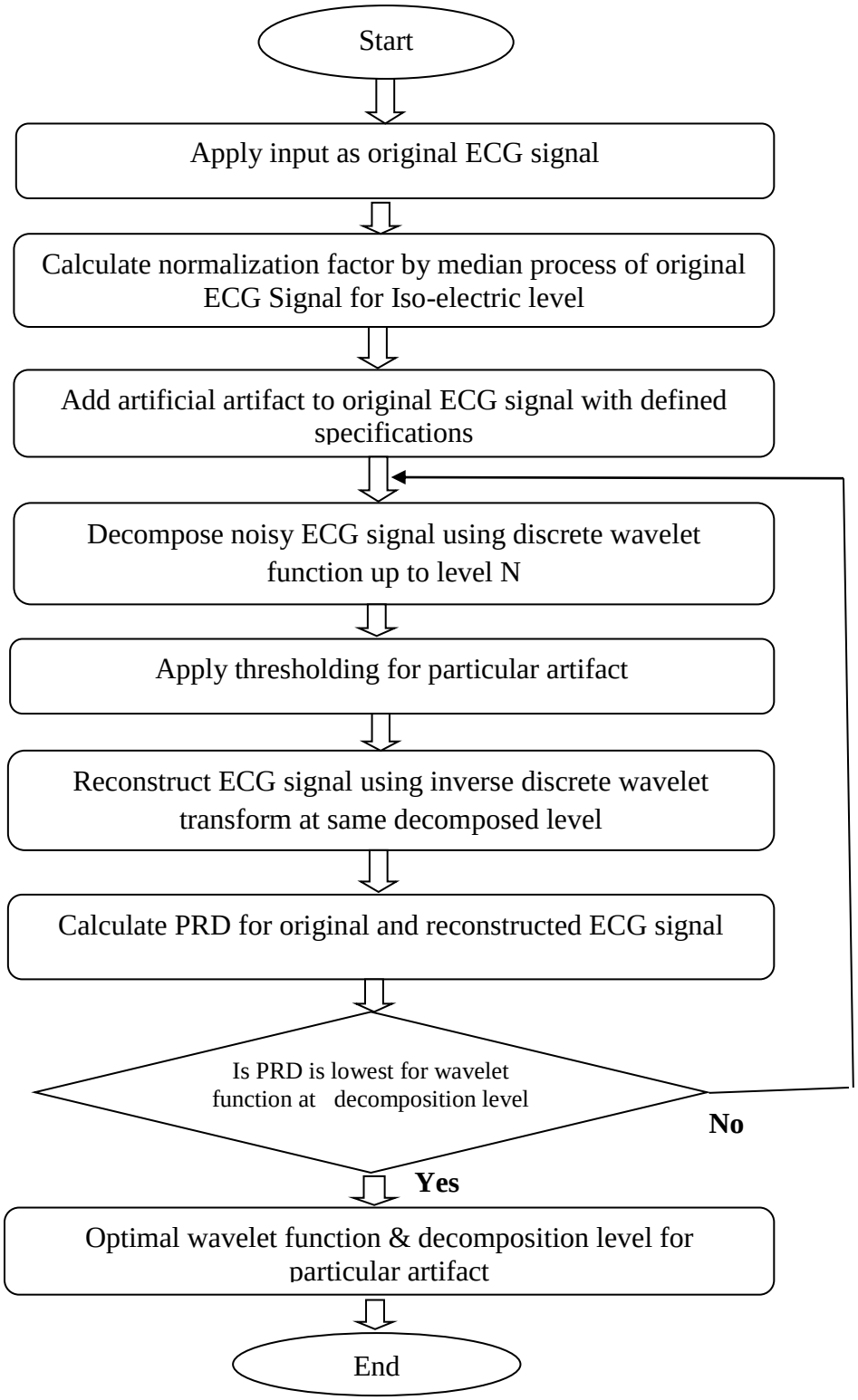

Figure 3.3: Flow Chart of algorithm for removal of artifacts in ECG signals

removal of baseline wander. Various wavelets at various decomposition levels db4 at 7^{th} , 8^{th}, 9^{th} and 10^{th} decomposition levels, db5, db5, db7 at 8^{th} decomposition levels , coif3 at 7^{th} and 8^{th} decomposition levels, coif4 at 7^{th} and 8^{th} decomposition levels, sym3 at 7^{th} , 8^{th} , 9^{th} and 10^{th} decomposition levels, sym4 at 7^{th} and 8^{th} decomposition levels have been employed. The rbio and biro families of wavelet are not found applicable for the removal of baseline wanders due to mismatch of these functions with baseline wandering ECG. The optimum value of wavelet function is db7 at 8^{th} level of decomposition having PRD of 0.1636% as shown in Figure 3.4. Table 3.1 shows the result of the various wavelet functions for calculating PRD for baseline wanders. Drifts-free signal is obtained. Moreover, the discarding of coefficients does not affect the original ECG signal morphology, particularly the ST segment, which is tremendously sensitive to the baseline wander [A. Kumar and M. Singh M, 2015; M.M. Beena et.al, 2014].

3.2.2 Removal of Power Line Interference

For removal of power line interference, we have taken 1,000 samples of ECG record (e0111) of European ST-T database of 250 Hz sampling frequency (x-axis is having no. of samples of record and y-axis is having voltage level in mV). For ECG normalization with respect to iso-electric line, median of ECG samples is taken and subtracted from original ECG, is called basic (noise free) signal. Then artificially generated sine wave of frequency 50 Hz is added to the original ECG signal in order to illustrate noisy signal as contaminated with PLI noise during recording from a human being because of specific reasons as discussed in earlier sections. The PLI contaminated ECG signal is decomposed for various wavelet functions at various decomposition levels. Then the value of sigma is found out for noise estimation, after that threshold factor is calculated by using sigma value. The hard thresholding technique has been applied for PLI by keeping the approximation coefficients at a value of two. Then reconstruction of a decomposed signal using the same wavelet function at the same decomposition level is performed. A particular wavelet function for which the reconstructed ECG signal is having close correlation of original ECG signal as well as having the lowest value of PRD is considered suitable for the removal of PLI, same as in the case of baseline wandering.

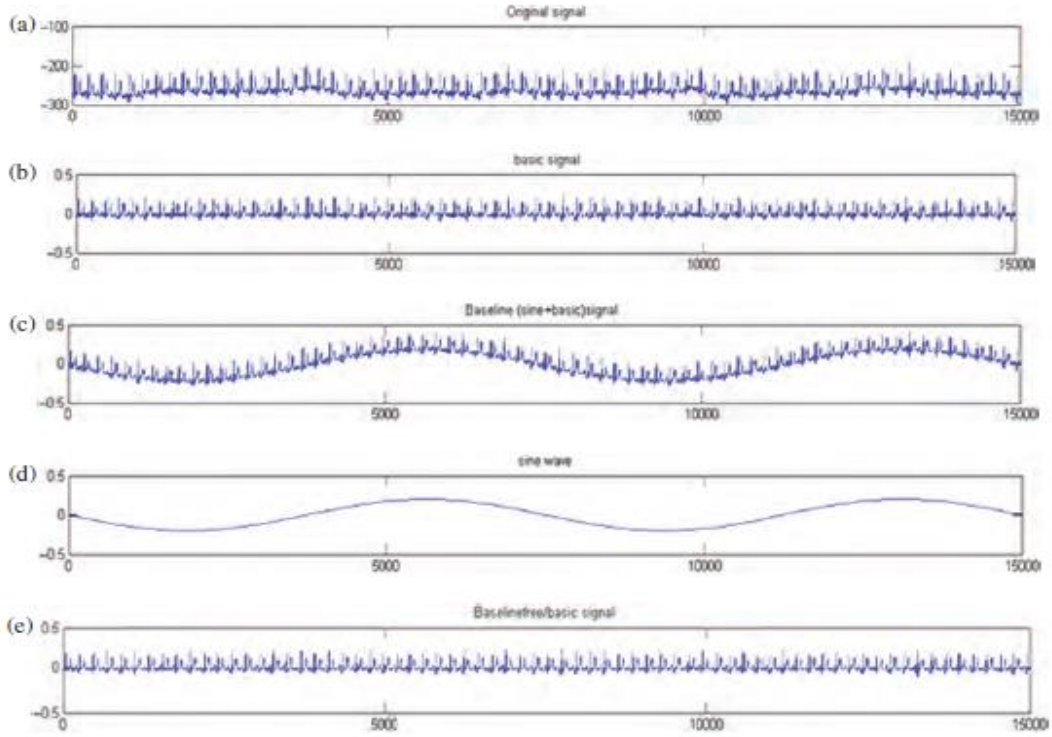

Figure 3.4: Results of artificial addition and removal of baseline wander for ECG signal, a) original ECG signal, b) ECG at iso-electric level, c) baseline wander contaminated ECG, d) estimated baseline, e) reconstructed ECG signal

Various wavelet functions at different decomposition levels are employed as sym3, sym4 at 8^{th} decomposition levels, sym5 at 6^{th}, 7^{th} and 8^{th} decomposition levels, coif4, coif3 and coif2 at 5^{th}, 6^{th}, 7^{th} and 8^{th} decomposition levels, db4, db5, db6, db7, db8 at 7th decomposition levels. The optimum value of wavelet function is coif2 at 5^{th} level of decomposition for PRD of 0.3980% as shown in Figure 3.5. The db, rbio and bior series families of wavelet are not found applicable for the removal of PLI, due to mismatch of these function with noisy ECG. Table 3.2 shows the performance of various wavelets for PRD for removal of PLI. The developed method has no destructive effects on the morphology of original ECG signal; all segments are giving exact values of intervals as before the decomposition [A. Kumar and M. Singh M, 2015; M.M. Beena et.al, 2014].

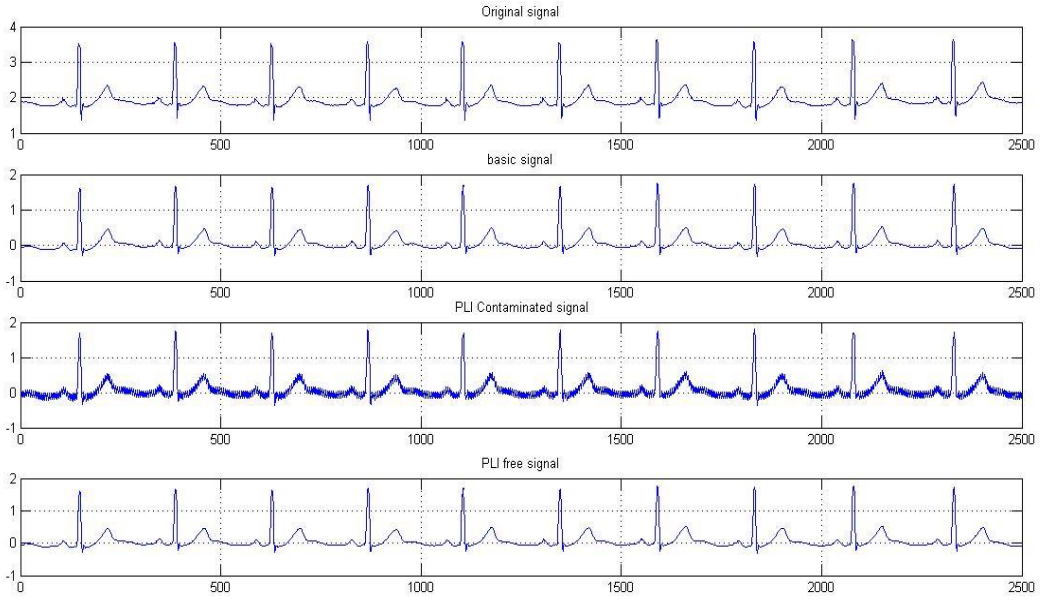

Figure 3.5: Results of artificial addition and removal of power line interference (PLI) for ECG signal, a) original ECG signal, b) ECG at iso-electric level, c) PLI contaminated ECG, d) reconstructed ECG signal

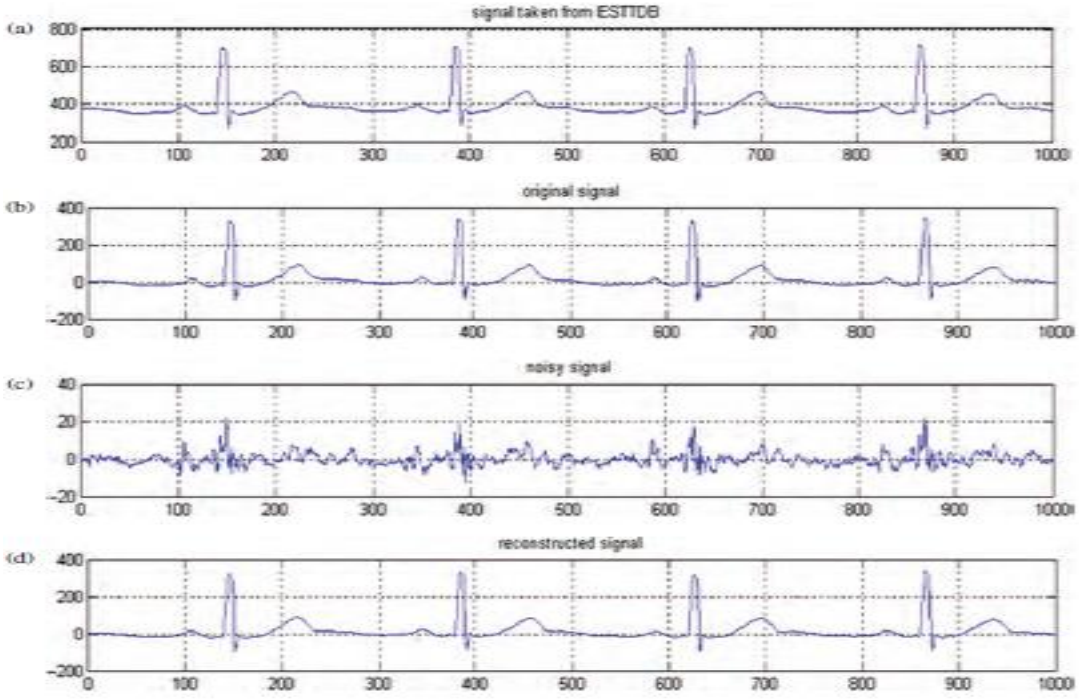

Figure 3.6: Results of artificial addition and removal of muscle tremors for ECG signal, a) original ECG signal, b) ECG at iso-electric level, c) muscle tremors contaminated ECG, d) reconstructed ECG signal

3.2.3 Removal of Muscle Tremors

For muscle tremor algorithm, we have taken 1000 samples of ECG record (e0111) of European ST-T database of 250 Hz sampling frequency (x-axis is having no. of samples of record and the y-axis is showing a voltage level in mV). The same procedure is adopted for normalization, as for above mentioned artifacts. We multiply the original ECG signal with white noise of ±1V, available in MATLAB to the original signal in order to illustrate ECG signal contaminated with muscle noise during recording from a human being because of specific reasons. The muscle tremor corrupts all segments of the ECG signal in real practices during recording. The muscle tremors contaminated ECG signal is decomposed for various wavelet functions at various decomposition levels. The value of sigma is found for noise estimation and then the value of the threshold is being calculated by sigma value. The soft thresholding technique has been applied while keeping the approximation coefficients at the value of one. The reconstruction takes place at the same level of decomposition by same wavelet function. The various wavelet functions are employed as sym4 at 6th, 7th and 8th decomposition levels, sym3 at 8^{th} decomposition levels, coif3 and coif4 at 6th, 7th and 8th level, db4, db5, db6, db7, db8 at 6th, 7th and 8th decomposition levels, rbio1.1, rbio1.3, rbio1.5 at 8th level, rbio2.2 at 9th, bior1.2 at 7th, bior1.3 at 8th and bior1.5 at 7th decomposition level. The optimum value of wavelet function PRD is 0.8959% for db7 at 8^{th} level of decomposition of this artifact is shown in Figure 3.6. The sym3, rbio and bior series families of wavelet are not found applicable for the removal of PLI; the reason for the same is due to the mismatch of these functions with noisy ECG. As in the case of power line interference, a particular wavelet function is considered to be suitable for removal of muscle tremor, which is having close correlation for original ECG with reconstructed signal as well as having lowest value of PRD. The performance of various wavelet functions at various decomposition levels for the removal of artificially added muscle noise has been presented in Table 3.3. The developed method has no adverse affect on the morphology of original ECG signal; all peaks and segments are having same values as before decomposition [A. Kumar and M. Singh M, 2015; M.M. Beena et.al, 2014].

Table 3.1: PRD values of various wavelets for removal of baseline wandering

Sr. No.	Wavelet Function	Decomposition Level	PRD (%)
1	db4	7	1.1421
2	db4	8	1.1418
3	db4	9	2.4433
4	db4	10	2.8017
5	db5	8	0.9623
6	db6	8	0.2137
7	**db7**	**8**	**0.1636**
8	coif3	8	0.8647
9	coif3	7	0.5066
10	coif4	7	0.6387
11	coif4	8	1.3986
12	sym3	7	1.2152
13	sym3	8	0.8972
14	sym3	9	0.6676
15	sym3	10	3.8274
16	sym4	8	1.0321
17	sym4	7	1.1155
18	rbio 1.1	7	N.A.
19	rbio 1.3	6	N.A.
20	rbio 1.5	7	N.A.
21	bior 1.1	6	N.A.
22	bior 1.3	6	N.A.
23	bior1.5	6	N.A.

Table 3.2: PRD values for various wavelets for removal of power line interference

Sr. No.	Wavelet Function	Decomposition Level	PRD (%)
1	coif4	8	0.3994
2	coif4	7	0.3994
3	coif4	6	0.3994
4	coif4	5	0.3994
5	coif3	8	0.4042
6	coif3	7	0.4042
7	coif3	6	0.4042
8	coif3	5	0.4042
9	coif2	8	0.3985
10	coif2	7	0.3983
11	coif2	6	0.3982
12	**coif2**	**5**	**0.3980**
13	db4	7	N.A.
14	db5	7	N.A.
15	db6	7	N.A.
16	db7	7	0.4226
17	db8	7	0.4420
18	db8	8	0.4420
19	sym3	8	N.A.
20	sym4	8	0.4021
21	sym5	8	N.A.
22	sym5	7	N.A.
23	sym5	6	N.A.
24	rbio 1.1	7	N.A.
25	rbio 1.3	6	N.A.
26	rbio 1.5	6	N.A.
27	bior 1.1	6	N.A.

28	bior 1.3	6	N.A.

Table 3.3: PRD values for various wavelets for removal of muscle tremors

Sr. No.	Wavelet Function	Decomposition Level	PRD (%)
1	coif4	8	0.9243
2	coif4	7	0.9263
3	coif4	6	0.9429
4	coif3	7	0.9140
5	coif3	6	0.9321
6	coif3	8	0.9113
7	sym3	8	N.A.
8	sym4	8	0.9169
9	sym4	7	0.9231
10	sym4	6	0.9379
11	db4	6	0.940
12	db4	7	0.9289
13	db4	8	0.9234
14	db5	8	0.9141
15	db5	7	0.9214
16	db5	6	0.9289
17	db6	6	0.9212
18	db6	7	0.9052
19	db6	8	0.8978
20	**db7**	**8**	**0.8959**
21	db7	7	0.9017
22	db7	6	0.9174
23	db8	6	0.9474
24	db8	7	0.9347
25	db8	8	0.9303

26	rbio1.1	8	N.A
27	rbio1.3	8	N.A
28	rbio1.5	8	N.A
29	rbio2.2	9	N.A
30	bior1.2	7	N.A
31	bior1.3	8	N.A
32	bior1.5	7	N.A

3.3 Comparison with Existing Methods

The various techniques are available in literature for removal of baseline wander, PLI & muscle tremors. The least mean square adaptive (LMS) method is mostly preferred, but this method is not capable of tracking the non stationary, QRS complex parameters [M. Merri et.al, 2012; N. V. Thakor, 1991]. The developed method overcomes the problems stated above and it preserves the small frequency waves of ECG (P and T wave) as analyzed by Dhono's method. There are more advantages of wavelet transforms over conventional techniques for baseline removal. Not only it is capable of eliminating the drifts, but also overcomes the problems mentioned in [K. Daqrouq, 2005]. Similarly, K. Daqrouq et.al has compared the values of PRD for moving average filter and median filter 0.9% & 1.65% respectively for ECG de-noising within a spectral band of frequency equal to 0.5-45 Hz and by using FIR filter, PRD is 0.511[K. Daqrouq and I.N. Qawasmi, 2008]. Likewise, M. Alfaouri et.al report is having PRD of 2.3243 for 8.2647 SNR using Donoho's relation and 0.4393 for 6.3674 SNR for filtration [M. Alfaouri and K. Daqrouq, 2008]. The proposed method is having the lowest value of PRD of 0.3980 for coif2 wavelet function at 5th decomposition level for filtration. The presented method gives more remarkable results than the notch filter [M.S. Chavan et.al, 2008] & finite impulse response (FIR) filter [V. J. A. Alste et.al, 1985] for removal of PLI. This method also addresses the issue of sensitivity to small changes in either the original signal or in the artifact, unless the basis-functions are trained on ECG signal as generated by neural networks [J. Mateo et.al, 2008] & PCA [M.P.S. Chawla, 2011]. Table 3.4 presents the comparison for performance evaluation with existing methods in literature for removal of baseline wanders in terms PRD.

Table 3.4: Performance evaluation of presented method for removal of artifacts

Sr. No.	Method	PRD (%)
1	Donoho's [S. Mukhopadhyay et.al, 1995]	0.187
2	FIR [M. Alfaouri, K. Daqrouq, 2008]	0.511
3	Presented method	0.1636

3.4 Preprocessing of ECG signals for Ischemia Detection

The ST segment is low amplitude and frequency segment in ECG signal. The main goal of pre- processing is to formalize the accurate and efficient delineation process. Total 10 representative records (e0103, e0104, e0105, e0108, e0113, e0114, e0147, e0159, e0162, e0206) have been processed for total eleven hours duration. Further, the portion under investigation is broken into segments of one minute each. A generalized diagram for wavelet transformation process for these pre-processing has been shown in Figure 3.7 and frequency corresponding to different artifacts after wavelet decomposition have been shown in Figure 3.8.

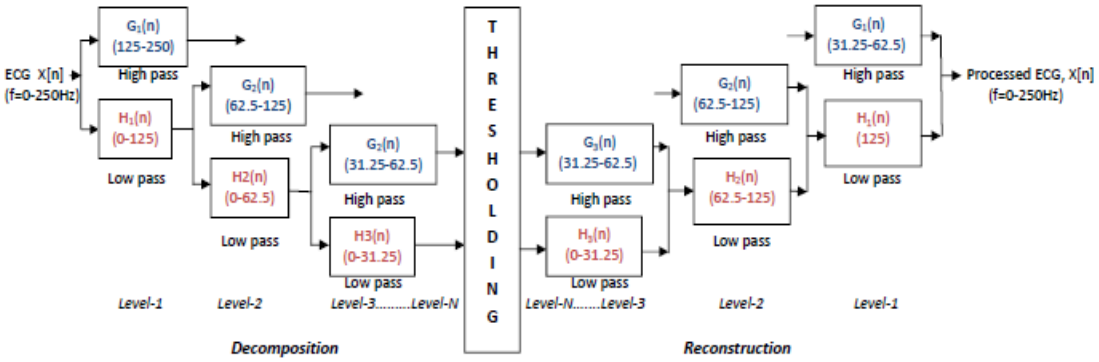

Figure 3.7: Wavelet transformation process for removal of artifacts in ECG records of European ST-T database

3.4.1 Removal of Baseline Wandering

The baseline wandering may be categorized as; the DC component which can be interpreted as TP or PQ segment voltage in ECG signal and the second involves baseline drift, a low frequency noise in the range of 0.5-1Hz. For elimination of DC component, mean of one minute ECG record samples is subtracted from original ECG signal. Then the ECG signal is decomposed to 8^{th} level using daubechies (db4) wavelet transform for

removal base line wander. As the baseline wanders lies usually in the frequency range of 0.5-1 Hz. Thresholding is applied after that. Thresholding involves the discarding of approximation coefficients to zero at the 8^{th} decomposition level followed by reconstruction [A. Kumar and M. Singh M, 2015; M.M. Beena et.al, 2014]. The db4 wavelet function is found suitable for removal of baseline wanders. The results in elimination of baseline wanders for 10 representative records of European ST-T database are shown in Figures 3.9 to 3.18.

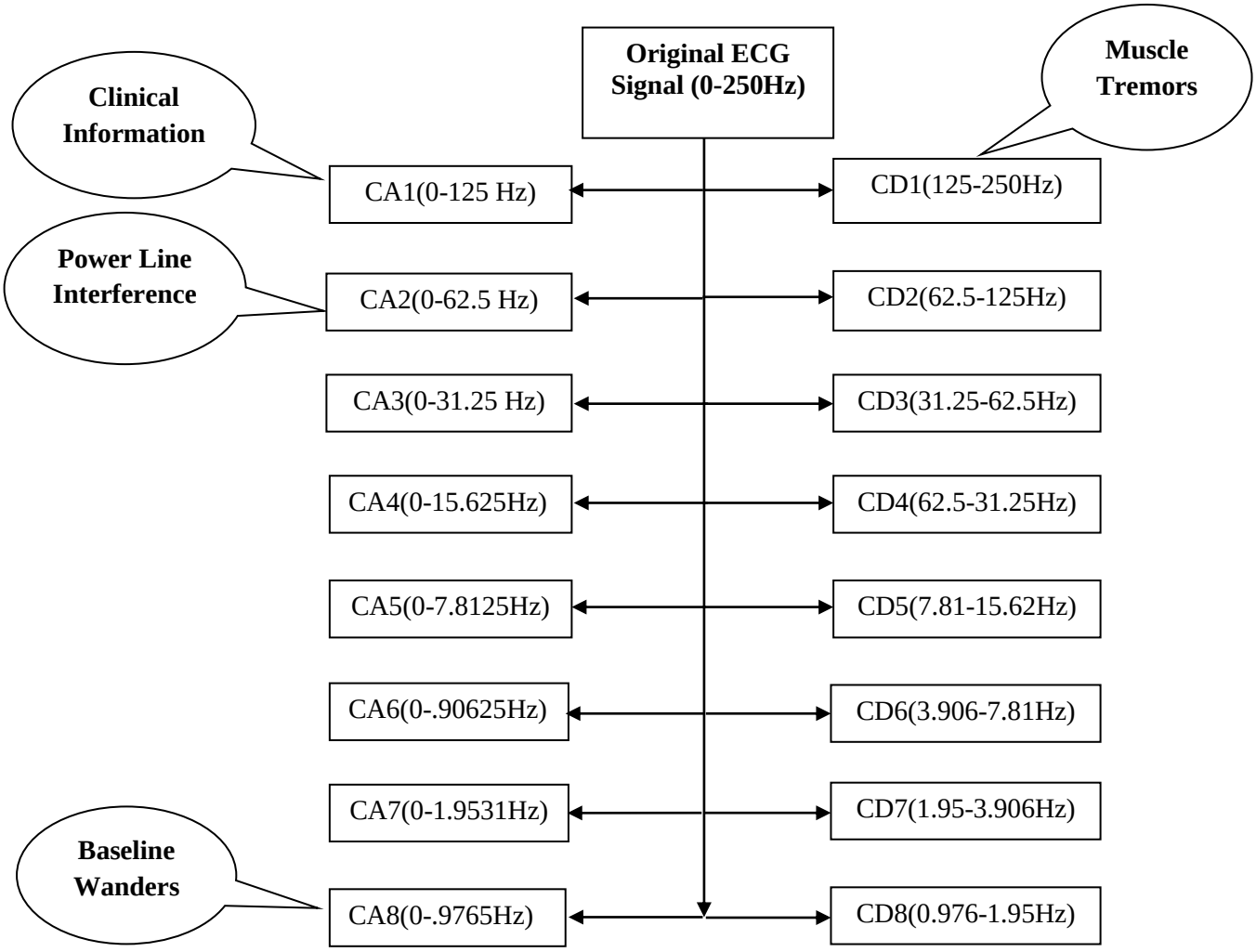

Figure 3.8: Frequency components of artifacts in wavelet decomposed ECG signals for European ST-T database

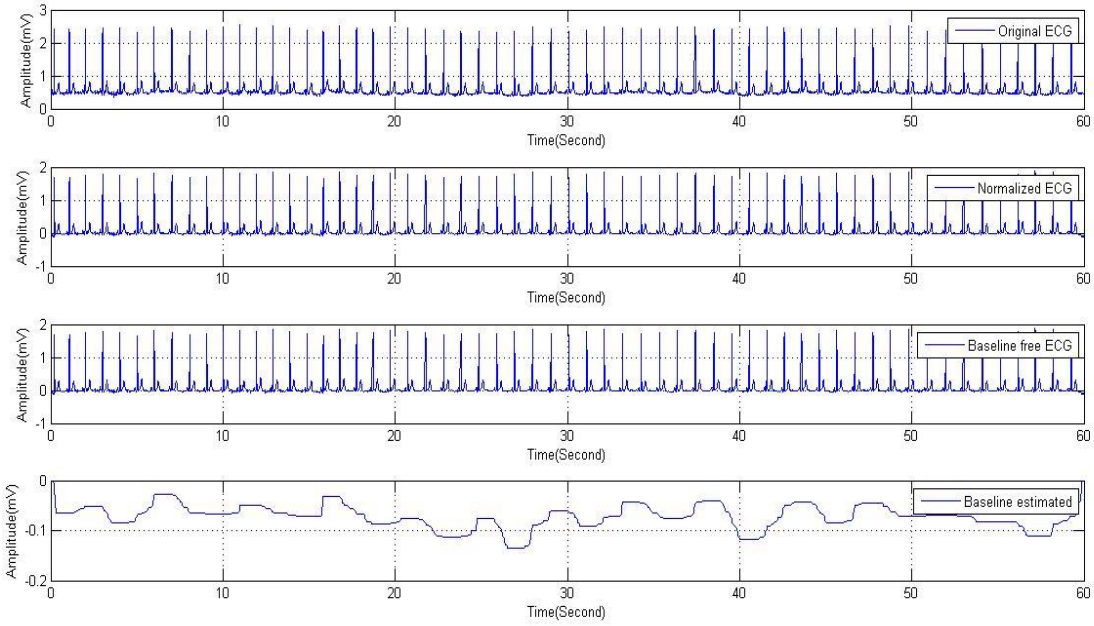

Figure 3.9: Results for removal of baseline wandering in e0103 record

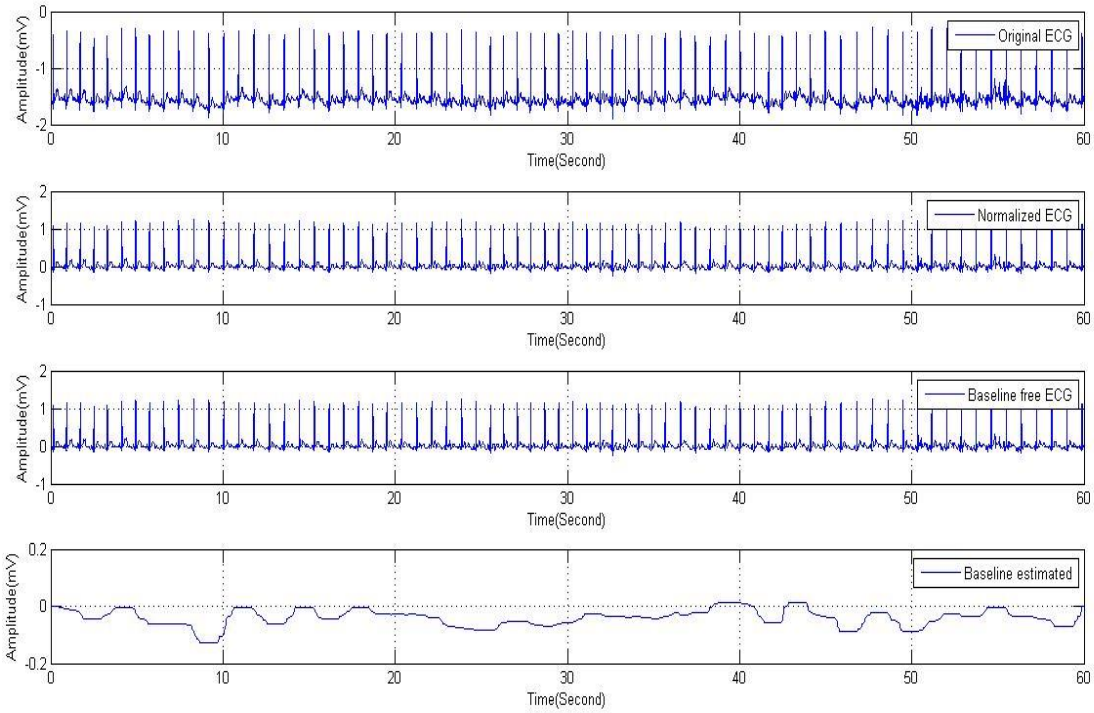

Figure 3.10: Results for removal of baseline wandering in e0104 record

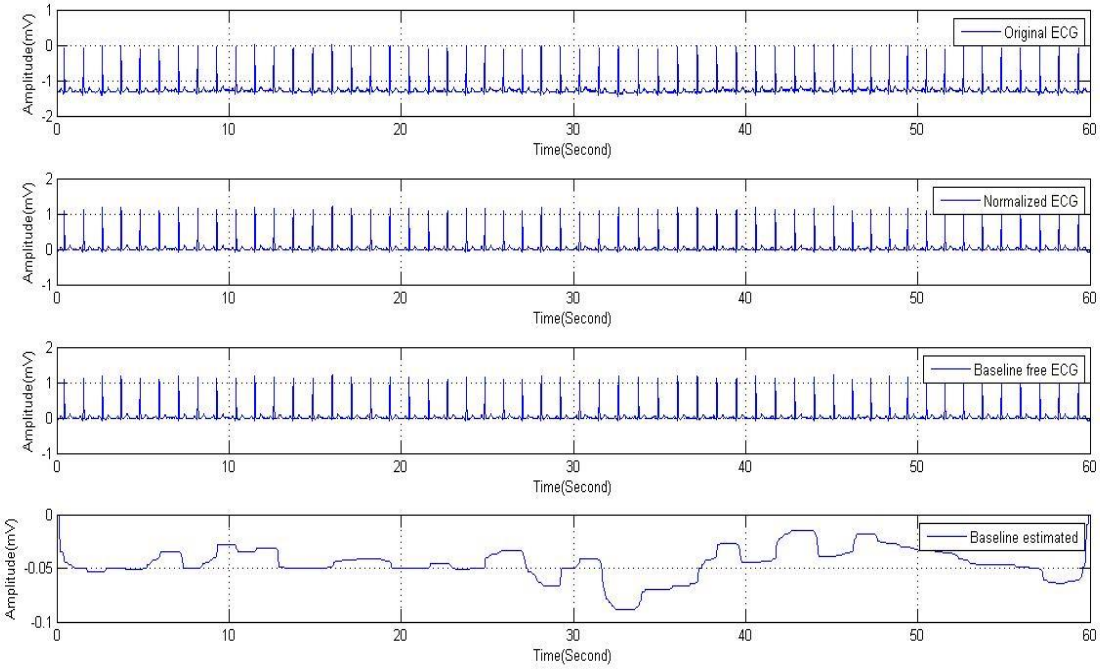

Figure 3.11: Results for removal of baseline wandering in e0105 record

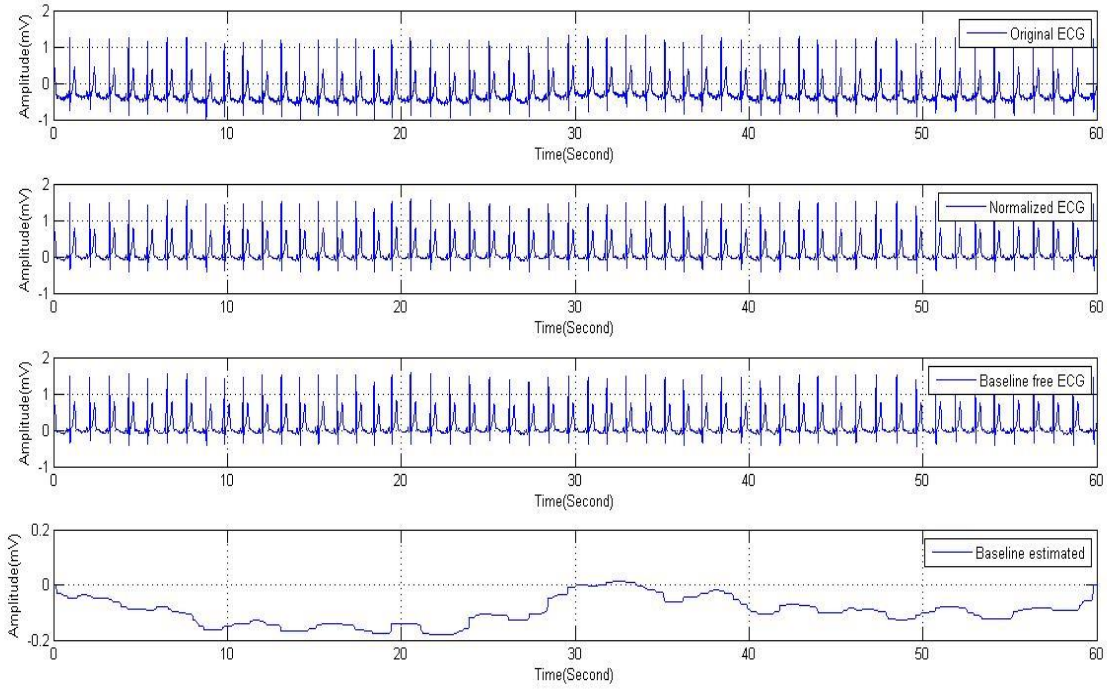

Figure 3.12: Results for removal of baseline wandering in e0108 record

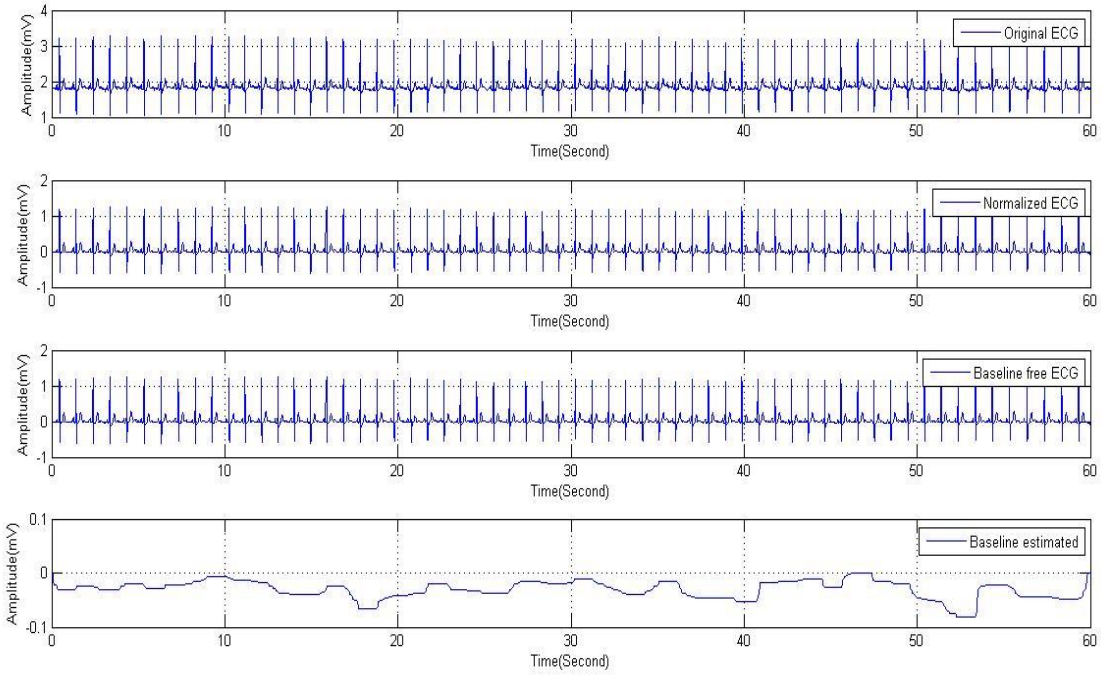

Figure 3.13: Results for removal of baseline wandering in e0113 record

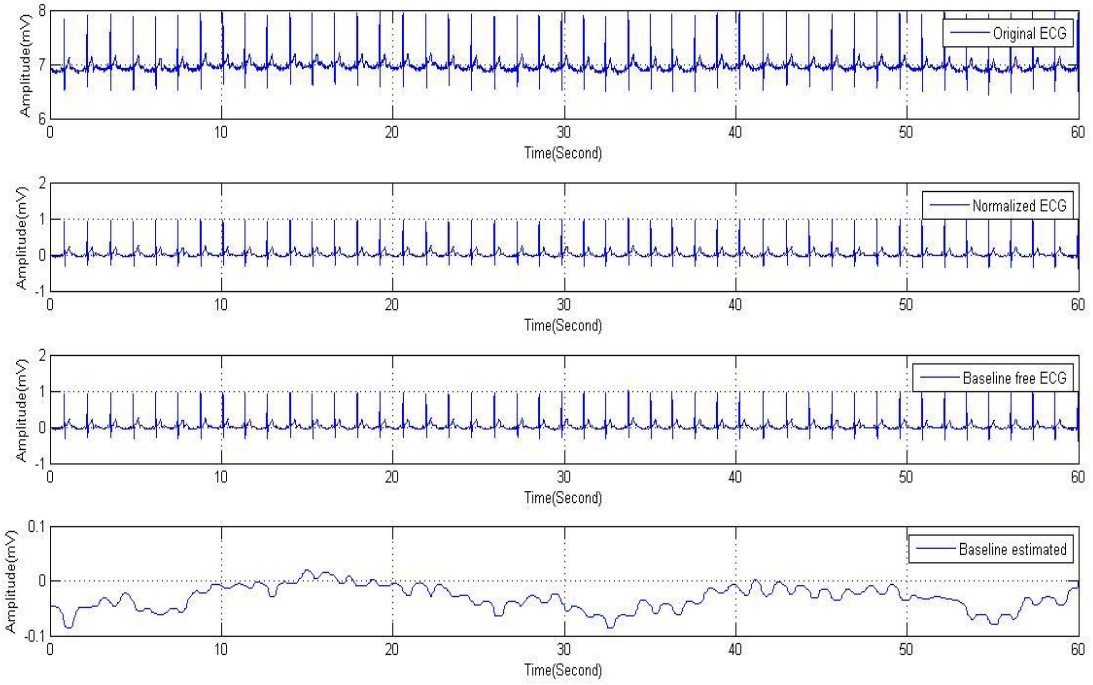

Figure 3.14: Results for removal of baseline wandering in e0114 record

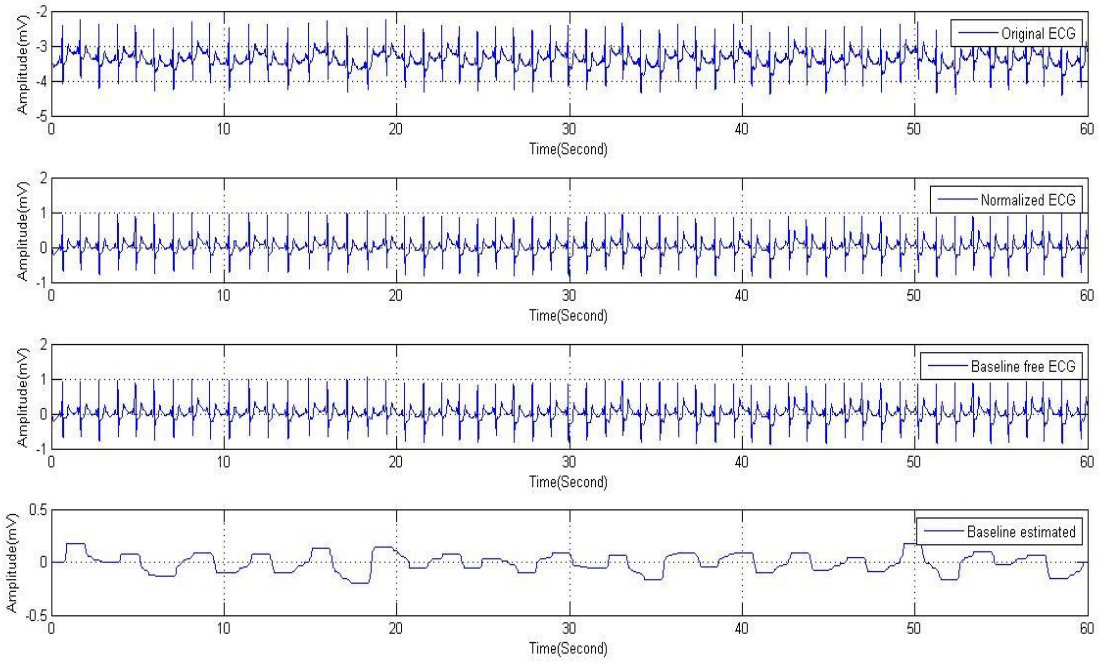

Figure 3.15: Results for removal of baseline wandering in e0147 record

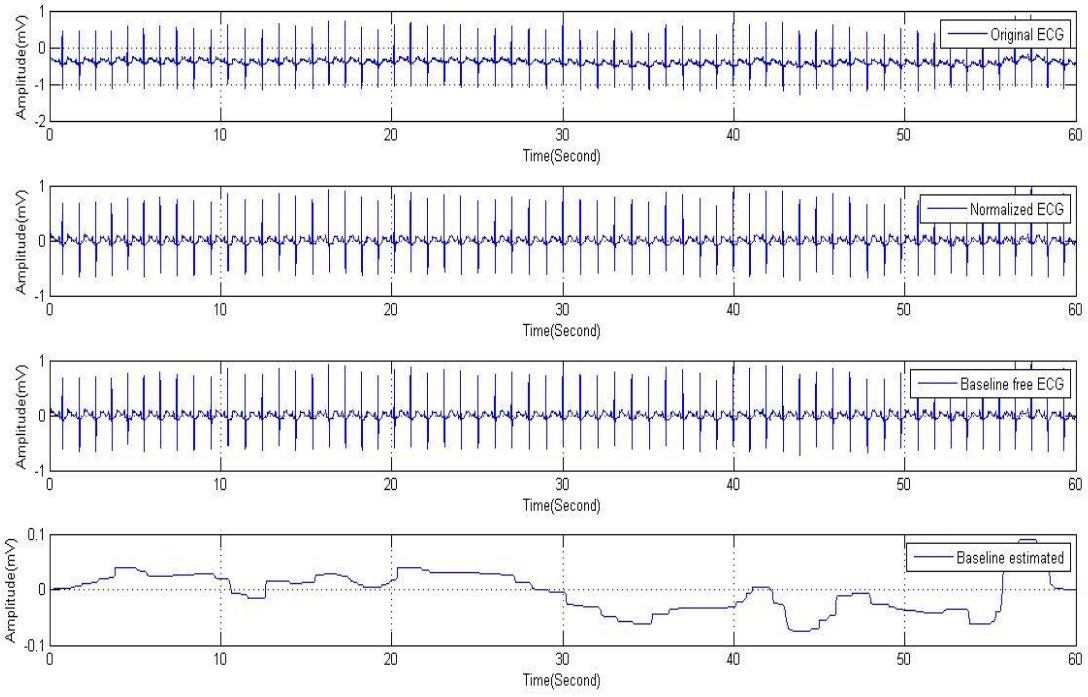

Figure 3.16: Results for removal of baseline wandering in e0159 record

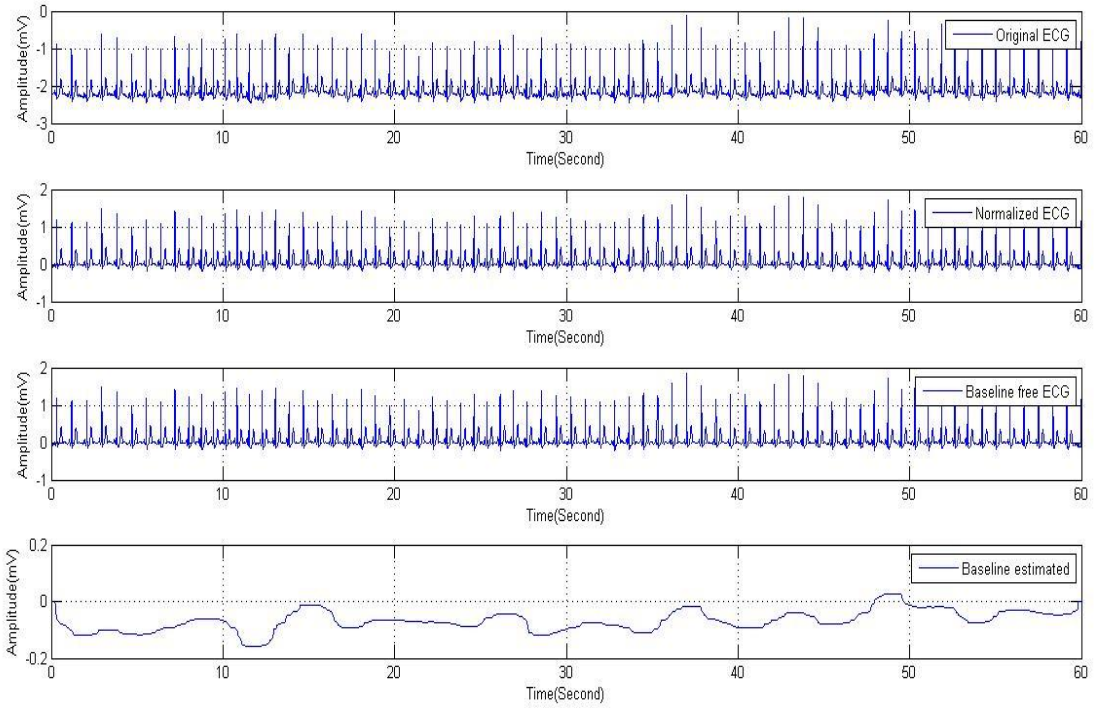

Figure 3.17: Results for removal of baseline wandering in e0162 record

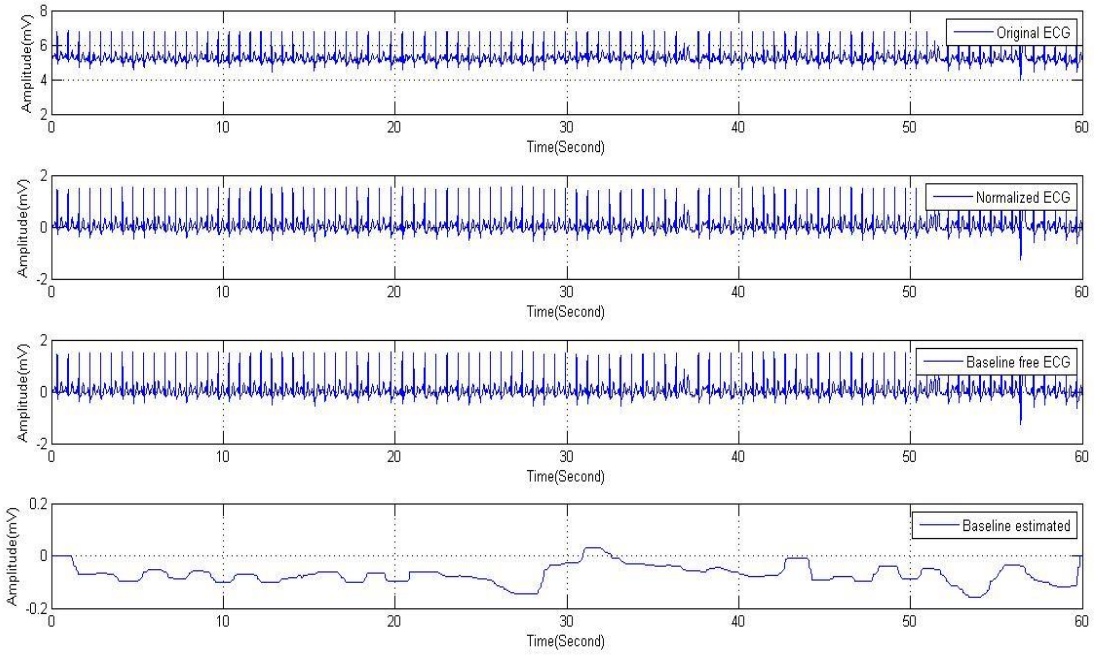

Figure 3.18: Results for removal of baseline wandering in e0206 record

3.4.2 Removal of Muscle Tremors

During recording, a low amplitude muscle tremors of skeletal are incorporated in ECG, often. This artifact mimics the iso-electric line in ECG signals. Coif-let (Coif4) wavelet function at 1st level of wavelet decomposition is found more suitable for removal of these noises in the frequency range of 100-150 Hz. Firstly the noise is estimated in the approximate coefficients of 1st level of ECG signal and is named as sigma and then the threshold is deliberated by using this sigma value. The soft thresholding technique [A. Kumar and M. Singh M, 2015; M.M. Beena et.al, 2014] has been applied for the discarding of detail coefficients while maintaining the approximation coefficients at unity value. After removal of these noises the ECG signal appears in the range of 0 to 125 Hz. The results of these noises removals in 10 representative records of European ST-T database are shown in figures 3.19 to 3.28.

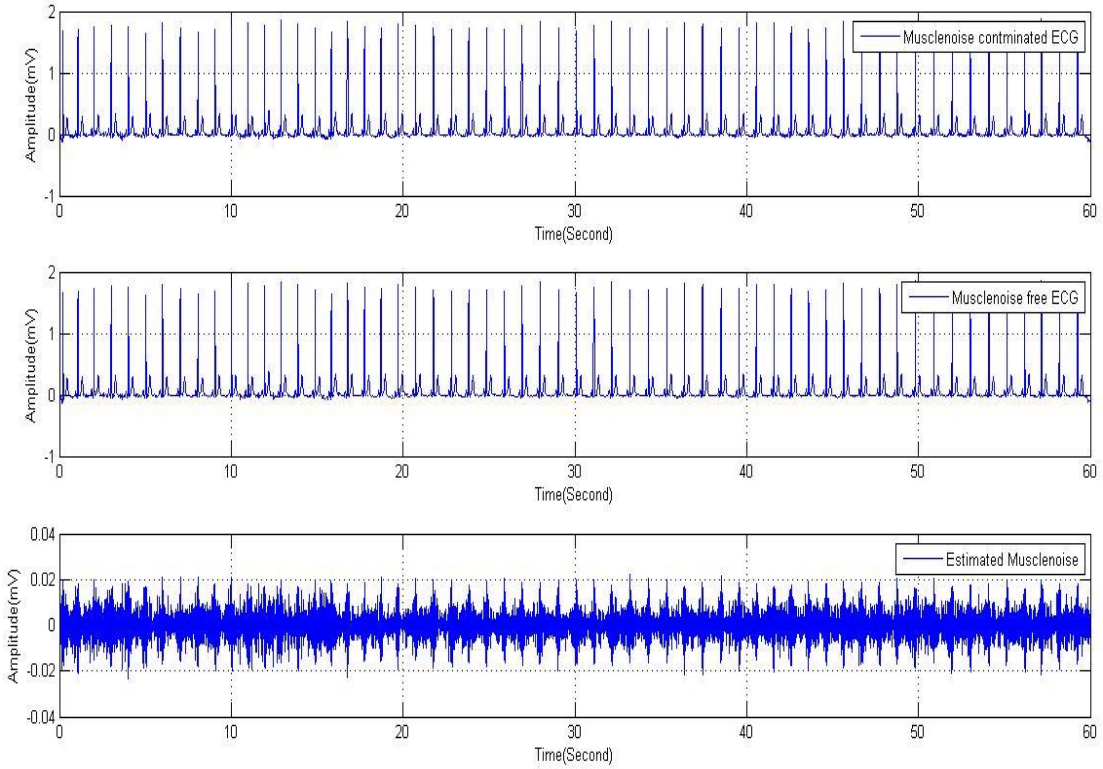

Figure 3.19: Results for removal of muscle tremors in e0103 record

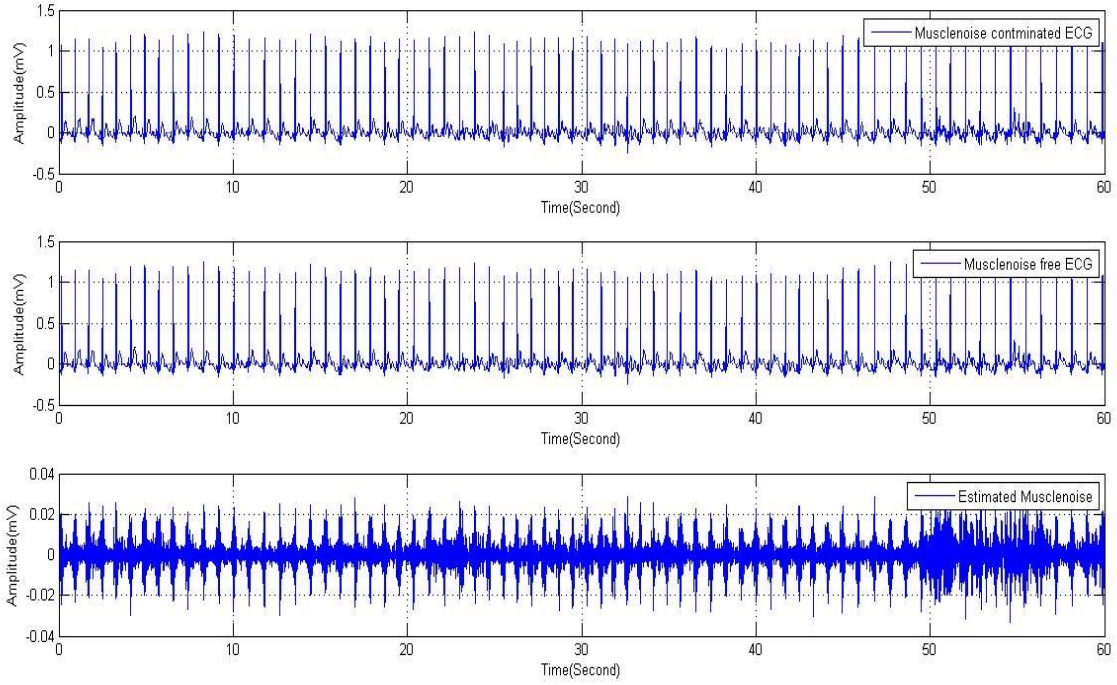

Figure 3.20: Results for removal of muscle tremors in e0104 record

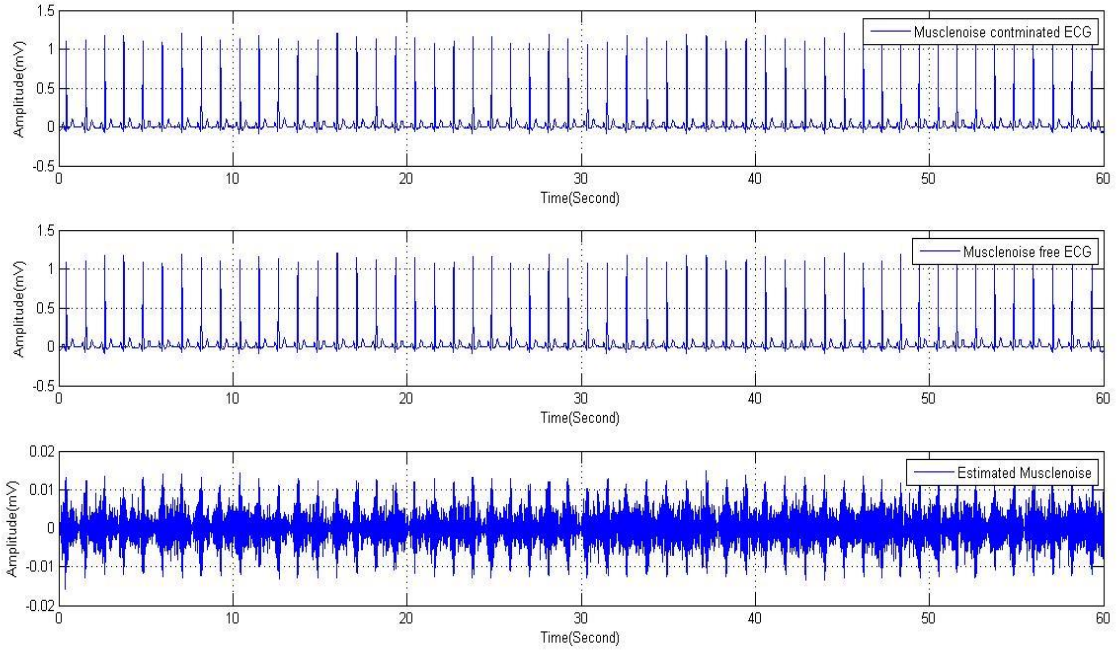

Figure 3.21: Results for removal of muscle tremors in e0105 record

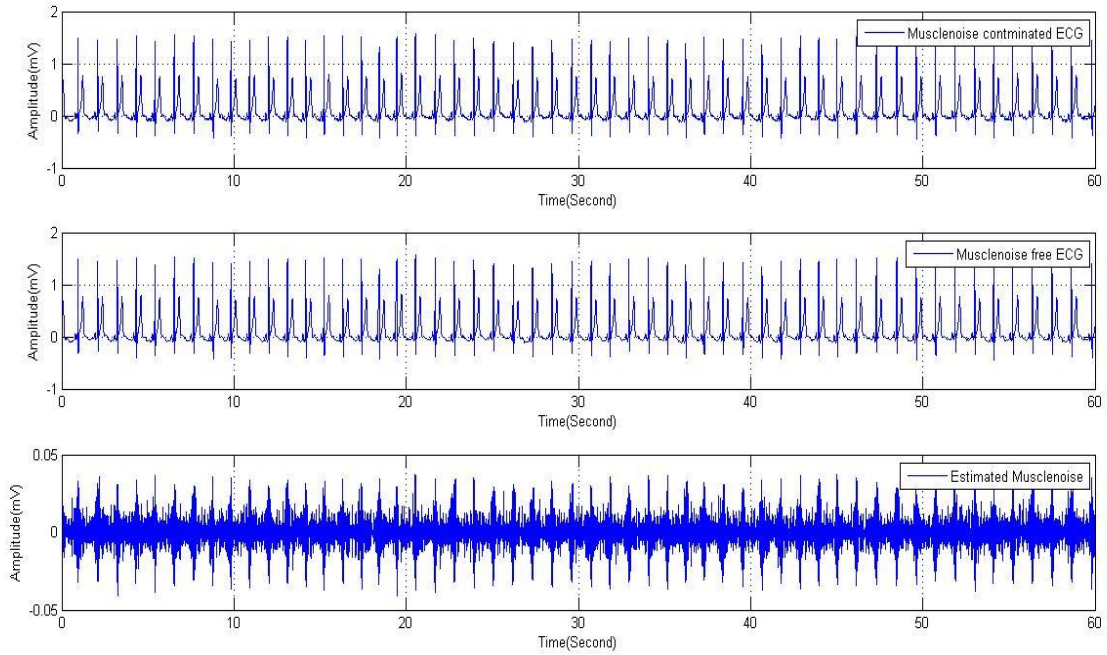

Figure 3.22: Results for removal of muscle tremors in e0108 record

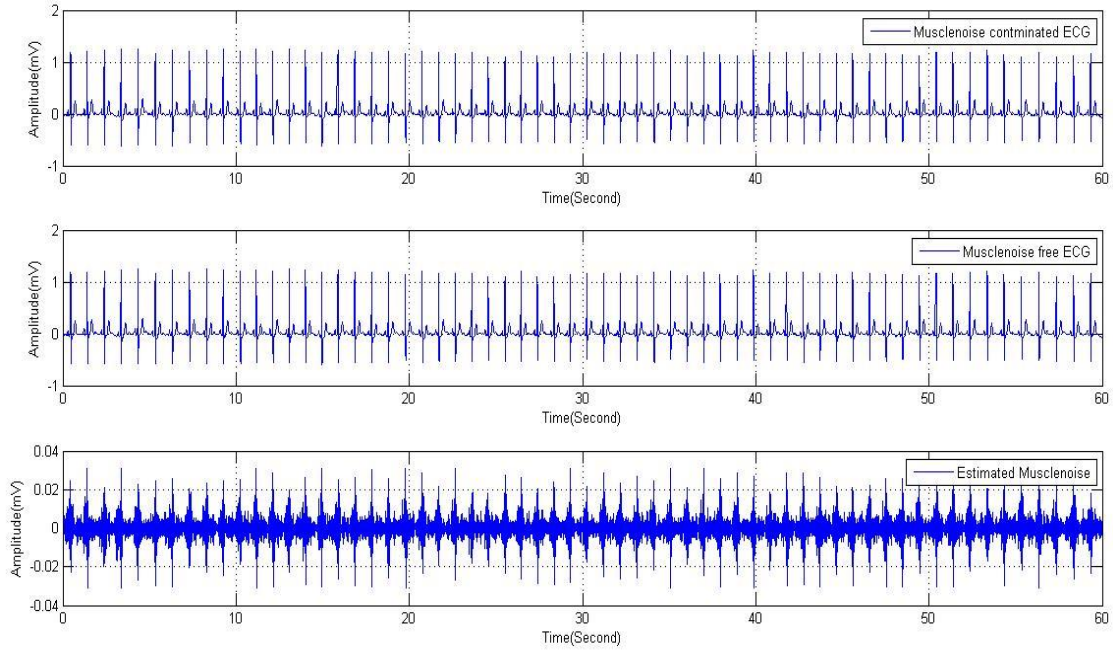

Figure 3.23: Results for removal of muscle tremors in e0113 record

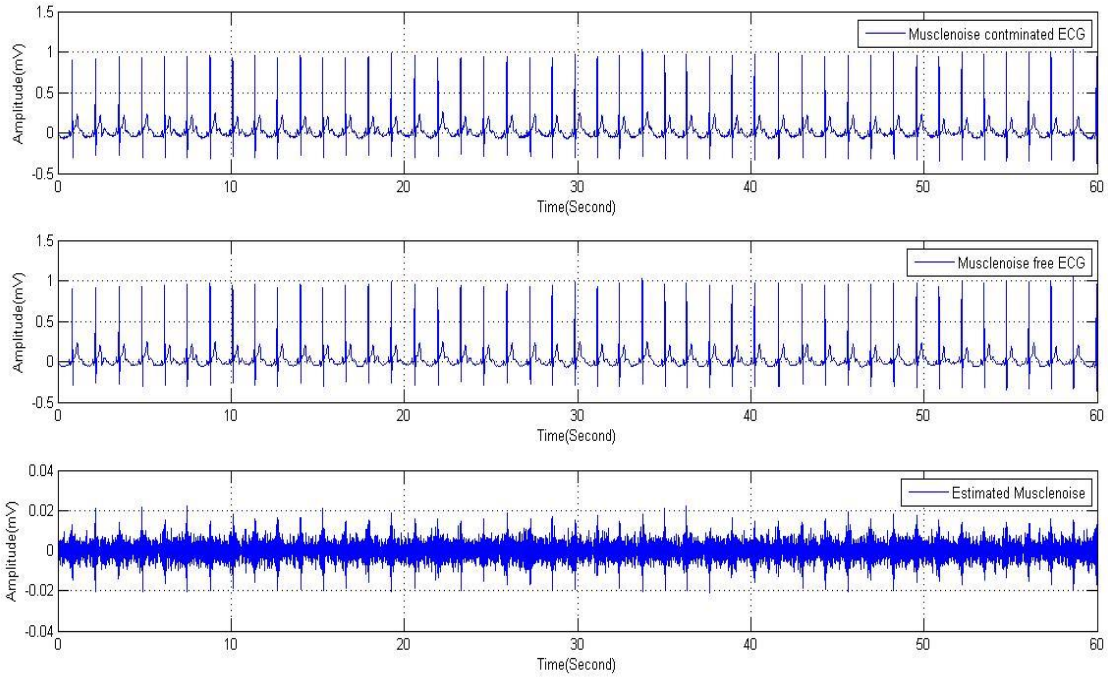

Figure 3.24: Results for removal of muscle tremors in e0114 record

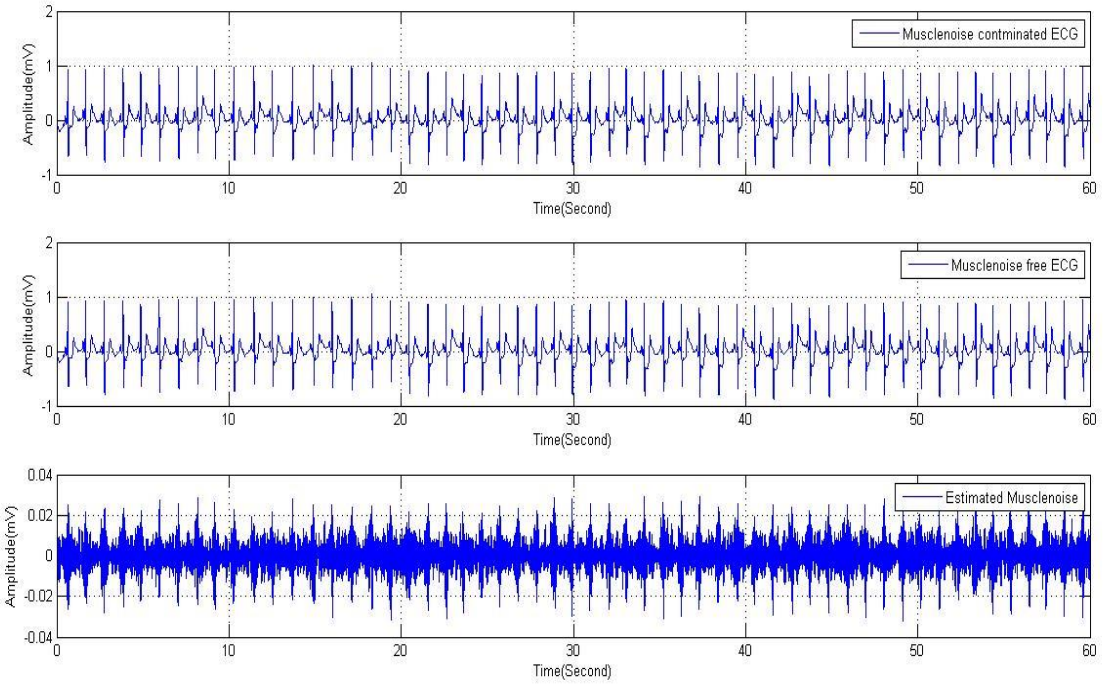

Figure 3.25: Results for removal of muscle tremors in e0147 record

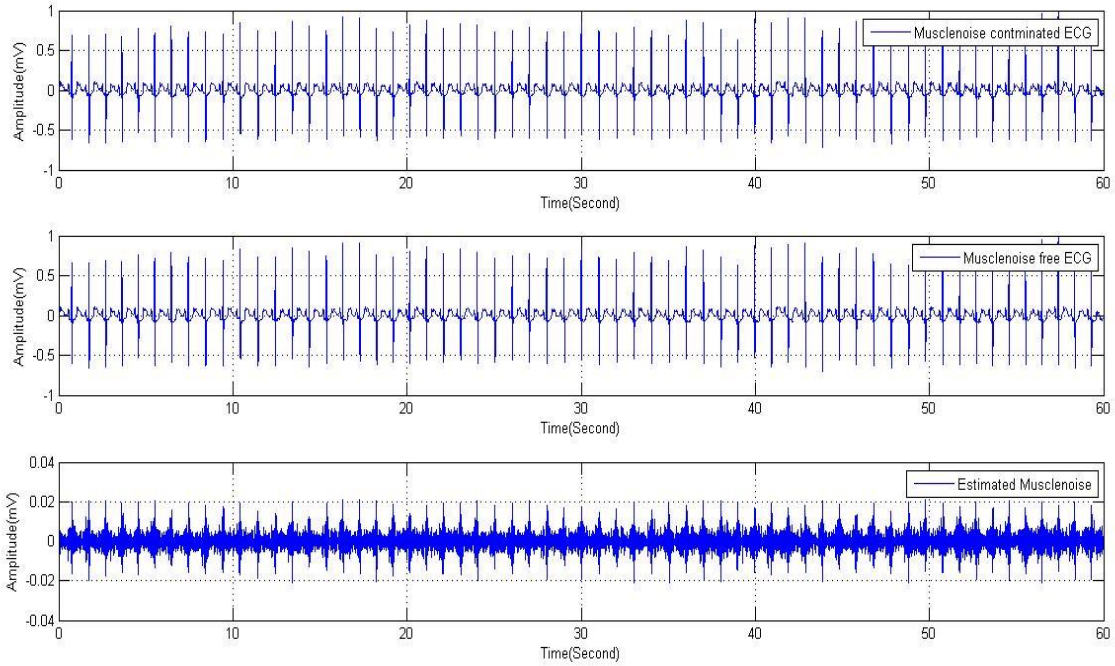

Figure 3.26: Results for removal of muscle tremors in e0159 record

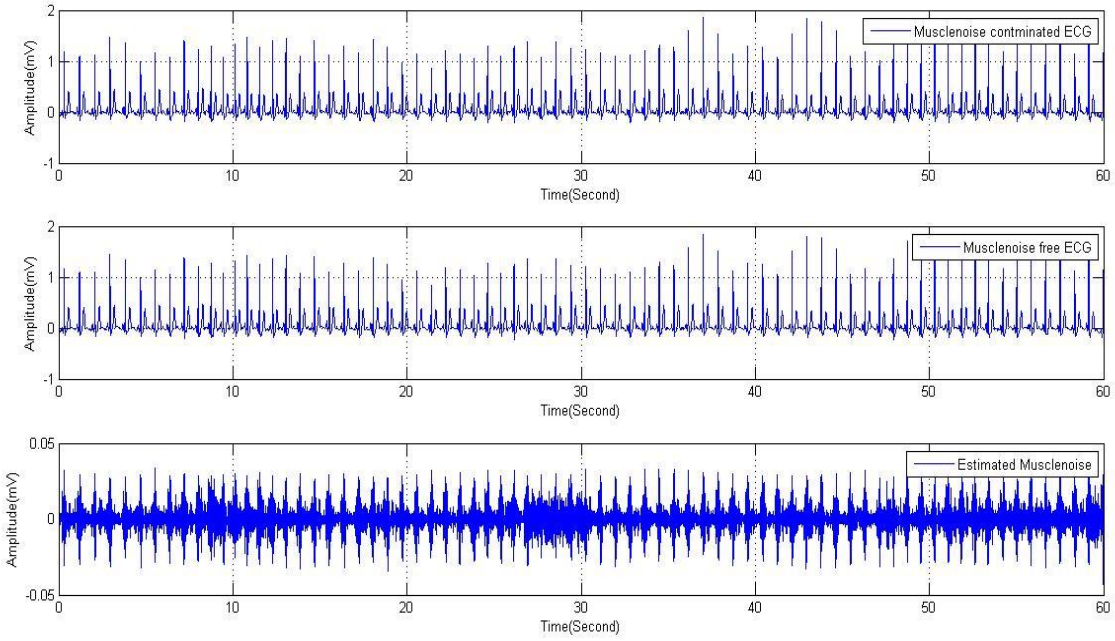

Figure 3.27: Results for removal of muscle tremors in e0162 record

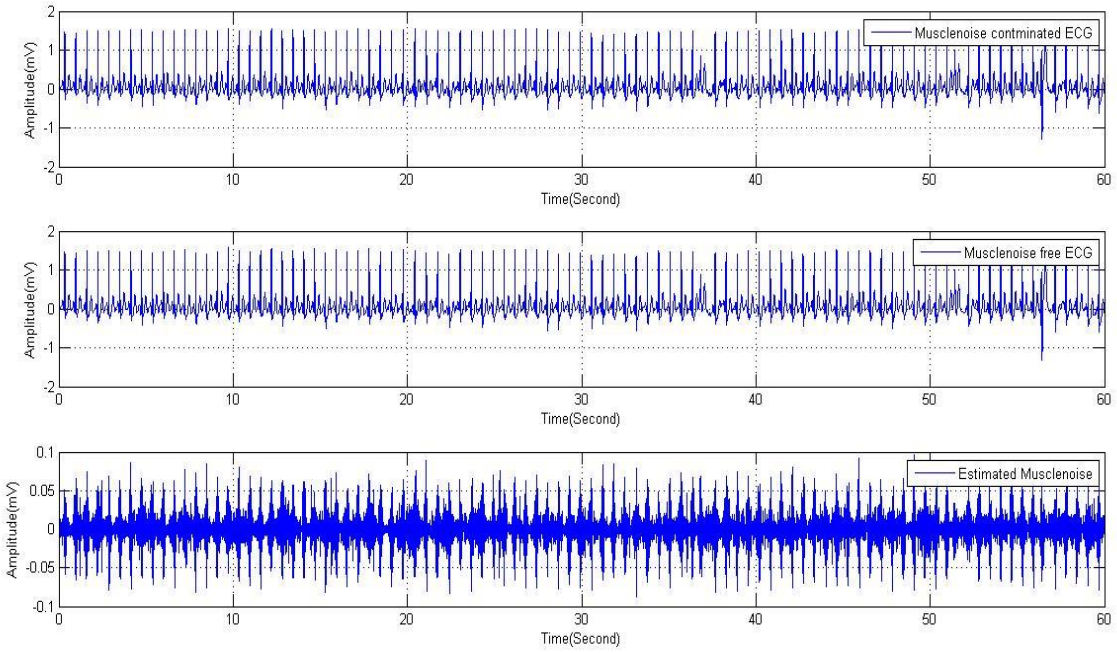

Figure 3.28: Results for removal of muscle tremors in e206 record

3.4.3 Removal of Power Line Interference (PLI)

During recording, power line interference is contaminated in ECG, if appropriate filters are not equipped with ECG recording machine. Symlet (Sym3), wavelet function at 2nd level of wavelet decomposition is found more suitable for removal of this artifact for a frequency of 50 Hz. Firstly the noise is estimated in the approximate coefficients of the 2nd decomposed level of ECG signal and is named as sigma and then the threshold is deliberated by using this sigma value. The hard thresholding technique [A. Kumar and M. Singh M, 2015; M.M. Beena et.al, 2014] has been applied for the discarding of detail coefficients while maintaining the approximation coefficients at unity value. The results of this noise removal in 10 representative records of European ST-T database are shown in figures 3.29 to 3.38.

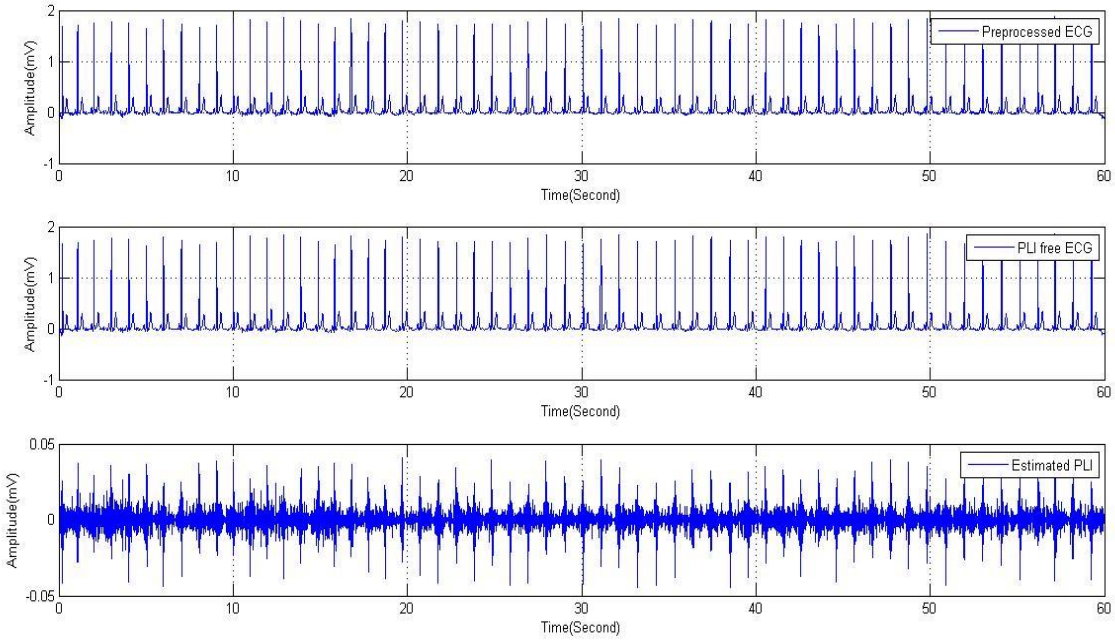

Figure 3.29: Results for removal of power line interference in e0103 record

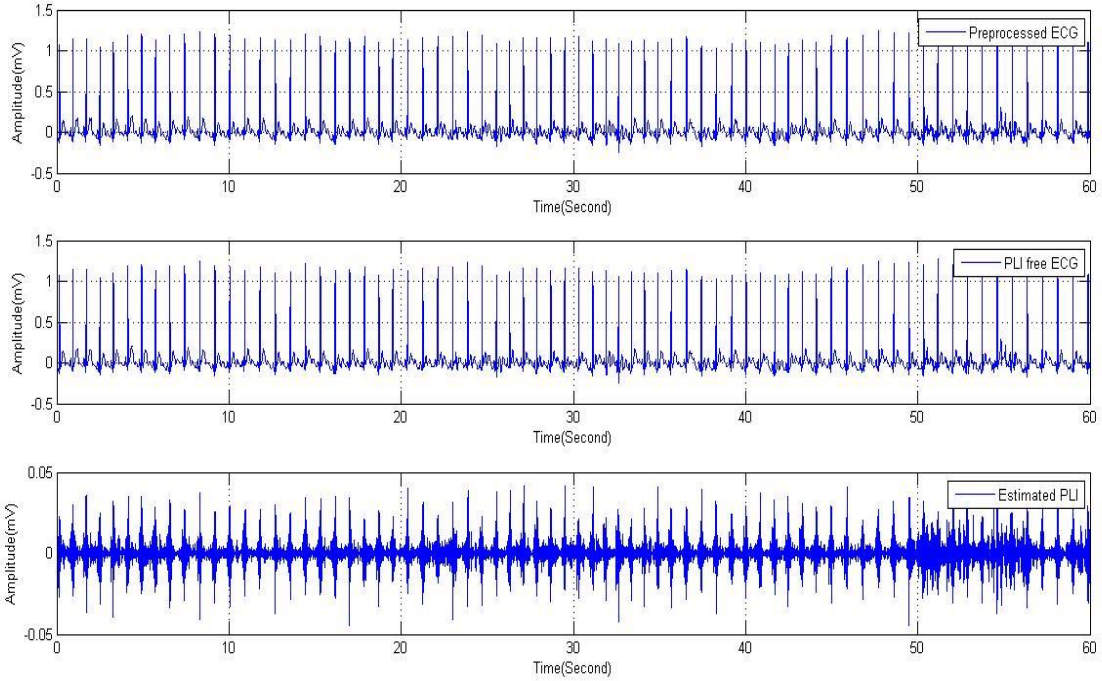

Figure 3.30, Results for removal of power line interference in e0104 record

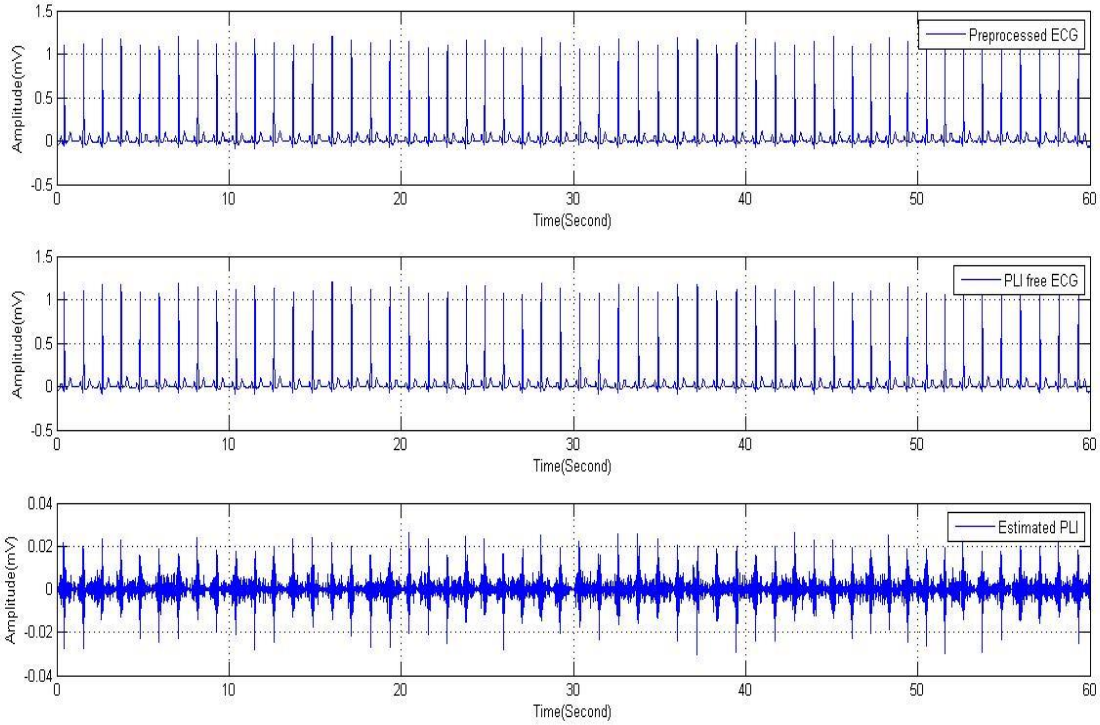

Figure 3.31: Results for removal of power line interference in e0105 record

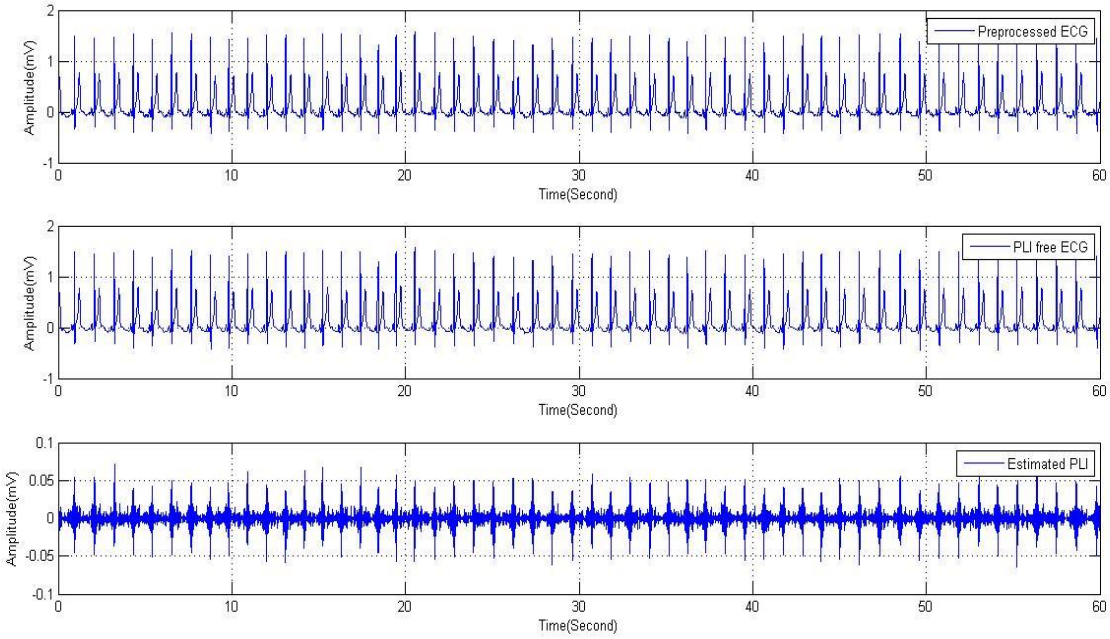

Figure 3.32: Results for removal of power line interference in e0108 record

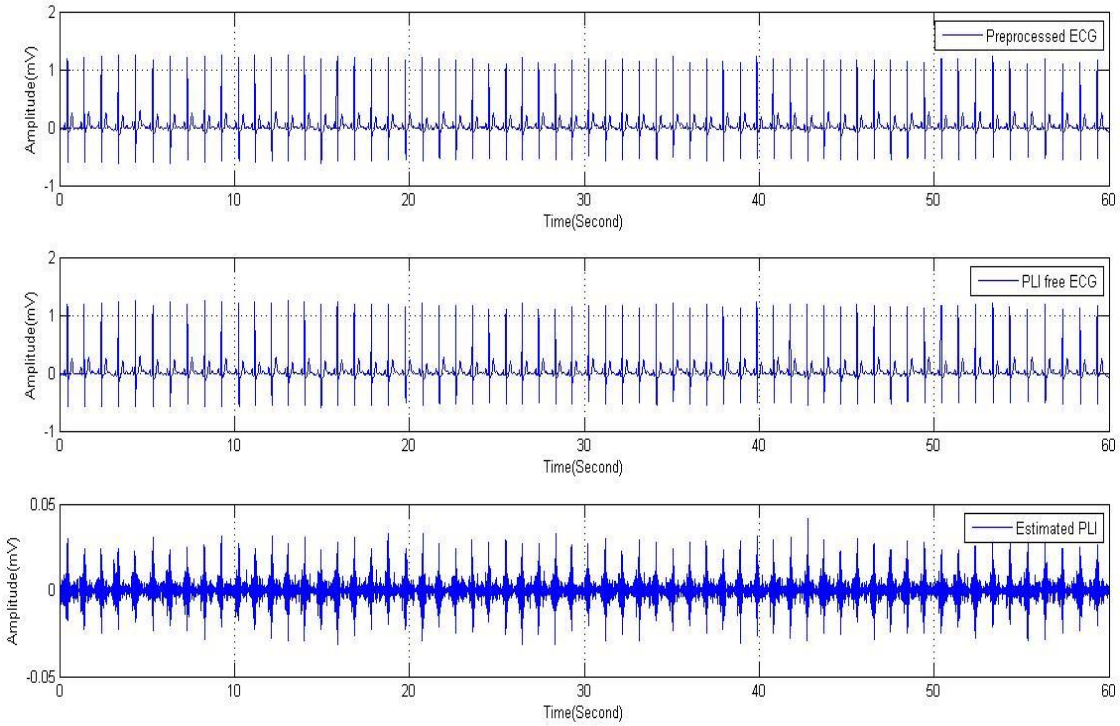

Figure 3.33: Results for removal of power line interference in e0113 record

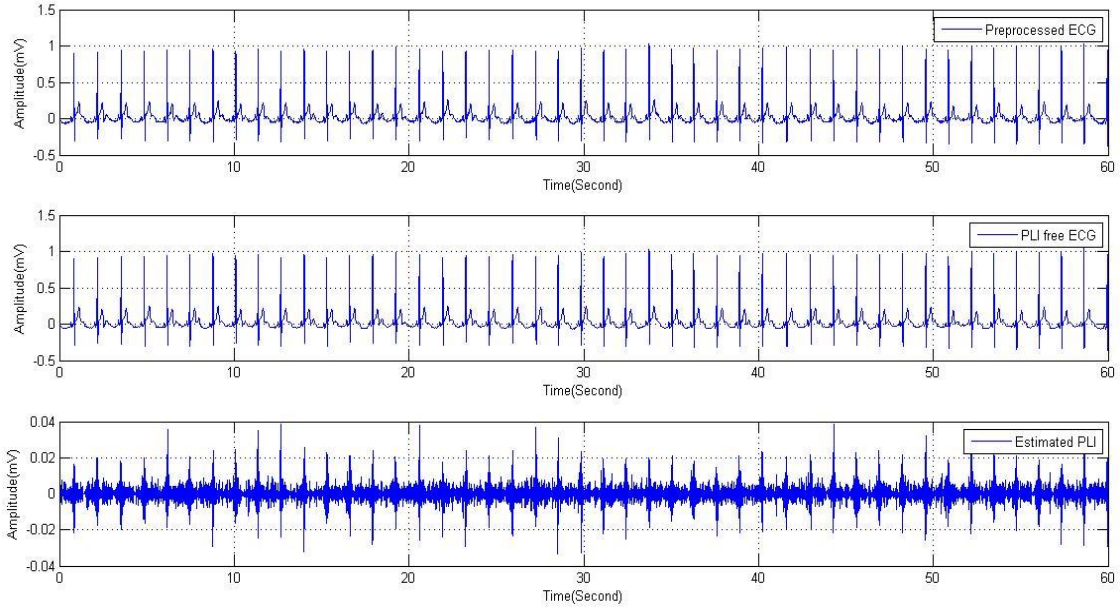

Figure 3.34: Results for removal of power line interference in e0114 record

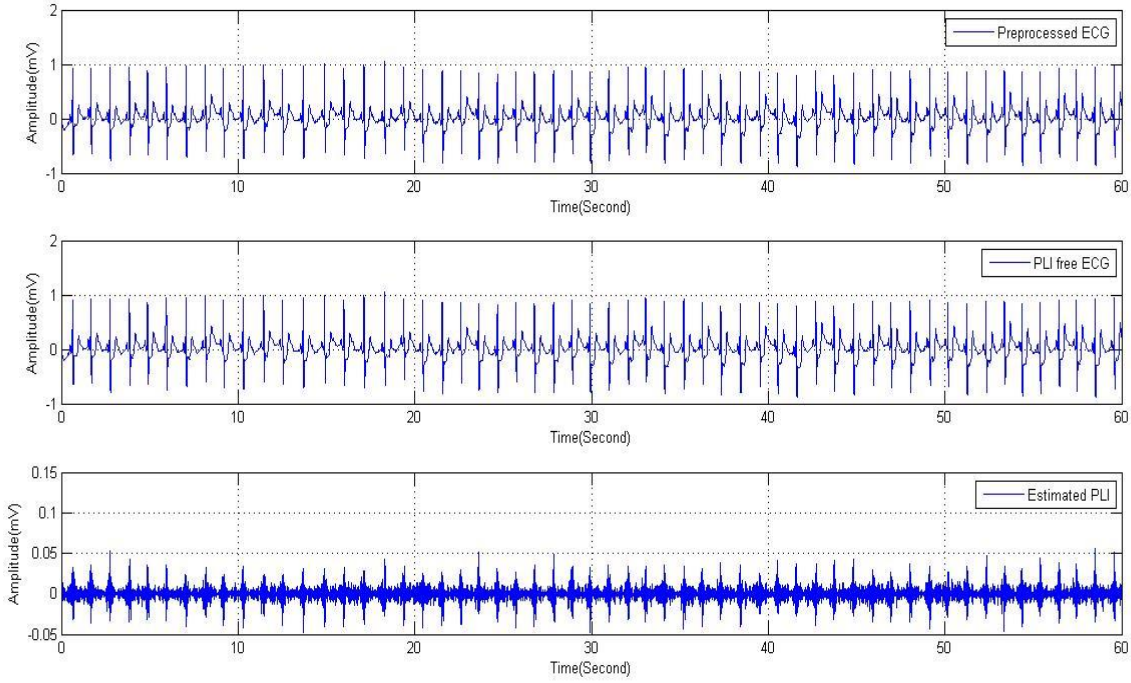

Figure 3.35: Results for removal of power line interference in e0147 record

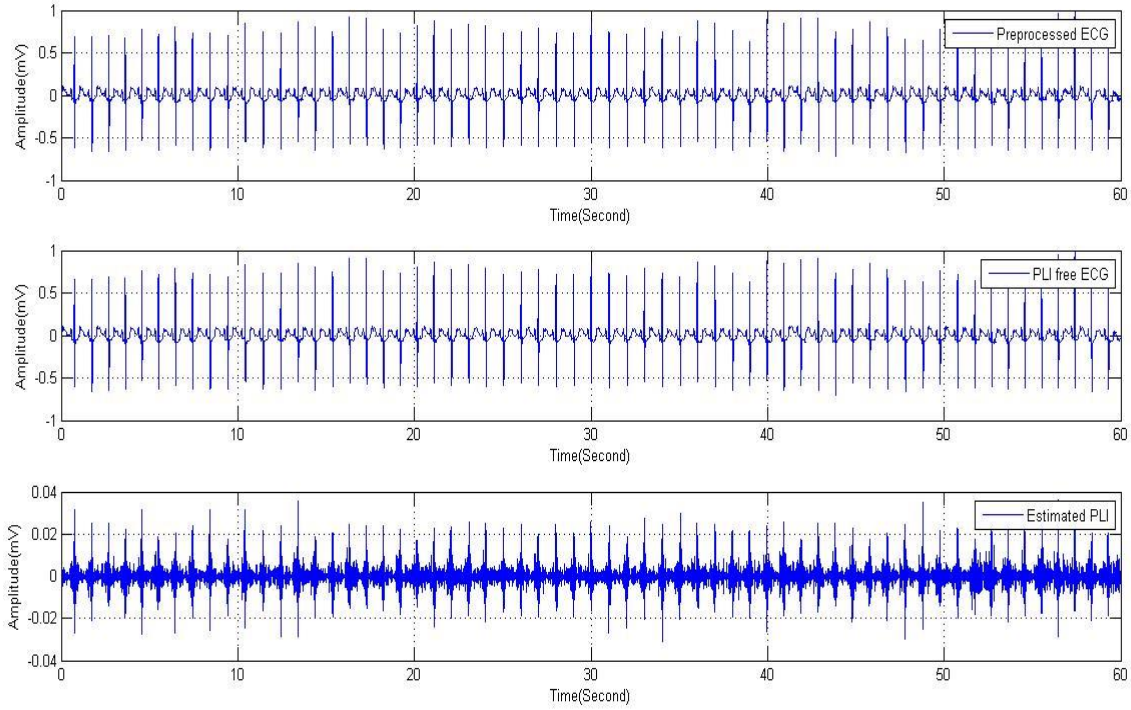

Figure 3.36: Results for removal of power line interference in e0159 record

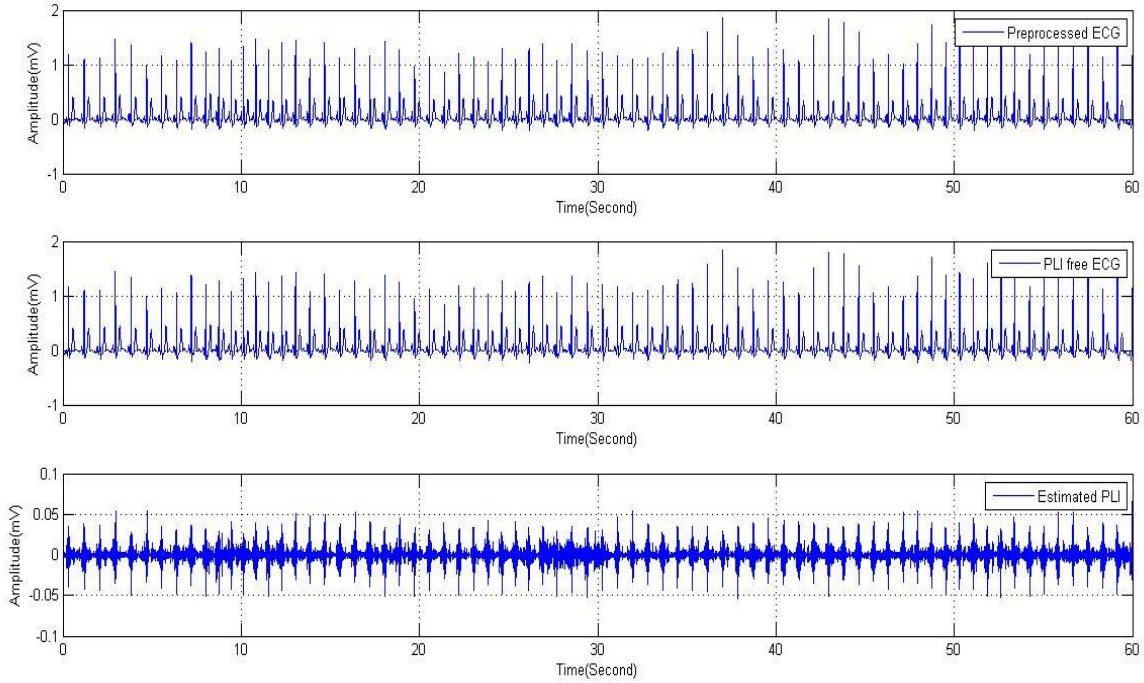

Figure 3.37: Results for removal of power line interference in e0162 record

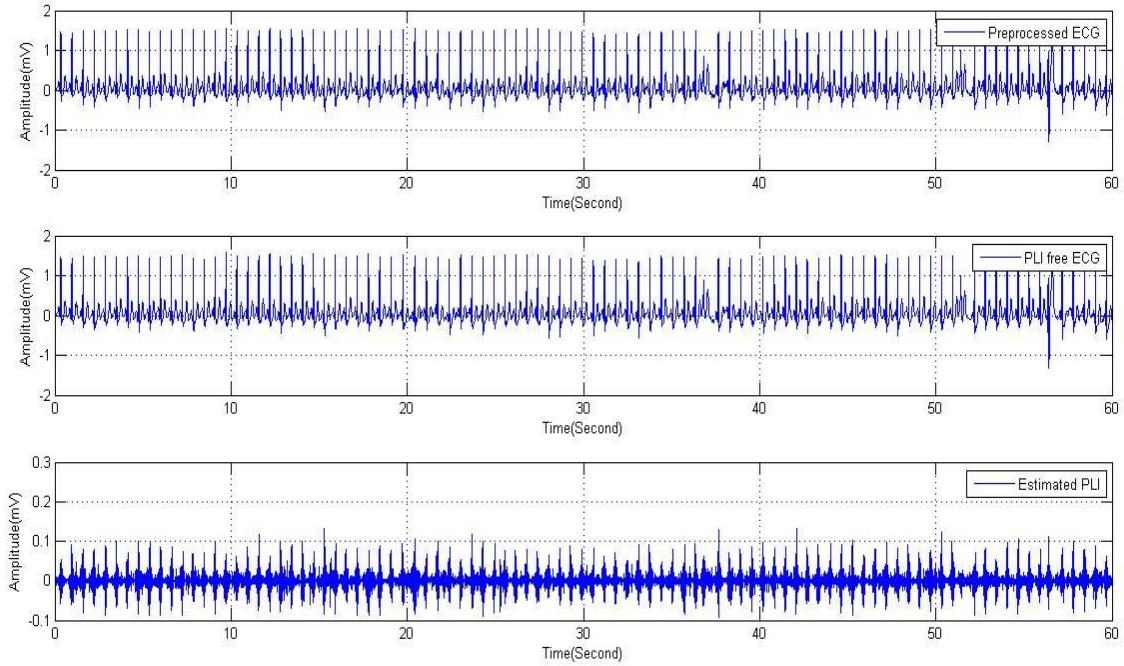

Figure 3.38: Results for removal of power line interference in e0206 record

CHAPTER 4

DELINEATION OF ECG SIGNALS

4. Introduction

ECG delineation is the automatic process of finding ECG features, such as amplitudes and time intervals. Formal definition of delineation implies the action of indicating the exact position of the boundary of a signal. In case of ECG, it implies detecting the R peaks in ECG signal to start with. This is followed by defining windows around the detected R peak for identifying QRS complex and other characteristic points like P wave, T wave and ST segment. A series of algorithms have been reported for feature extraction of characteristic points in the ECG. Many algorithms have been reported in literature for QRS detection of ECG. Like, wavelet based QRS detection [C. Saritha, et.al, 2008; P. Ranjit, 2003], Pan and Tomkins method in assembly language [J. Pan and W.J. Tomkins, 1985], software based QRS detection [O. Pahlm and L. Sornmo, 1984], based on mathematical models [F. Gritzali, 1988; A. Ghaffari, 2008]. Review of the principles of software QRS detection [B.U. Kohler, 2002] can be studied. Similarly, for comparison of nine QRS detection algorithms [G.M. Friesen et.al, 1990] may be studied. Other approaches include matched filters [A.S.M. Koeleman et.al, 1985], second order derivatives [J.G.C et.al, 1994] , ECG slope criteria [I.K. Daskalov et.al, 1998], Hidden Markov Models (HMM) [M.J. Vaessen et.al, 2006], Bayesian approach [C. Lin et.al, 2010], wavelet transforms [A.K. Manocha, M. Singh, 2013; B.M. Evangelos et.al, 2010; C.Li et.al, 1995, S. Banjerjee et.al, 2012; J.S. Sahambi et.al, 1997; J.P. Martnez, 2004; S.C. Saxsena et.al, 2002], correlation based delineation of ECG waves [M.R. Homaeinezhad et.al, 2014], K-nearest neighbor based algorithm for P and T waves delineation [I. Saini et.al, 2014], method based on evolutionary optimization process [J. Dumont et.al, 2010], support vector machine based [S.S. Mehta and N.S. Lingayat, 2009], quality-supported analysis of characteristic templates [A. Karimipur and M.R. Homaeinezhad, 2014] methods have been carried out. It is still a challenge for the researchers to develop an automated diagnosis system which accurately delineates the ECG, for many reasons. Like, the P wave is characterized by low amplitude and may be

missed by muscular noise or electrode motion. By reviewing the literature, it is concluded that the multi-resolution feature of wavelets transform is a boon for non-stationary ECG signals, which decomposes the signals in the required scales used for accurate analysis of non stationary signals [I. Daubechies, 1990; A. Grap, 1995, D.L. Fugel, 2009]. For an accurate delineation and analysis of ECG signals, it is also essential that the transform should exhibit good resolution in both the frequency and time domain. Many frequency-time analysis methods available in literature to represent the ECG signals having their advantages and disadvantages. The advantage and disadvantage of these methods have been discussed in [R. J. Martis et.al, 2014]. The best way to analyze the non-stationary ECG signals is the use of multi-resolution wavelet transform, which incorporates the feature of variable time-frequency resolution over the time-frequency plane. The size and dimensions of the reconstructed signal are about the same as the decomposed signal, which makes wavelet transform a very powerful technique in signal processing. We have developed and validated a new method for delineation of ECG characteristic points using wavelet transform and window search method. A general flow chart of the developed method has been shown in Figure 4.2.

4.1 Detection of ECG Characteristic Points

While looking for characteristic points in the pre-processed ECG signal, we have appended 100 sample points (zeros) before and after to the pre-processed one minute ECG segments. The entire ECG segment is scanned for local maxima. These maxima are stored in an array named, maxh. Further the highest value of this array is taken as ECG_max. Average entire value of all sample points in the signal is stored in a variable named ECG_mean. We define ECG_amp = (ECG_max – ECG_mean)/2. Threshold for detecting R wave is taken as ECG_thresh = (ECG_max)*(ECG_amp) for detecting all R peaks. All peaks of ECG record that crosses this threshold level is classified as R peaks [A. Kumar, M. Singh, 2015; S. Banerjee et.al, 2012; C. Li et.al, 1995]. The time position and amplitude of each R peak is stored in R_INDEX. After successful detection of R peaks, search traverses forth and back for maxima and minima for P, Q, T, S peaks. Firstly search is initiated in window [R_INDEX-400ms: R_INDEX-200ms] for local maximum, which indicates the P peak. In the same manner window of [R_Index-200ms:

R_INDEX-40ms] is employed for a local minimum where in gives Q peak. With similar logic, search for a local minimum in the window [R_INDEX+20ms: R_INDEX+100ms] for S peak and local maximum in window [R_INDEX+200ms: R_INDEX+400ms] for T peak is employed. The corresponding sample locations and amplitudes of the detected characteristic waves are stored in P_INDEX, Q_INDEX, S_INDEX, and T_INDEX. As shown in Fig 6, '^' symbolize the P, Q, R, S and T peaks for 10 representative records of the European ST-T database. The detected sample time values corresponding to these peaks (location) for normal (e0103), elevated (e0103) and depressed (e0105) signals for 10 second duration are mentioned in Table 4.2, 4.3 and 4.4.

4.2 Detection of Onset and Offset Points

For detection of onset and offset points of each characteristic waves, again the search is initiated within the window for corresponding INDEX to check the slope sign inversion. The slope is computed by expression Newton's difference quotient as mentioned in Eqn. 4.1. The window is taken as [INDEX-80ms: INDEX] for onset and [INDEX: INDEX+80ms] for offset.

$$\frac{f(x+h) - f(x)}{h} \tag{4.1}$$

A simple two point estimation has been used to find the slope of a secant line through the points, (x+h, f (x+h)) and (x, f (x)). Here, 'h' is taken as one sample interval. The resulting onset and offset points are having almost zero slopes. Then equivalent onset and offset sample values are stored in ON and OFF indices. Figure 6 shows, onset and offset sample values are represented by blue and black stars, respectively [A. Kumar, M. Singh, 2015; .M R. H. Ghaffaria et.al, 2009; Z. Zidelmala et.al, 2012]. The detected sample time value for onset and offset points for normal, elevated (e0103) and depressed (e0105) signals for 10 second duration are mentioned in Table 4.2, 4.3 and 4.4. Delineation results for 10 representative records have been shown in figures 4.1 & 4.3 to 4.11.

4.3 Heart Rate Determination

The heart rate is calculated as the distance between the two corresponding R-R intervals and is expressed in beats per minute (BPM). It is the mean of time taken between R-R

intervals in the 60 seconds in an ECG record. The detected heart rate for normal (e0103), elevated (e0103) and depressed (e0105) signals for 10 second duration has been mentioned in Table 4.2, 4.3 and 4.4.

4.4 Detection of Isoelectric Reference (IR)

The iso-electric reference is defined in the TP segment, i.e. region connecting the offset of current beat and onset of the next beat. This segment is a flat line between these two points, practically voltage in this segment is nearly zero. For each record, the mean of isoelectric reference value for all the beats is measured. The detected isoelectric reference for normal (e0103), elevated (e0103) and depressed (e0105) signals for 10 second duration has been mentioned in Table 4.2, 4.3 and 4.4.

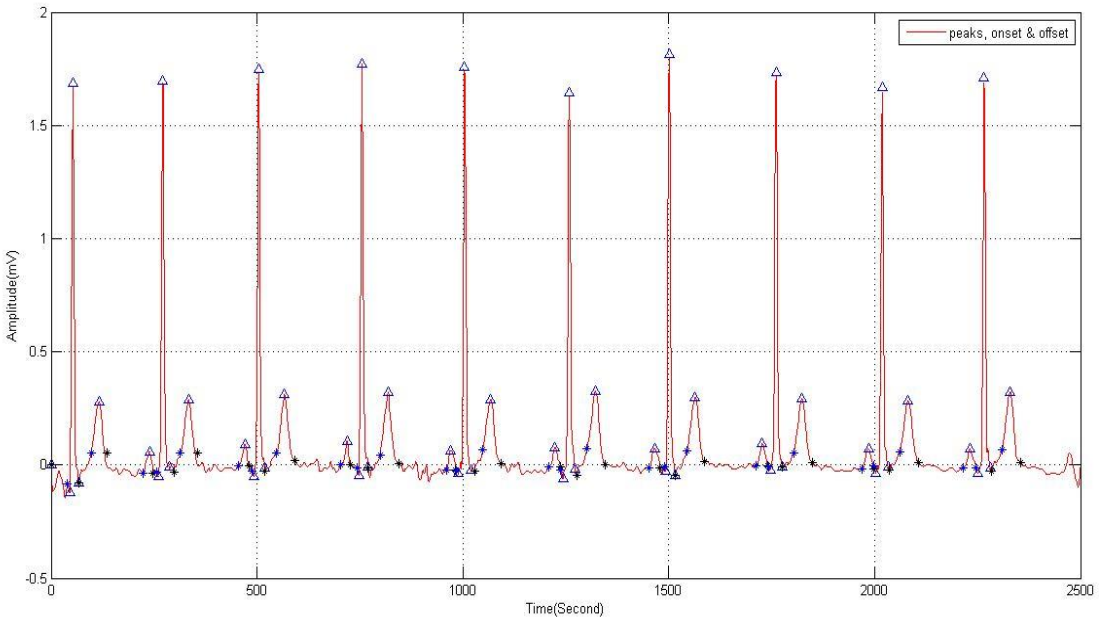

Figure 4.2: Delineation results for e0103 record

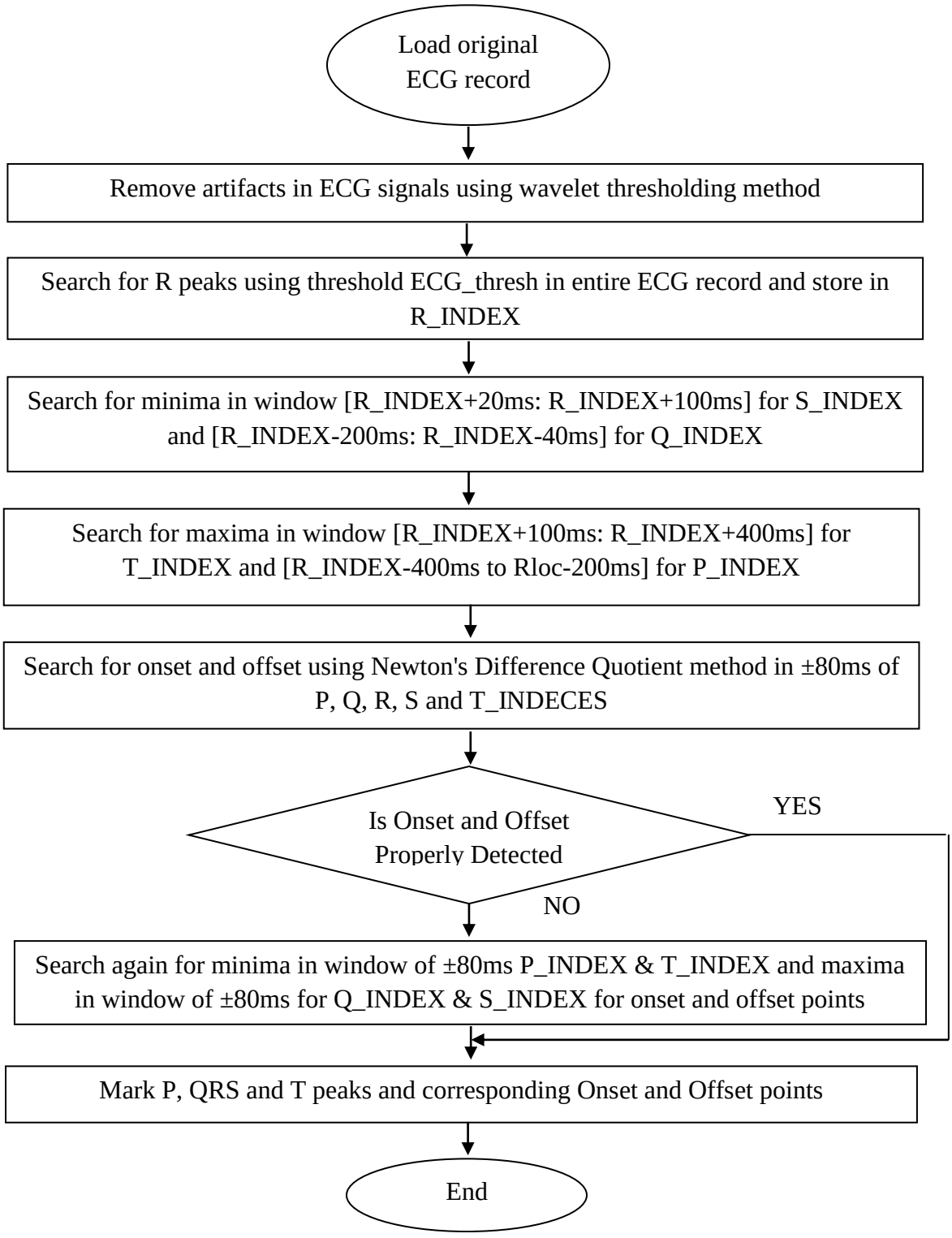

Figure 4.1: Flowchart for developed method for delineation process

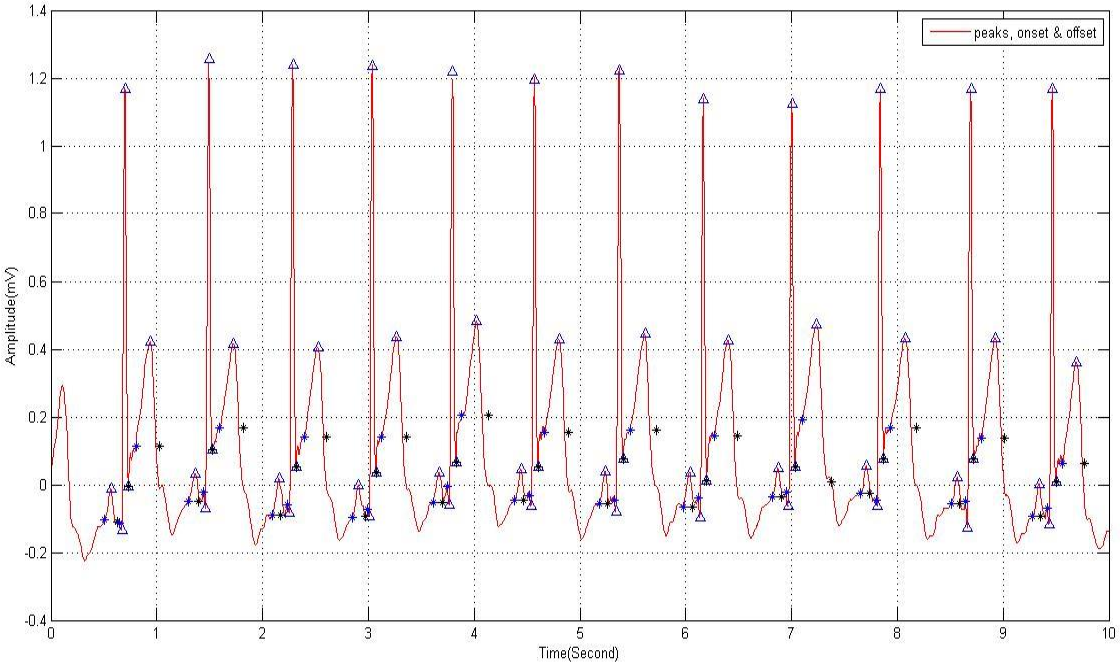

Figure 4.3: Delineation results for e0104 record

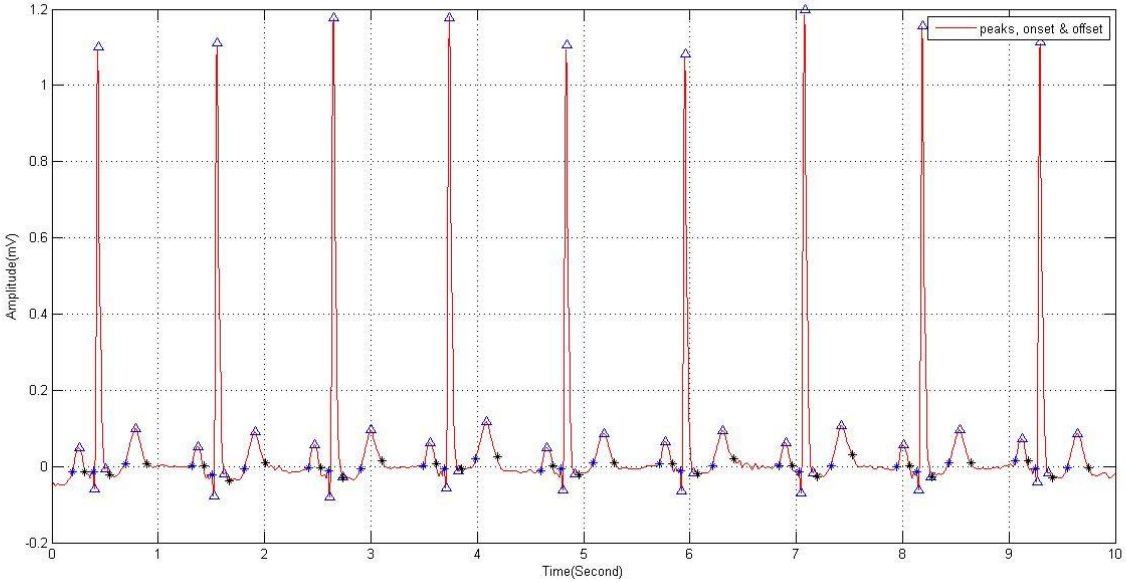

Figure 4.4: Delineation results for e0105 record

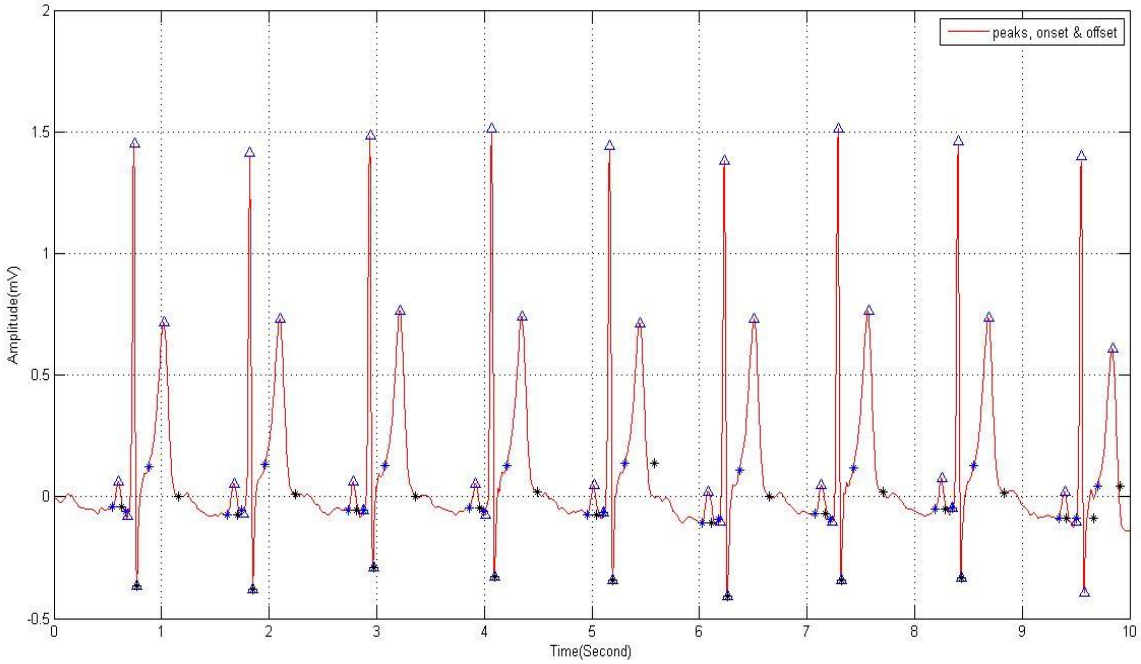

Figure 4.5: Delineation results for e0108 record

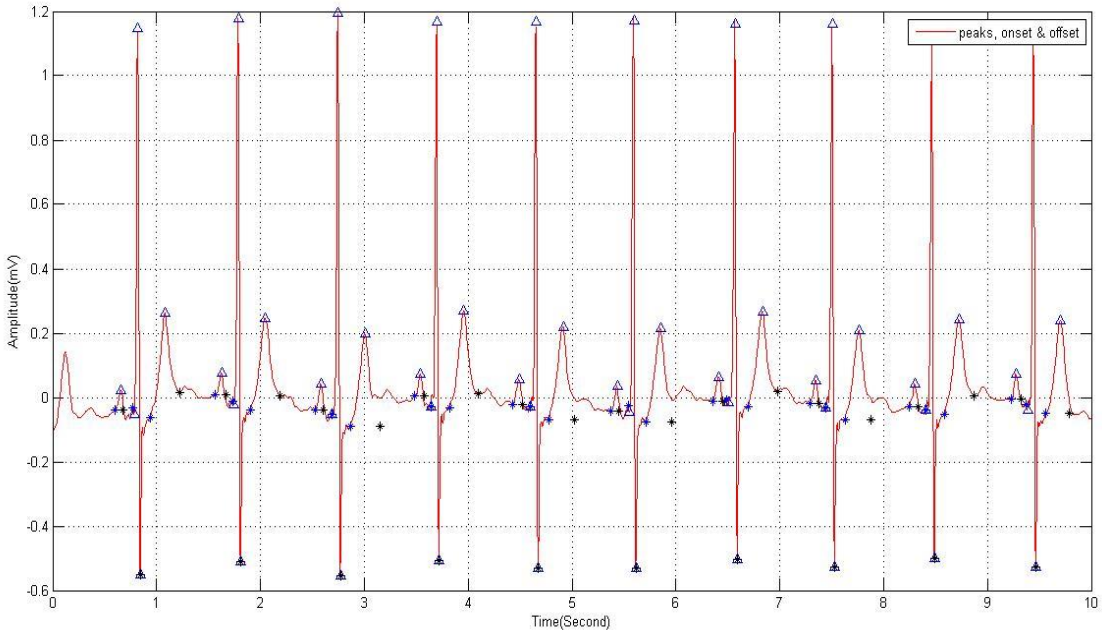

Figure 4.6: Delineation results for e0113 record

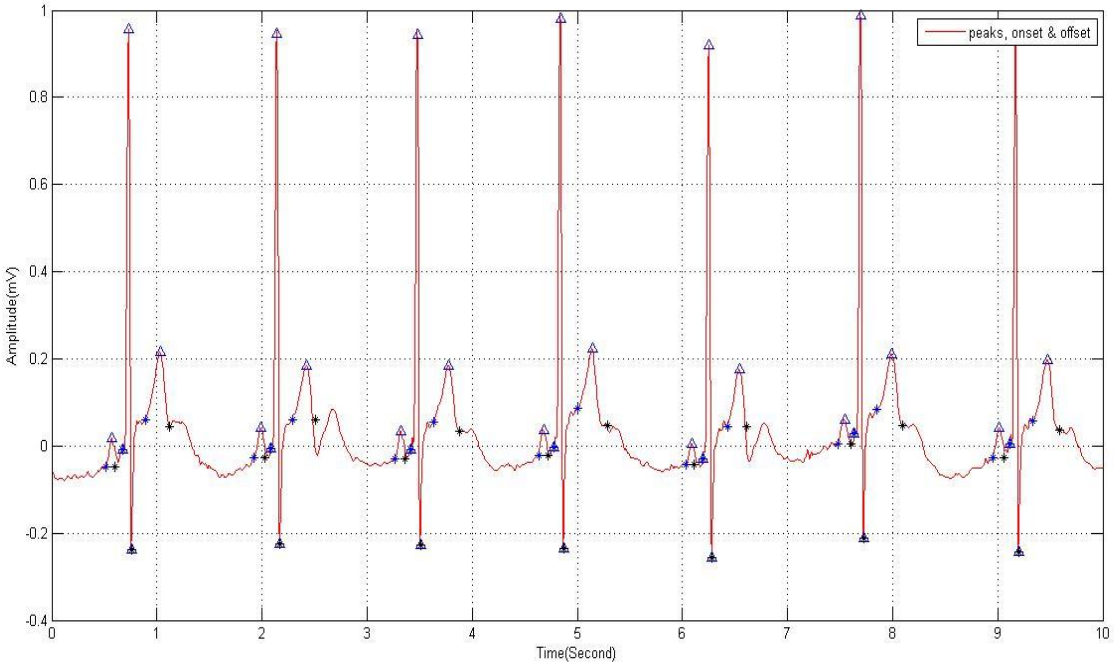

Figure 4.7: Delineation results for e0114 record

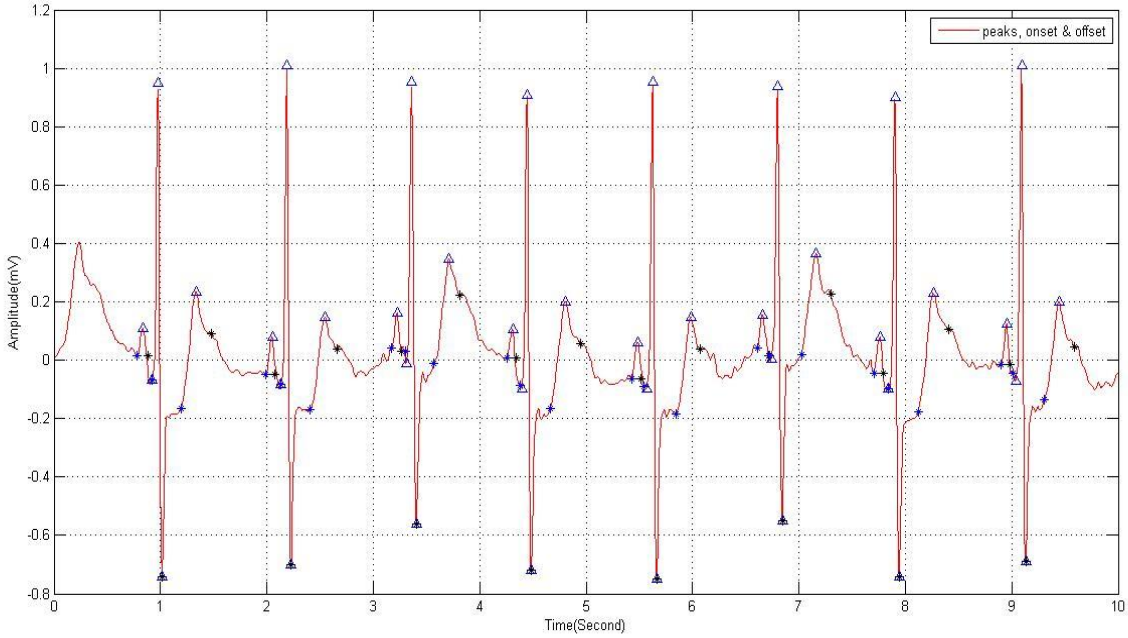

Figure 4.8: Delineation results for e0147 record

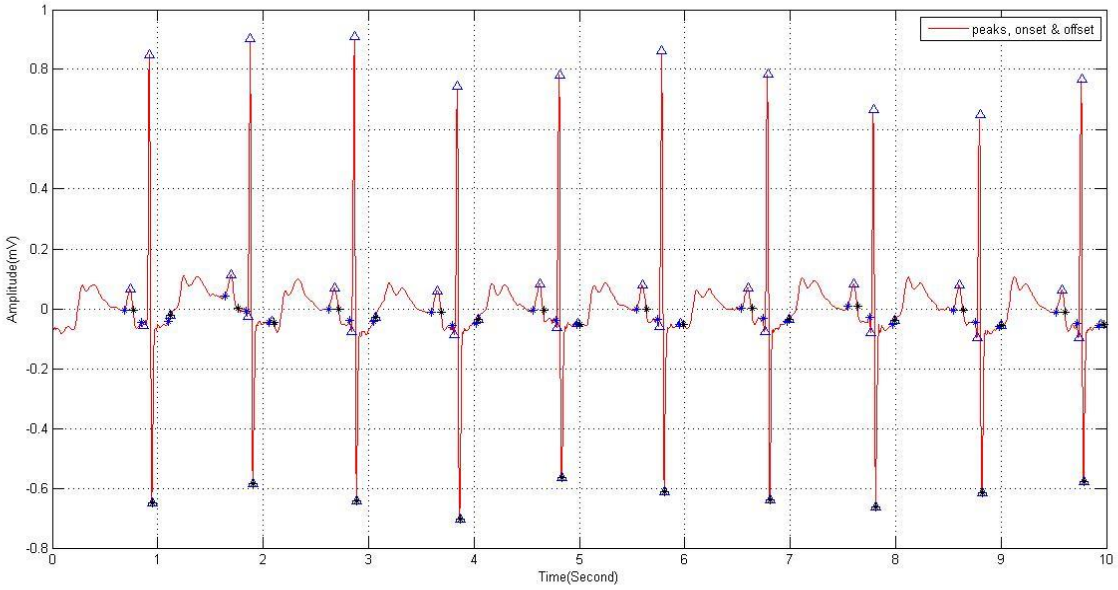

Figure 4.9: Delineation results for e0159 record

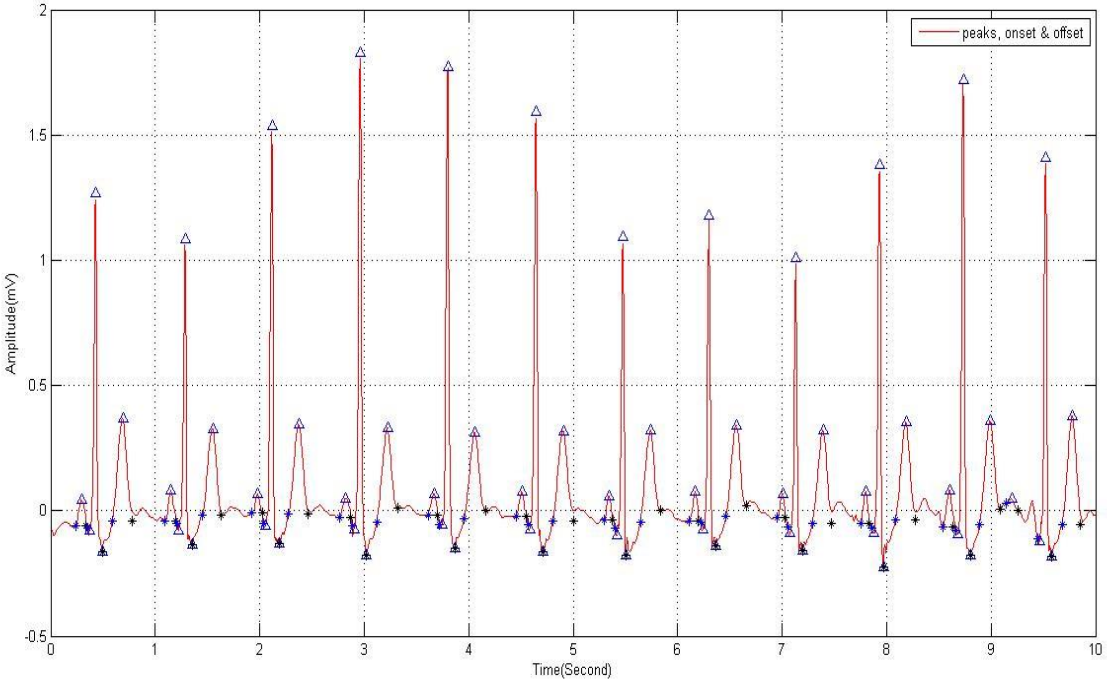

Figure 4.10: Delineation results for e0162 record

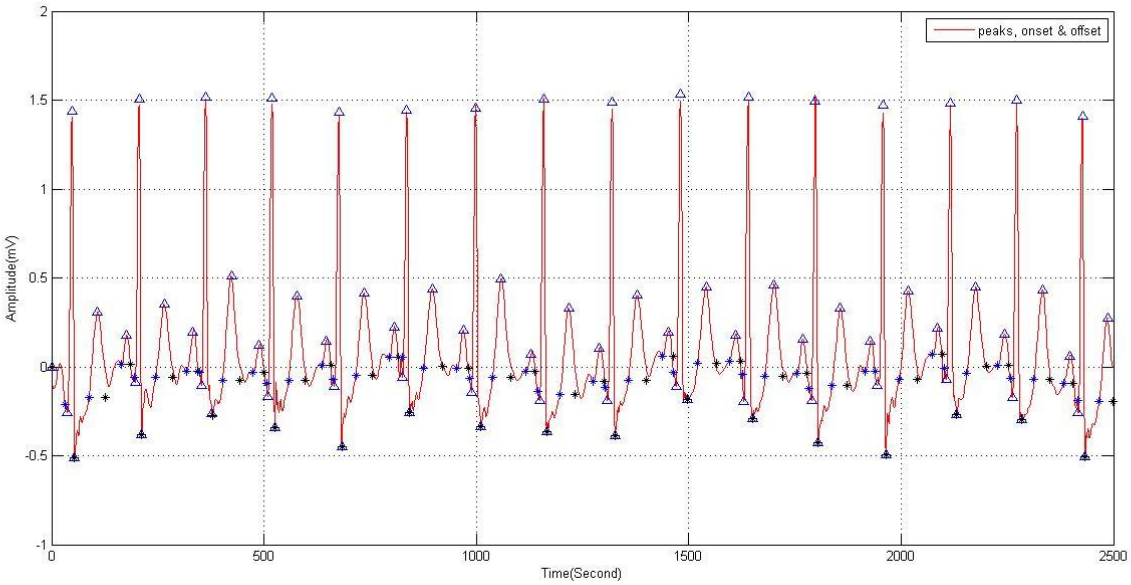

Figure 4.11: Delineation results for e0206 record

4.5 Determining Amplitude Features

The amplitude features from detecting characteristic points are deliberated as

Q height = QRS onset amplitude – Q peak amplitude

R height = R amplitude – isoelectric reference from TP region

S height = QRS offset amplitude - S amplitude

P height = P amplitude – isoelectric reference from TP region

T height = T peak amplitude – isoelectric reference from TP region

4.6 Determining Time Plane Features

The time-plane features from detecting onset and offset points of characteristic waves are determined as

R–R interval = Distance between two consecutive R peaks

PR interval = P onset: R peak location

QRS width = QRS onset: QRS offset

ST interval= S onset: T offset

QT interval = QRS onset: T offset

The normalized value of the QT interval is corrected (hypothetically at a rate of 60 beats per minute) and is given by $QTc = \frac{QT\ Interval}{\sqrt{R-R\ interval}}$

The amplitude and time plane feature for normal (e0103), elevated (e0103) and depressed (e0105) records for 10 second duration are shown in Table 4.2, 4.3 and 4.4 respectively.

4.7 Results and Validation

The developed method for delineation process is implemented and validated in MATLAB2012a for 10 representative ECG records of European ST-T database (EDB) of the Physio-bank. Additionally, the peaks of all characteristic points of ECG and their corresponding onset and offset sample values are also validated manually in Microsoft excel against their original ECG sample values. The proposed method has been validated for 10 representative records, namely whole e0104 recording and the first hour of the e0103, e0105, e0108, e0113, e0114, e0147, e0159, e0162, and e0206 recordings. These records yielded a dataset of 43, 876 cardiac beats for one lead used for recording. After removing the artifacts and the mis-detected beats in delineation process, the final dataset contained 43,762. The proposed method is not suitable for detection of bi-phasic T waves (e0159 record), for which T offset points have been detected carefully. Table 4.1 shows average sensitivity 99.72% and positive predictivity of 99.78% for 10 representative records except T waves of e0159 records. The performance evaluation, sensitivity (S_E) and positive predictivity (+P) measures have been used for these records defined as

$$\text{Sensitivity } (S_E) = [TP/(TP+FN)] * 100 \quad (4.2)$$

$$\text{Positive predictivity } (+P) = [TP/(TP+FP)] * 100 \quad (4.3)$$

Where TP stands for true positive, FP denotes false positive & FN denotes false negative detection. Eqn. 4.2 & 4.3 defines sensitivity and the positive predictivity measures. The developed delineation method has also been validated another dataset, in addition to the above, which carries 37,333 for first 30 minutes of e0103, e0104, e0105, e0106, e0107, e0108, e0111, e0113, e0114 and e0116. The developed method for this dataset achieves 99.94% sensitivity and 99.98% positive predictivity.

Table 4.1: Performance measures for 10 representative records

Sr. No.	Record No.	No. of beats	S_E (%)	+P(%)
1	e0103	3696	99.98	99.87
2	e0104	7824	99.92	99.81
3	e0105	3357	99.81	99.84
4	e0108	3301	99.82	99.63
5	e0113	4225	99.38	99.67
6	e0114	2858	99.47	99.77
7	e0147	3261	99.64	99.69
8	e0159	4449	99.76	99.91
9	e0162	5294	99.78	99.86
10	e0206	5611	99.68	99.78
Total		**43,876**	**99.72**	**99.78**

4.8 Statistical Analysis of Amplitude and Time Plane Features

The statistical analysis [S. Banjeree et.al, 2012; I. I. Amr et.al, 2010] of measured amplitude and time plane feature can also be used for the validation of results for all measurements of single detected characteristic points. This involves standard deviations (S.D.) along with the coefficient of variation (C.V.) are deliberated. Here x_i = ith beat and n = number of beats in the record.

$$\text{Mean} = \frac{\sum x_i}{n}$$

$$\text{Standard Deviation (S.D.)} = \sqrt{\frac{\sum(x_i - mean)^2}{n}}$$

$$\text{Coefficient of Variation (C.V.)} = \frac{S.D.}{Mean} * 100$$

The S.D. measures the absolute dispersion about the mean in a data series. Whereas, C.V. expresses the dispersion within a series of data in percentage value, represents the consistency. The statistical values of amplitude and time plane features for normal, depressed and elevated signals are mentioned in Table 4.5.

e0103 normal signal of 10 second duration										
Parameter	Beat1	Beat2	Beat3	Beat4	Beat5	Beat6	Beat7	Beat8	Beat9	Beat10
Pon(sec)	0	0.896	1.824	2.816	3.844	4.836	5.804	6.848	7.88	8.864
Poff(sec)	0	0.988	1.92	2.908	3.928	4.948	5.916	6.96	7.988	8.984
Qon(sec)	0.16	1.024	1.948	2.968	3.936	4.952	5.956	6.968	7.992	8.984
Soff(sec)	0.268	1.192	2.076	3.08	4.12	5.104	6.064	7.104	8.14	9.136
Ton(sec)	0.388	1.256	2.188	3.196	4.192	5.204	6.176	7.212	8.244	9.236
Toff(sec)	0.54	1.424	2.368	3.376	4.372	5.384	6.348	7.392	8.424	9.416
Ploc(sec)	0	0.956	1.884	2.876	3.88	4.896	5.864	6.908	7.94	8.924
Qloc(sec)	0.144	1.04	1.968	2.988	3.952	4.972	5.968	6.988	8.012	9.004
Rloc(sec)	0.204	1.08	2.012	3.012	4.012	5.028	6	7.036	8.068	9.06
Sloc(sec)	0.264	1.132	2.072	3.072	4.072	5.088	6.06	7.096	8.128	9.12
Tloc(sec)	0.468	1.336	2.268	3.276	4.272	5.284	6.256	7.292	8.324	9.316
P_height(mV)	0.082	0.086	0.1008	0.1108	0.0857	0.0999	0.0978	0.104	0.0792	0.0821
Q_height(mV)	0.0394	0.0189	0.0234	0.0349	0.0063	0.0394	0.0199	0.0152	0.0303	0.026
R_height(mV)	1.767	1.725	1.757	1.77	1.782	1.664	1.837	1.743	1.675	1.732
S_height(mV)	-0.0215	-0.0236	-0.013	-0.0054	-0.00493	-0.0295	-0.00192	-0.0025	-0.01408	-0.0153
T_height(mV)	0.3623	0.3164	0.3179	0.3278	0.3127	0.3467	0.3232	0.3016	0.2872	0.3213
I. R.(in mV)	-0.0825	-0.0296	-0.0081	-0.0063	-0.0224	-0.0216	-0.0242	-0.0069	-0.0052	-0.0031
QRS width(sec)	0.108	0.172	0.132	0.116	0.188	0.156	0.112	0.14	0.152	0.156
QTinterval(sec)	0.402	0.404	0.424	0.412	0.44	0.436	0.396	0.428	0.436	0.436
QTc(sec)	__	0.433	0.438	0.411	0.441	0.429	0.404	0.406	0.43	0.44
PRinter(sec)	__	0.192	0.196	0.208	0.176	0.2	0.204	0.2	0.196	0.204
STint(sec)	0.271	0.236	0.296	0.3	0.256	0.284	0.288	0.292	0.288	0.284
R-R interval (sec)	0.91	0.872	0.932	1.004	0.996	1.016	0.972	1.04	1.028	0.992
Heart Rate(bpm)	67.78									

Table 4.2: Amplitude and time plane features for delineated characteristic waves for normal signal

e0103 elevated signal of 10 second duration										
Parameter	**Beat1**	**Beat2**	**Beat3**	**Beat4**	**Beat5**	**Beat6**	**Beat7**	**Beat8**	**Beat9**	**Beat10**
Pon(sec)	0.232	1.228	2.184	3.152	4.108	5.092	6.08	7.012	7.96	8.928
Poff(sec)	0.312	1.336	2.296	3.252	4.216	5.212	6.188	7.116	8.056	9.024
Qon(sec)	0.372	1.344	2.296	3.264	4.248	5.22	6.2	7.152	8.1	9.06
Soff(sec)	0.496	1.488	2.456	3.408	4.38	5.408	6.352	7.28	8.204	9.212
Ton(sec)	0.6	1.596	2.548	3.508	4.48	5.468	6.444	7.376	8.324	9.288
Toff(sec)	0.776	1.752	2.716	3.664	4.628	5.64	6.596	7.54	8.496	9.444
Ploc(sec)	0.292	1.288	2.236	3.212	4.168	5.152	6.14	7.072	8.02	8.988
Qloc(sec)	0.372	1.364	2.316	3.284	4.248	5.236	6.22	7.152	8.116	9.076
Rloc(sec)	0.432	1.424	2.376	3.344	4.308	5.296	6.276	7.212	8.156	9.12
Sloc(sec)	0.492	1.484	2.432	3.404	4.368	5.356	6.336	7.272	8.204	9.18
Tloc(sec)	0.68	1.676	2.628	3.588	4.56	5.548	6.524	7.456	8.404	9.368
P_height(mV)	0.073	0.097	0.096	0.109	0.095	0.114	0.103	0.098	0.088	0.09
Q_height(mV)	0.0014	0.0003	0.013	0.0003	0.0019	0.033	0.021	0.018	0.019	0.03
R_height(mV)	1.789	1.723	1.743	1.778	1.803	1.783	1.772	1.847	1.87	1.788
S_height(mV)	-0.0004	-0.0041	-0.0079	-0.0067	-0.0193	-0.0058	-0.0024	-0.0177	-0.00532	-0.00642
T_height(mV)	0.286	0.258	0.246	0.264	0.262	0.254	0.237	0.283	0.274	0.267
I. R. (in mV)	-0.0482	-0.0188	-0.00254	-0.0206	-0.0286	0.0069	-0.0095	-0.0434	-0.0106	-0.0146
QRS width(sec)	0.144	0.148	0.164	0.148	0.136	0.192	0.156	0.132	0.108	0.156
QTinterval(sec)	0.404	0.412	0.424	0.404	0.384	0.424	0.4	0.392	0.4	0.388
QTc(sec)	0.425	0.414	0.441	0.41	0.395	0.426	0.412	0.406	0.411	0.395
PRinter(sec)	0.2	0.2	0.196	0.196	0.204	0.208	0.2	0.204	0.2	0.196
STint(sec)	0.26	0.268	0.264	0.26	0.252	0.236	0.248	0.264	0.296	0.236
R-R interval (sec)	0.942	0.992	0.952	0.968	0.964	0.988	0.982	0.936	0.944	0.964
Heart rate(bpm)	62.21									

Table 4.3: Amplitude and time plane features for delineated characteristic waves for elevated signal

e0105 depressed signal of 10 second duration									
Parameter	**Beat1**	**Beat2**	**Beat3**	**Beat4**	**Beat5**	**Beat6**	**Beat7**	**Beat8**	**Beat9**
Pon(sec)	0.3	1.396	2.484	3.584	4.652	5.728	6.8	7.888	8.948
Poff(sec)	0.404	1.512	2.6	3.684	4.764	5.848	6.92	7.996	9.06
Qon(sec)	0.484	1.576	2.68	3.768	4.836	5.92	7	8.072	9.132
Soff(sec)	0.644	1.692	2.776	3.952	5.024	6.024	7.1	8.256	9.24
Ton(sec)	0.808	1.9	2.988	4.08	5.16	6.228	7.308	8.396	9.456
Toff(sec)	0.988	2.08	3.168	4.26	5.34	6.408	7.488	8.576	9.636
Ploc(sec)	0.36	1.456	2.544	3.644	4.712	5.788	6.86	7.948	9.008
Qloc(sec)	0.504	1.596	2.692	3.784	4.856	5.932	7.012	8.088	9.152
Rloc(sec)	0.532	1.624	2.716	3.812	4.884	5.96	7.04	8.116	9.18
Sloc(sec)	0.592	1.684	2.776	3.872	4.944	6.02	7.1	8.176	9.24
Tloc(sec)	0.888	1.98	3.068	4.16	5.24	6.308	7.388	8.476	9.536
P_height(mV)	0.082	0.088	0.086	0.082	0.084	0.078	0.085	0.082	0.0829
Q_height(mV)	0.061	0.031	0.042	0.063	0.045	0.04	0.055	0.057	0.017
R_height(mV)	1.39	1.42	1.35	1.29	1.37	1.38	1.36	1.31	1.39
S_height(mV)	-0.047	-0.025	-0.011	-0.039	-0.054	0.005	0.009	-0.061	-0.008
T_height(mV)	0.13	0.151	0.152	0.143	0.138	0.139	0.141	0.141	0.124
I. R. (in mV)	-0.021	-0.013	-0.021	-0.021	-0.02	-0.0015	-0.016	-0.013	-0.01
QRS width(sec)	0.16	0.12	0.1	0.188	0.192	0.108	0.104	0.188	0.112
QTinterval(sec)	0.504	0.508	0.492	0.496	0.508	0.492	0.492	0.508	0.508
QTc(sec)	0.484	0.493	0.473	0.473	0.493	0.473	0.472	0.474	0.496
PRinter(sec)	0.236	0.232	0.236	0.232	0.236	0.236	0.244	0.232	0.236
STint(sec)	0.344	0.392	0.396	0.312	0.32	0.388	0.392	0.324	0.4
R-R interval (sec)	1.087	1.092	1.092	1.096	1.072	1.076	1.08	1.076	1.064
Heart Rate(bpm)	55.92								

Table 4.4: Amplitude and time plane features for delineated characteristic waves for depressed signal

Parameter	e0103 normal signal for 10 second duration			e0103 elevated signal for 10 second duration			e0105 depressed signal for 10 second duration		
	Mean	S.D.	C.V.	Mean	S.D.	C.V.	Mean	S.D.	C.V.
P_height(mV)	0.0928	0.0111	11.96	0.0963	0.011	11.42	0.0833	0.0029	3.48
Q_height(mV)	0.0254	0.0108	42.51	0.0138	0.124	95.38	0.0457	0.0151	33.04
R_height(mV)	1.7452	0.0507	2.9	1.7896	0.043	2.4	1.3622	0.04	2.93
S_height(mV)	-0.0132	0.0095	-6.64	-0.0076	0.006	85.71	-0.0257	0.025	-97.27
T-height(mV)	0.3217	0.0212	6.6	0.2631	0.154	58.58	0.1399	0.008	5.71
I.R. (mV)	-0.021	0.0236	112.38	-0.019	0.172	894.72	-0.0152	0.006	-40
QRS width(sec)	0.1432	0.026	18.18	0.1484	0.021	14.18	0.141	0.04	28.36
QTinterval(sec)	0.4214	0.016	3.8	0.4032	0.013	3.22	0.5009	0.007	14
QTc(sec)	0.4258	0.148	34.82	0.4135	0.014	3.38	0.481	0.01	2.07
PRinter(sec)	0.1973	0.009	4.56	0.2004	0.004	2	0.235	0.003	1.27
STint(sec)	0.2795	0.0199	2.03	0.2584	0.017	6.58	0.363	0.037	10.27
R-R interval (sec)	0.9762	0.547	56.04	0.9632	0.019	1.97	1.08	0.01	0.92

Table 4.5: Statistical analysis values for amplitude and time plane features for delineated characteristic waves for normal, elevated and depressed signal

4.9 Artifacts Removal Effects on Delineation Process

As discussed earlier, the artifacts have an adverse effect on the computerized delineation of ECG. It is very significant to recognize the artifact frequencies and to discriminate these artifact changes from genuine changes to prevent mis-diagnosis, unnecessary testing and therapeutic interventions. Like, ST segments in ECG signal are affected by baseline wanders, either ST segment depression or elevation can occur, which can be misinterpreted as myocardial ischemia. Similarly, PLI introduces tall T-waveforms, which may be mis-identified in the measurement of R-R intervals (a basis of heart rate variability). Sometimes, muscle tremors overlap with QRS complex, which may mimic atrial flutter or fibrillation. Obscuring of P waves may resemble a heart block [S. Scheidt, 1984]. As shown in Figure 3.8, the discarding of wavelet coefficients corresponding to artifact frequencies of original ECG signal has no destructive effects on the morphology of original ECG signal, which is significantly improving the ability of doctors to characterize the patient's prescribe treatment. To support the claim of improved sensitivity of ischemia detection, normal ECG ST Segment of the e0103m record from European ST-T database were selected. A baseline wanders of 0.25 Hz was superimposed to mimic artifact on account of breathing of 1809 beats analyzed. 1186 beats were detected as normal, which the remaining 623 beats were detected as ischemic. Due to the false positive sensitivity of normal signal reduces to 65.56%. On removing to this baseline wander using the proposed algorithm, the sensitivity attained again became 100%. This removal of baseline alone can significantly improve the sensitivity in the case of computer aided ischemia detection.

4.10 Comparisons with Existing Methods

Although, it is very difficult to make comparisons of the proposed method with existing methods, because of the availability of the many databases available in the literature for the validation process. QRS detection methods are divided into three categories as syntactic, non-syntactic and hybrid. Syntactic method [E. Pietka, 1991] is time consuming due to the need of grammatical inference. Whereas non-syntactic methods [Q. Z. Xie et.al, 1992; P.S. Hamilton and W.J. Tompkins, 1986] preferred band pass filters, which suppress the P and T waves. Most of the reported methods are not able to detect

the P wave after the QRS complex detection as generally is embedded in artifacts. The Proposed method in [F. Gritzali et.al, 1989] can detect P and T wave by length transformation, but it is not robust to noise and artifacts. The pan-tomkins method [J. Pan and W.J. Tomkins, 1985] used nonlinear transformation like derivatives and squaring for detection of QRS complexes, but this method suffers from the following bottlenecks; 1). The signal frequency band of the QRS complex is different for beats even for the same subject. 2). Frequency bands of artifacts and QRS complex overlaps. The proposed method conserves the small frequency waves of P and T wave as analyzed by Dhono's method [K. Daqrouq, 2005]. Table 4.6 compares the performance of the developed method with existing methods in literature for European ST-T database records. It should be mentioned that the comparative methods does not have the same number of datasets. The developed method for delineation achieves 99.72% sensitivity and 99.78% positive predictivity for 10 representative ECG records. The developed method achieves highest positive predictivity against available methods.

Table 4.6: Performance evaluation of developed method with existing method: application to European ST-T database

Detection Algorithm	**S_E (%)**	**+ P (%)**
Developed method	**99.72**	**99.78**
Ghaffari et.al [A. Ghaffari et.al, 2006]	99.60	99.47
Martinez et.al [J.P. Martinez et.al, 2004]	99.61	99.48
Moody and Mark [G.B. Moody & R. G. Mark, 1982]	95.09	98.63
A. Ghaffaria et.al [A. Ghaffaria, 2009]	99.63	99.55
Luigi Y Di & Lorenzo Chiari [L.Y.D. Macro & L.Chiari, 2011]	99.81	99.56

CHAPTER-5

ISOELECTRIC ENERGY FUNCTION

5. Introduction

Myocardial ischemia is universally detected by observing ST segment elevation or depression with respect to isoelectric reference. The normal ST segment with respect to the isoelectric reference (TP segment) has been shown in Figure 5.1a, ST segment depression and ST segment elevation is shown in Figure 5.1b Figure 5.1c respectively. An alternate method (as presented in Figure 5.2) to detect the elevation or depression of ST segment with respect to isoelectric reference is to define a mathematical function that detects these deviations in a rugged manner. The main requirement of this function is that its value should increase as the ST segment hugs isoelectric reference level, while it should decrease as ST segment tries to move away from the isoelectric reference. The motivation behind developing this function is to go in for a simpler but reliable threshold based classification for detecting myocardial ischemia.

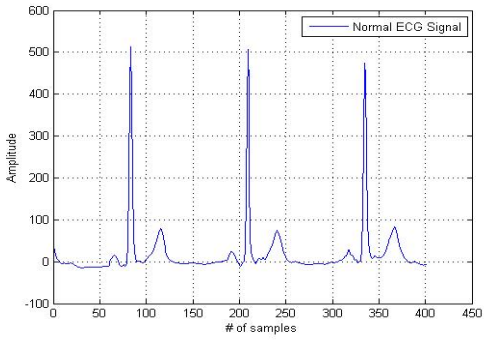

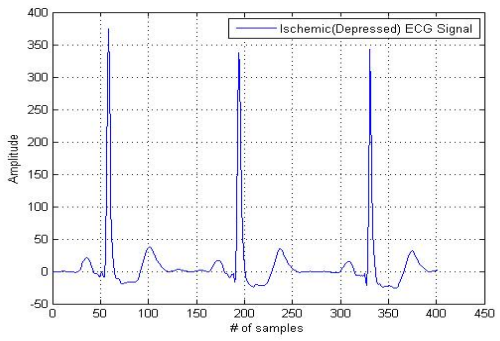

Figure 5.1: (a) Normal ECG **(b) Ischemic (depressed ST) ECG**

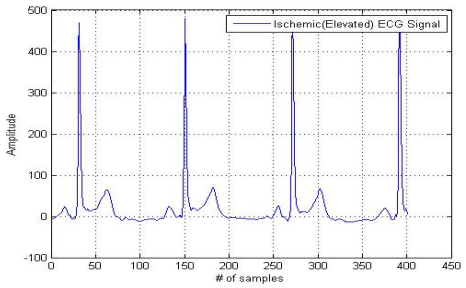

(c) Ischemic (elevated ST) ECG

5.1 Region of Interest for ST Segment

We have defined region of interest corresponds to ST segment (ROI_{ST}). This ROI is having almost the same length of ST segment as criteria of J point, is mentioned as

ROI_{ST}
STS = R-R/8 (8^{th} part of R-R interval samples)
ROI_{ST}= abs (Rpeak+3.2ms: STS)

5.2 Measurement of Isoelectric Reference (IR)

The isoelectric reference (IR) is defined in TP segment (Toffset: Ponset). This segment is having a flat line between these two points; practically voltage in this segment is nearly zero.

5.3 Isoelectric Energy Measurement

The isoelectric energy for each sample in the ST segment is measured, the proposed isoelectric energy function (IEEF) is defined in Eqn. 5.1.

$$\mathbf{IEEF} = \frac{\sum\left[\left[\left(\mathrm{ST(i)}\right) - \mathrm{Avg(IR)}\right]^2 + \alpha\right]^{-1}}{\mathrm{Length\ (ST)}} * \beta \qquad (5.1)$$

Where i =1, 2, 3--------up to length of samples in an ST segment

ST = voltage values for each sample of an individual ST segment in a record

Avg (IR) = average of voltages in isoelectric references in a record

α= 0.01, artificial added constantly to prevent IEEF acquiring infinite value

β is to keep the threshold for classification of the beat as unity

Length (ST) is the number of samples in individual ST segment in a record.

The IEEF is developed by keeping in view that the samples of the segments, which are nearest to isoelectric line will contribute more energy as compared to the far away samples from the isoelectric line.

5.4 Defining Thresholds

After measurement of isoelectric energy for each ST segment in a particular record, we define the threshold β as mentioned in Eqn. 5.1. The normal beat will always have more

value of IEEF than the ischemic (elevated or depressed) beat. The normal beats are annotated by 1 and ischemic by 0 is called as preliminary stage.

Ischemic Beat Classification
If isoelectric energy ≥ 1
Then the beat is normal
Else the beat is ischemic

5.5 Characterization of Beats

An ischemic beat characterization algorithm has been developed for the records in which after detecting all possible ischemic or normal beats, filter out the spurious ischemic or normal beat in the final stage. Steps involved in proposed algorithm are

1. The entire ECG record of 60 minute is divided into 60 sections of one minute each.
2. Each section is de-noised, delineated and each ST segment examined.
3. Each section with all its beats properly identified and classified for being ischemic or normal.
4. Each beat is annotated as 1 if it is normal and annotated as 0 if it is ischemic.
5. All sections of 60 minute ECG record with annotations are recombined. The recombination gives an array of L entries, where L is the numbers of beats in 60 minutes ECG record. Each entry is either 0 (for ischemic beat) or 1 (for normal beat).
6. To implement an algorithm for nth beat where $1 \leq n \leq L$, the record has appended with four extra entries, i.e. two at the beginning and two at the end. The record now starts at -1 and ends at L+2. The extended array will have [-1, 0, 1, 2, ------L, L+1, L+2].
7. The extended array is now filtered from n=1 to n = L for spurious entries using following algorithm

5.6 Ischemia Episode Detection

As per the advice of European society of cardiology, the ischemic episode detection process should consider minimum 30 seconds duration of ECG signals. Search starts for the ischemic beats in entire 60 minute record. One ischemic episode must consist

Ischemic Beat Characterization Algorithm

Let $S_n = \sum_{k=0}^{k=2} x(n+k)$

Where x(n) =1 for n^{th} beat being normal

and x(n) =0 for n^{th} beat being ischemic

If S_n = 3, then x(n) =1

Else if S_n = 0, then x(n) =0

Else let $P_n = \sum_{k=-2}^{k=0} x(n+k)$

If P_n = 3, then x(n) =1

Else if P_n = 0, then x(n) =0

Else let $T_n = \sum(x(n-2), x(n-1), x(n+1), x(n+2)$

$T_n = 4$, then x(n) =1

Else if $T_n = 0$, then x(n) =0

Else x(n)= 0.5, beat is unclassified

of at least 90% ischemic beats of all beats for at least 30 seconds duration or more in a record is named as ischemic window.

Detection of Ischemic Episode

If [(No. of ischemic beats) / (All beats)] ≥ 90%)

The window is ischemic

Else The window is normal

5.7 Ischemia Classes

After characterization of the beats and detection of ischemic episodes, we have identified the class of detected ischemic episodes as Subendocardial or Transmural Ischemia. As explained in earlier sections, Ischemia is of two types. Depressed ST segments represent Subendocardial Ischemia, while elevated ST segments represent Transmural Ischemia. To achieve this classification, we find the sample that lies in the middle of the ST segment. Its value is stored in ST_{mid}. Similarly, we identify the middle sample of the isoelectric reference segment. Its value is stored in IR_{mid}. It is obvious that for Transmural

ischemia [ST_{mid} - IR_{mid}] shall be a positive value, while this value shall be negative for Subendocardial ischemia. Thus, knowing the value of [ST_{mid} - IR_{mid}] helps us in identifying the ischemic beat and episodes as Transmural or Subendocardial Ischemia.

5.8 Results and Validation

The pre-processing & delineation algorithms are implemented using wavelet transform toolbox in MATLAB2012a. We have validated the developed method for 10 representative records of the annotated European ST-T database, namely whole e0104 recording and the first hour of the e0103, e0105, e0108, e0113, e0114, e0147, e0159, e0162, and e0206 recordings for mentioning one lead. These records have 20 ischemic ST segment episodes. These records covered both elevated ST segment and depressed ST segment. These records yielded a dataset of 43,876 ST segments characterized as normal, ischemic or artifact. After removal of the artifacts and the mis-detected beats in delineation process, the final dataset have 43,762 ST ST segments to be diagnosed as normal or ischemic. We have measured isoelectric energy for each sample in the ST segment using proposed function and classify the beats as normal or ischemic in two stages. The philosophy of isoelectric energy is to form a function that has high value, if the ST segment is closer to the isoelectric line. This value would decrease as the ST segment moves either above or below the isoelectric line. The pre-processing will reduce the drift in the isoelectric line (TP segment) to nearly zero value. We have measured isoelectric reference in TP segment instead of PQ segments, as high heart rate or conduction abnormalities may distort PQ segment in some cases. To avoid isoelectric energy function becoming infinite on account of zero in the denominator, an artificial constant (α) with value 0.01 has been added. In the same way, constant β is multiplied to keep the threshold for classification of the beat as unity in primarily stage. For normal ST segment, the value of IEEF lies in the range of 93.3 to 98.5 and for the ischemic ST segment, the value of IEEF lies in the range of 63.2 to 67.5. Hence, we define threshold β as 1/80. The Length (ST) is the number of samples in individual ST segment in a record, the length of ST segment will be adjusted according to the RR interval in a particular record. The function will contribute more energy for ST segment, which are horizontal or down sloping as compared to up-sloping depressed ST segments. The proposed function

has specifically been designed to classify the beats on simple thresholding technique and thus does not require any training set. After successful detection of all 20 ischemic episodes, means achieving 100% sensitivity for ischemic episodes, a class of detecting episode has also been detected. Table 5.1 is showing detected class for above mentioned 10 representative records. The most preferred terms for performance evaluation used are sensitivity (S_E), specificity (S_P) and positive predictivity (+P) as defined in Eqn. 5.2, 5.3 and 5.4 respectively.

$$S_E = [TP/ (TP+FN)]*100 \quad (5.2)$$

$$S_P = [TN/ (TN+FP)]*100 \quad (5.3)$$

$$+P = [TP/ (TP+FP)]*100 \quad (5.4)$$

Where TP presents true positive, FN denotes false negative, TN presents true negative and the FP denotes false positive detection. Table 5.2 shows 98.12% average Sensitivity, 98.16% average specificity and average positive predictivity is 98.36% for these 10 representative ECG records of annotated European ST-T database. The second classification stage includes beat characterization algorithm helps to filters out the spurious beats in records by checking annotated beats in the first stage. The advantage of the two stage classification algorithms involves the automatic discarding of clinical irrelevant data, noisy beats.

Table 5.1: Detected class of ischemia for 10 representative records

Sr. No.	Record No.	Lead of detecting record	No. of ischemic episodes detected	Class of Ischemia
1	e0103	V4	4	Transmural
2	e0104	V4	3	Transmural
3	e0105	V4	3	Subendocardial
4	e0108	V4	1	Subendocardial
5	e0113	V4	1	Transmural
6	e0114	V4	2	Transmural
7	e0147	V4	3	Subendocardial
8	e0159	V4	1	Subendocardial
9	e0162	V4	1	Subendocardial
10	e0206	V5	1	Transmural

5.9 Comparison with Existing Methods

This research proposes a new function, named isoelectric energy function for detection of ischemia, which does not involve any complex calculations. The performance of the algorithm has been validated on above mentioned 10 records of European ST-T database for making comparison with existing methods. This database is used as a standard

Table 5.2: Performance measure values for 10 representative records

Sr. No.	Record No.	S_E (%)	S_P (%)	+P (%)
1	e0103	99.19	98.68	99.22
2	e0104	98.02	98.18	98.32
3	e0105	99.21	97.92	99.52
4	e0108	97.85	98.73	98.53
5	e0113	98.18	98.22	98.46
6	e0114	98.47	98.27	98.16
7	e0147	97.64	97.18	98.06
8	e0159	97.83	98.12	97.49
9	e0162	97.67	98.17	98.02
10	e0206	97.18	98.18	97.88
Average		**98.12**	**98.16**	**98.36**

reference for myocardial ischemia. Specifically, it was considered that every annotated episode in the database contained only ischemic beats. Our method performance cannot be judged against the mentioned methods [S. Papadimitriou et.al, 20001; T. Stamkopoulos et.al, 1998; D. Lemire et.al, 2000; H. Rabbani et.al, 2011; N. Maglaveras et.al, 1998; P. Ranjit et.al, 2003; H. Haraldsson et.al, 2004; L. Drance et.al, 2006; S. Don et.al, 2013 and N. Maglaveras et.al, 1998], since either they have been evaluated with other datasets or employed different performance measures or different database. The obtained results are better than those of other approaches [C. Papaloukas et.al, 2004; T.P. Exarchos et.al, 2007; J. Park et.al, 2012; C. Papaloukas et.al, 2002; D. Fotiadis et.al, 2002; Y. Goletsis et.al, 2003; C. Papaloukas et.al, 2001; S. Murgan and S. Radhakrishnan, 2010] in terms of both sensitivity and specificity. It should be mentioned that most of the previously reported method has measured ST segment with fixed lengths after J point, proposed method have taken window lengths depends on the RR interval. The methods mentioned above are having their own advantages and disadvantages. Like, digital analysis techniques [H. Rabbani et.al, 2011; D. Lemire et.al, 2000; P. Ranjith et.al,

2003] are easy to implement in real time. Similarly, rule based algorithms [C. Papaloukas et.al, 2001] provides exact decision as of experts. A limitation of this methodology is the requirement of a representative training set in order to extract reliable rules for validation. HMM [R. V. Andero et.al, 2004] achieves best average statistics in ischemic episode detection, but not suitable for non-ischemic episode detection. Fuzzy logic [T. P. Exarchos et.al, 2007; M. G. Tsipouras et.al, 2007] based systems is having great importance in the diagnosis of ischemia of validating the rules, but still need further investigation in order to improve the diagnosis performance. The neural network based systems [C. Papaloukas et.al, 2002] can detect the ischemia more reliable than the other existing systems, but are not able to provide interpretation of diagnosis because of black box nature in hidden layers. In the same way, genetic algorithm [C. Papaloukas et.al, 2004], support vector machine and kernel density estimation [J. Park et.al, 2012] and multi-criteria decision analysis [Y. Goletsis et.al, 2003] based algorithms take more time for decision as it involves many complex calculations for the optimization process. This paper is having relevance with ST segment area and deviations based methods, as [B. Rotman et.al, 1988; A. Smrdel and F. Jager, 2004; C. Papaloukas et.al, 2000; L.O. Resende et.al, 2012] to distinguish ischemic from normal ST segments. We have measured isoelectric energy based on ST segment deviations which also could employ additional morphological features of ST segments. Our method has two major advantages. The method could provide an interpretation of the results. This is of great importance when designing a device for medical decision support and will assist doctors to reach a diagnosis faster and safer. This would also help with patient in CCU without knowing its past reference. Second, it involves the direct analysis based on isoelectric energy without involvement of any complicated algorithm. In Table 5.3, results have been compared in terms of sensitivity and specificity with the existing methods for European ST-T database. Filtering and delineation has been performed in such a well-organized manner, which makes possible to attain significantly better results than the existing methods. The disadvantage of the proposed method is not applicable to analyze T waves for ischemia detection and also, one lead of each record of a database has been used for detection. Furthermore, in order for the described method to be used in clinical

practice, the database records could be extended and additional types of ischemic and normal ECG waveform patterns could be included.

Table 5.3: Comparison of developed method with existing methods: application to European ST-T database

Methods	**S_E (%)**	**+S_P (%)**
ANN and PCA [C. Papaloukas et.al, 2002]	90	90
ANN and parametric modeling [D. I. Fotiadis et.al, 2002]	81	84
Rule based [C. Papaloukas et.al, 2001]	70	63
Multi-criteria decision analysis [Y. Goltesis et.al, 2003]	91	91
Ant miner [S. Murgan and S. Radhakrishnan, 2010]	92.3	94.3
SVM [J. Park et.al, 2012]	95.7	95.3
KDE [J. Park et.al, 2012]	94.5	94.3
Fuzzy based [T.P. Exarchos et.al, 2007]	91.2	90.9
GA & MCDA [C. Papaloukas et.al, 2004]	91.2	92.2
Developed method	**98.12**	**98.16**

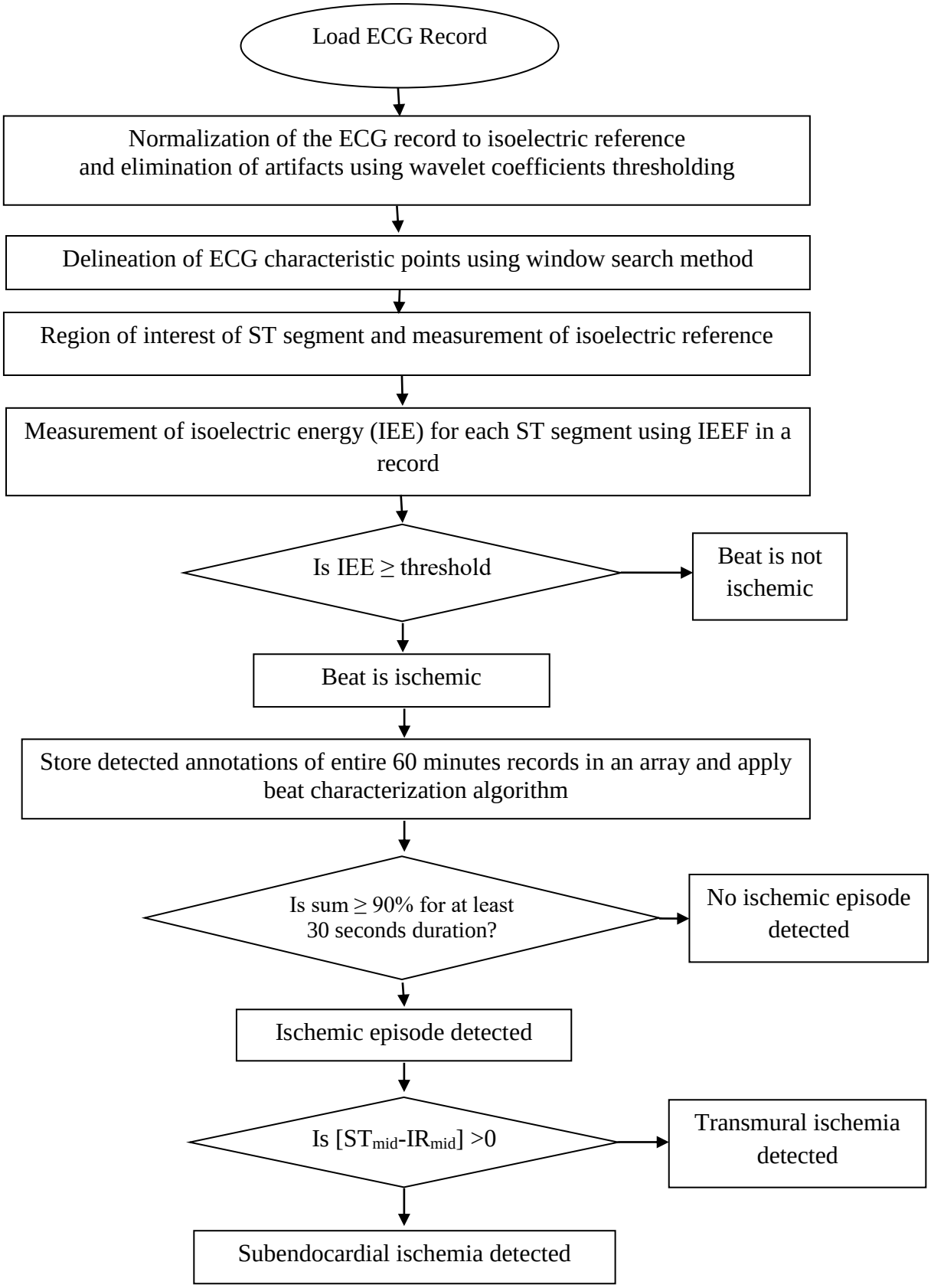

Figure 5.2: Flowchart for developed ischemia detection method

CHAPTER 6

CONCLUSIONS AND FUTURE PROSPECTIVE

6.1 Conclusions

We have successfully developed and validated a simple, reliable and rugged method for detection of ischemia. The developed method is a mathematical function, an alternate method to detect the elevation or depression of ST segment with respect to isoelectric reference in ECG signals. The main requirement of this function is that its value should increase as the ST segment hugs isoelectric reference level, while it should decrease as ST segment tries to move away from the isoelectric reference. The motivation behind developing this function is to go in for a simpler but reliable threshold based classification for detecting myocardial ischemia. Our contribution towards diagnosis of ischemia is of twofold. First, developed method could provide an interpretation of the results. This is of great importance in medical decision support for patient in the critical care unit (CCU) without knowing its past reference. Second, it involves the direct analysis based on isoelectric energy without involvement of any complicated calculations. We strongly believe that this research would surely decrease the mortality of patients that are prone to have ischemia, and those that are anguish from it. The performance of the algorithm has been validated for 10 representative records of European ST-T database for making comparison with existing methods. This database is used as a standard reference for detection of myocardial ischemia. The main highlights of this research are as follows:

- Recent developments in digital signal processing methods, wavelet transform is found more appropriate for non-stationary ECG signal analysis, pre-processing and delineation process. Using the present method, wavelet transform, the limitations of conventional methods can be avoided
- We have proposed an improved method for removal of artifacts in ECG signals. Simulated results show that the optimal value of the wavelet function for elimination of these artifacts as, db7 at 8^{th} decomposition level for baseline wander with

percentage root mean square difference (PRD) of 0.1636%, coif2 at a 5th decomposition level for power line interference with PRD of 0.3980% and db7 at 8^{th} decomposition level for muscle tremor with PRD of 0.8959% in selected records of European ST-T database

- The proposed method for delineation of ECG characteristic points attains 99.72% sensitivity and 99.78% positive predictivity for European ST-T database records after validation
- The proposed does not require any complex calculations and also could employ additional morphological features of ST segments
- It should be mentioned that most of the previously reported method has measured ST segment with fixed lengths after J point, proposed method have taken window lengths depends on the RR interval
- A proposed characterization algorithm for beats annotation by filtering out spurious beats in a record. The advantage of the two stage classification algorithms involves the automatic discarding of clinical irrelevant data, noisy beats
- The proposed method makes classification of detecting ischemic episodes as transmural or subendocardial ischemia
- Filtering and delineation has been performed in such a well-organized manner, which makes possible to achieve higher performance than the available method in literature, 98.12% average sensitivity, 98.16% average specificity and 98.36% average positive predictivity. In addition, 100% sensitivity for ischemic episodes. These results are significantly better than existing methods.

6.2 Future Prospective

- Though this research is thriving in detecting and diagnosing myocardial ischemia, there are still many challenges that need to be addressed. The research has been developed using the European ST-T database datasets. Applying this research directly to patients in real-time, which can lead to improved diagnostic decisions
- In order for the developed method to be used in clinical practice, the database records could be extended and additional types of normal and ischemic ST segments patterns could be included

- Developed method performance may be validated for additional functionality, for example, for multiple leads and with other classification methods
- The increasing demand for achievement of higher sensitivity and specificity values is still challenging for researchers. Future scope includes the remarkable results in terms of their performance and capabilities with respect to standard databases are possible, using a combination of promising algorithms.

References

[1]. V.L. Roger, A.S. Go, D.M. Lloyd-Jones, E.J. Benjamin, J.D. Berry, W.B. Borden, D.M. Bravata, S. Dai, E.S. Ford, C.S. Fox, et al. Heart Disease and Stroke Statistics – 2012 Update a Report from the American Heart Association. Circulation, 125(1):e2–e220, 2012.

[2]. GBD 2013, Mortality and Causes of Death, Collaborators, Global, regional, and national age-sex specific all-cause and cause-specific mortality for 240 causes of death, 1990-2013: a systematic analysis for the Global Burden of Disease Study 2013. Lancet 385, 2015: 117–71. doi:10.1016/S0140-6736 (14)61682-2.

[3]. D. Singh, D. Singh, S. S. Han. Fabrication of three dimensional macro-porous matrix for cardiac regeneration. Inter. J. Applied Eng. Res. 7(11) 2012: 1226-1228.

[4]. P.K. Dash. Electrocardiogram monitoring. Indian J. Anaesth. 46 (4) 2002: 251-260.

[5]. J. Brownfield, M. Herbert, "EKG criteria for fibrinolysis: what's up with the J point" Western J. of Emergency Med. 9(1) 2008: 40–42.

[6]. M. Gheorghiade, G. Sopko, L. De Luca, E.J. Velazquez, J.D. Parker, P.F. Binkley, Z. Sadowski, K.S. Golba, D.L. Prior, J.L. Rouleau, et al. Navigating the crossroads of coronary artery disease and heart failure. Circulation. 114(11) 2006: 1202–1213.

[7]. E. Carmeliet. Cardiac ionic currents and acute ischemia: from channels to arrhythmias. Physiological Reviews. 79(3) 1999: 917–1017.

[8]. N. Luqman, R.J. Sung, C.L. Wang, and C.T. Kuo. Myocardial ischemia and ventricular fibrillation: pathophysiology and clinical implications. International Journal of Cardiology 119 (3) 2007: 283–290.

[9]. G. S. Wagner, P. Macfarlane, H. Wellens et al. AHA/ACCF/HRS Recommendations for the Standardization and Interpretation of the Electro-cardiology Rhythm Society: Endorsed by the International Society for Computerized on Clinical Cardiology; the American College of Cardiology Foundation; and the Heart American Heart Association Electrocardiography and Arrhythmias Committee, Council, Circulation. 119 2009: e262-e270.

[10]. D. R. Perez. Characterization, detection and quantification of acute myocardial ischemia from depolarization ECG-derived indices. Ph. D thesis, Aragon Institute for Engineering Research (I3A), University of Zaragoza. 2013.

[11]. M. T. Keating and M. C. Sanguinetti. Molecular and cellular mechanisms review of cardiac arrhythmias. Cell 104 2001:569–580.

[12]. E. Pueyo, J.P. Mart´ınez, and P. Laguna. Cardiac repolarization analysis using the surface electrocardiogram. Philosophical Transactions of the Royal Society A: Mathematical, Physical and Engineering Sciences. 367(1887) 2009: 213–233.

[13]. M. Singh. Introduction to biomedical instrumentation. Prentice Hall of India, New Delhi. 2010.

[14]. R. Myerburg A. Castellanos. Heart disease: a textbook of cardiovascular medicine, ch. Cardiac arrest and sudden cardiac death. Philadelphia: WB Saunders, 2001.

[15]. C. R. Conti, A. A. Bavry, J. W. Petersen. Silent ischemia-clinical relevance. J. American College of Cardio. 59 (5) 2012: 435-441.

[16]. G. Gupta. Ischemia Detection: By Identification of Isoelectric Line and ST Segment. M.E. Thesis, Department of Electrical Engineering Thapar University, Patiala, Punjab, India 2010.

[17]. F. S. Barnes, B. Greenebaum .Bioengineering and biophysical aspects of electromagnetic field. Handbook of Biological Effects of Electromagnetic Fields, Taylor and Francis, 3rd Edition 2006.

[18]. J. Garcia, G. Wagner, L. Sornmo, S. Olmos, P. Lander, and P. Laguna. Temporal evolution of traditional versus transformed ECG-based indexes in patients with induced myocardial ischemia. Journal of Electrocardiology. 33(1) 2000:37–47.

[19]. P. H. Stone. Ischemia dictates outcome, not symptoms. J. American College of Cardiology. 61 (7) 2013: 712-713.

[20]. M.D. Thames, D. R. Sease, A. Damain, Ischemic heart disease: An overview, advanced studies in medicine 4(10B) 2004: 794-802.

[21]. A. J. Grau, F. Buggle, S. Heindl, C. S.Wiehn et.al. Recent Infection as a Risk Factor for Cerebrovascular Ischemia. American Heart Association, 1994.

[22]. T. Huebner, M. Goernig, M. Schuepbach, E. Sanz, R. Pilgram, A. Seeck, A. Voss. Electrocardiologic and related methods of non-invasive detection and risk stratification in myocardial ischemia: state of the art and perspectives. Ger Med Sci. 8 2010. doi: 10.3205/000116.

[23]. A. Gacek , W. Pedrycz. ECG Signal Processing, Classification and Interpretation-A Comprehensive Framework of Computational Intelligence, Springer London Dordrecht Heidelberg New York, ISBN 978-0-85729-867-6, doi: 10.1007/978-0-85729-868-3. 2012.

[24]. P. E. McSharry, G. D. Clifford, L. Tarassenko, L. Smith .A dynamical model for generating synthetic electrocardiogram signals. IEEE Trans Bio. Med. Eng. 50 2003: 289-294.

[25]. E. J. Berbari. Principles of electrocardiography: the biomedical engineering handbook, CRC Press, 2nd ed. Boca Raton 2000.

[26]. K. H. W. J. Ten Tusscher, A.V. Panfilov. Cell model for efficient simulation of wave propagation in human ventricular tissue under normal and pathological conditions. Physics in Medicine and Biology. 51(23) 2006: 6141.

[27]. R.S. Khandpur. Handbook of Biomedical Instrumentation, Tata MacGrawHill Publishing, India, 1992.

[28]. W. F. Ganong et al. Review of medical physiology, volume 21. McGraw-Hill Medical New York:, 2005.

[29]. E. Frank. An accurate, clinically practical system for spatial vectorcardiography. Circulation. 13(5) 1956:737–749.

[30]. L. Cromwell, F. J. Wiebell, E. A. Pfeiffer. Biomedical Instrumentation and Measurements, Prentice Hall , 2nd edition, ISBN: 978-81-203-0653-0. 2000.

[31]. D. J. Bronzino. The Biomedical Engineering Handbook. 2nd ed. vol. 1. IEEE Publisher. 2000.

[32]. A. R Houghton; D. Gray. Making Sense of the ECG, Third Edition. Hodder Education. p. 214. 2012. ISBN 978-1-4441-6654-5.

[33]. M.S. Sabatine. Pocket Medicine (Pocket Notebook). Lippincott Williams & Wilkins. ISBN 0-7817-1649-7. 2000.

[34]. E. B. Hanna, D. L. Glancy, ST-segment depression and T-wave inversion: Classification, differential diagnosis, and caveats, Clevel and Clinic Journal of Medicine 78(6), 2011,

404-415. doi:10.3949/ccjm.78a.10077.

[35]. A. Smrdel , F. Jager, Automatic classification of long-term ambulatory ECG records according to type of ischemic heart disease, Bio-Medical Engineering On-Line 10 2011:107-117.

[36]. K. Matsumura, R. W. Jeremy, J. Schaper, L. C. Becker, Progression of Myocardial Necrosis During Reperfusion of Ischemic Myocardium, circulation. American Heart Association 1998: 795-804.

[37]. A. Goldberger. New noninvasive approaches to evaluating coronary heart disease: electrocardiogram in ischemic heart disease. The western journal of medicine. 135 (2) 1981: 104-109.

[38]. J. Park, W. Pedrycz, M. Jeon. Ischemia episode detection in ECG using kernel density estimation, support vector machine and feature selection. Biomed. Eng. On-line 11(30) 2012: 1-22.

[39]. B. L. Chia. Ischaemic heart disease. Clinical Electrocardiography, 3rd edition, Singapore World Scintific. 1998.

[40]. A. S. Fauci et al. Harrison's principles of internal medicine, volume 2. McGraw-Hill Medical New York. 2008.

[41]. S.A. Jones. ECG notes: Interpretation and management guide. FA Davis Company. 2005.

[42]. C. M. Travieso, J. B. Alonso, J. R. Ticay-Rivas, M. Pozo-Baños. Apnea Detection Based on Hidden Markov Model Kernel. Advances in Nonlinear Speech Processing. Lecture Notes in Computer Science. 70(15) 2011: 71-79.

[43]. G. Clifford, F. Azuaje, P. McSharry. ECG Statistics, Noise, Artifacts and Missing Data: Advanced Methods and Tools for ECG Data Analysis, Artech House, London, chapter 3 2006: 55-99.

[44]. P. Coumel, O. Garfien. Electrocardiography: past and future. Ann. NY Acad. Science 601. 1990: 1-4.

[45]. L. Schamroth. An introduction to electrocardiography Wiley Blackwell Scientific 7th Ed. India 2009.

[46]. ECG artifacts notes, 2006, available :http://www.mauvila.com/ECG/ecg_artifact.html.

[47]. J. G. Webster, Medical Instrumentation-Application and Design, Wiley India Student Edition. 2009.

[48]. R. J. Martis, U. R. Acharya, H. Adeli, Current methods in electrocardiogram characterization, Computers in Biology and Medicine 48 2014:133–149.

[49]. H. Y. Lin, S. Y. Liang, Y. L. Ho, Y. H. Lin, H. P.Ma. Discrete-wavelet-transform-based noise removal and feature extraction for ECG signals, IRBM, Elsevier 35 2014: 351–361.

[50]. N. Maglaveras, T. Stamkopolos, C. Papaas, M. G. Strinzis. An adaptive back propagation neural network for real time ischemia episodes detection: development and performance analysis using the European ST-T database. IEEE Tran. Biomed. Eng. 45(7) 1998: 805-813.

51. T. Stamkopolous, N. Maglaveras. ECG analysis using nonlinear PCA neural network of ischemia detection. IEEE Tran. Signal Process. 46(2) 1998: 3058-3067.

[52]. C. Papaloukas, D. I. Fotiadis, A. Likas, A. P. Liavas, L. K. Michalis, A knowledge-based technique for automated detection of ischaemic episodes in long duration electrocardiograms, Medical & Biological Engineering & Computing 38 2000: 1-8.

[53]. S. Papadimitriou, S. Mavroudi, L. Viadutu, A. Bezerianos. Ischemia detection with a self organizing map supplemented by supervised learning. IEEE Tran. Neural Networks. 12 (3) 2001: 2342-2353.

[54]. A. Cimponeriu, C. F. Starmer. Theoretical analysis of acute ischemia and infraction using ECG reconstruction on a 2-D model of Myocardium. IEEE Tran. Biomed. Eng. 48 (1) 2001: 41-54.

[55]. C. Papaloukas , D. I. Fotiadisb, A. Likasb , L. K. Michalis, An ischemia detection based on artificial neural networks, Artificial Intelligence in Medicine 24 2002: 167–178.

[56]. C. Papaloukas, Y. Goletsis, D.I. Fotiadis, A. Likas, L.K. Michals. HySMID: an ischemia diagnosis system using genetic algorithms and multi criteria decision analysis. Computers in Cardiology. 2003: 343-346.

[57]. P. Ranjith, P.C. Baby, P. Joseph. ECG analysis using wavelet transform: application to myocardial ischemia detection. Elsevier, ITBM-RBM 24. 2003: 44-47.

[58]. H. Haraldsson, L. Edenbrandt, M. Ohlsson. Detecting acute myocardial infraction in the 12 lead ECG using hermite expansions and neural networks. Artificial Intel. Medicine. 2004: 127-136.

[59]. T. Goletsis, C. Papaloukas, D. I. Fotiadis, Aristidis and L. K. Michalis. Automated ischemic beat classification using genetic algorithm and multi criteria decision analysis. IEEE Tran. Biomed. Eng. 51 (10) 2004: 1717-1725

[60]. R.V. Andreao., B. Dorizzi., J. Boudy, J.C.M. Mota. Online beat segmentation and classification through hidden markov models. Proc. IIICLAEB, Joao Pessoa, Brazil, 2004: 234-244.

[61]. I. Niwas, S. S. Kumari, V. Sadasivam. Artificial neural network based automatic cardiac abnormalities classification. 6th international conf. on Computational Intelligence and Multimedia Applications. 2005: 41-46.

[62]. L. Dranca, A. Goni, A. Illarramendi. Using decision trees for real Time ischemia detection. Proc. of 19th IEEE Sym. on Computer based Medical Systems. 2006: 1-5.

[63]. M. C. Maclachlan, B. F. Nielsen, M. Lysaker, A. Tveito .Computing the Size and location of myocardial ischemia using measurement of ST segment shift. IEEE Tran. Biomed. Eng. 53(6) 2006: 1024-1031.

[64]. M. G. Tsipouras, V. Costas, D.I. Fotiadis. A frame-work for fuzzy expert System creation- application to cardiovascular disease. IEEE Tran. Biomed. Eng. 54 (11) 2007: 2089-2105.

[65]. J.Q. Xue. Adapting ECG morphology changes from reduced lead set by specifically trained algorithm for acute ischemia detection. Computers in Cardiology 2007: 709-712.

[66]. C. Zizzo, A. H., Delphine Turner. Automatic detection and imaging of ischemic changes during electrocardiogram monitoring. IEEE Tran. Biomed. Eng. 55(3) 2008: 1343-1348.

[67]. A. Gharaviri, M. Teshnehlab, H.A. Moghaddam. Ischemia detection via ECG using ANFIS. Proc. of 30th Annual Inter. Conf. on Biomed. Sys. British Columbia, Canada 2008: 1163-1166.

[68]. E. Pueyo, L. Sornmo, P. Lguna. QRS slopes for detection and characterization of myocardial ischemia. IEEE Tran. Biomed. Eng. 55(2) 2008: 468-477.

[69]. T. S. Ruud , B.F. Nielsen M. Lysaker, J. Sundnes .A computationally efficient method for determining the size and location of myocardial ischemia. IEEE Tran. Biomed. Eng. 56(2) 2009: 263-272.

[70]. A. Minchole, F.Jager, P.Laguna. Discrimination between ischemic and artifactual ST segment events in Holter recordings. Biomedical Signal Processing and Control 5 2010: 21–31.

[71]. S. Murugan, S. Radhakrishnan. Rule based classification of ischemic ECG beats using ant-miner, Inter. J. of Eng. Sci. and Tech. 2 2010: 3929–3935.

[72]. H. Rabbani H, M. P. Mahjoob, E. Farahabadi, A. Farahabadi, A. M. Dehnavi. Ischemia detection by electrocardiogram in wavelet domain using entropy measure Journal of Research in Medical Sciences 16 2011: 1473–1482.

[73]. X. Tang , L. Xia, W. Liu, Y. Peng, T. Gao, Y. Zeng, An approach to determine myocardial ischemia by hidden Markov models, Computer Methods in Biomechanics and Biomedical Engineering, 15(10) 2012: 1065-1070, DOI: 10.1080/10255842.2011.570341.

[74]. S. Don, D. Chung, D. Min. Analysis of electrocardiogram signals of arrhythmia and ischemia using fractal and statistical features J. of Mechanics in Medicine and Biology 13 2013: 1350008-8.

[75]. V. Hellemond, S. Bouwmeester, C.W. Olson, M. Hassell, H.E. Bøtker, A.K. Kaltoft, S.S. Nielsen, C. J. Terkelsen, C. Maynard, M. P. Andersen, A. P. Gorgels, G.S.Wagner , Consideration of QRS complex in addition to ST segment abnormalities in the estimation of the 'risk region' during acute inferior myocardial infarction. J Electrocardiol. 46(3) 2013:215-20.

[76]. P. Gomis, P. Caminal, Evaluation of very low amplitude intra-QRS potentials during the initial minutes of acute transmural myocardial ischemia, Journal of Electrocardiology 47 2014: 512–519.

[77]. R. Correa, P. D. Arini, L. S. Correa M. Valentinuzzi, E. Laciar. Novel technique for ST-T interval characterization in patients with acute myocardial ischemia, Computers in Biology and Medicine 50 2014: 49–55.

[78]. A. Graps. An introduction to wavelets. IEEE Tran. Comput. Sci. Eng. 2(2) 1995: 50-61.

[79]. A. Taddei, G. Distante, M. Emdin, P. Pisani, G. B. Moody GB, Zeelenberg, C. Marchesi. The European ST-T database: standard for evaluating systems for the analysis of ST-T changes in ambulatory electrocardiography European Heart Journal, 13 1992: 1164–1172.

[80]. P. M. Louis, A. Rieder. Wavelets theory and applications, John Wiley & Sons 1997.

[81]. C. L. Liu. A Tutorial of the wavelet transform 2010, available online:

[82]. R. Polikar. The engineer's ultimate guide to wavelet analysis, the wavelet tutorial, available online: http://users.rowan.edu/~polikar/WAVELETS/WTpart1.html

[83]. S. Mallat. A theory for multi-resolution signal decomposition: the wavelet representation. IEEE Pattern Anal. Machine Intell. 11(7) 1989: 674-693.

[84]. G. Strang, T. Nguyen. Wavelets and filter banks Wellesley Cambridge Press 1996.

[85]. I. Daubechies. The wavelet transform: time-frequency localization and signal analysis. IEEE Tran. on Inform. Theory 36 1990: 961–1005.

[86]. V. K. Mukamia. Baseline Wander Estimation for ECG Characterization. Electrical and instrumentation engineering department, Thapar university, Patiala, India, 2010.

[87]. Wavelet transform tutorial, The image and vision science laboratory. available: http://visl.technion.ac.il.

[88]. J. Kovacevic, W. Sweldens, Wavelet Families of Increasing Order in Arbitrary Dimensions, IEEE Trans. Image Proc. 9(3) 2000: 480-496.

[89]. U.M. Chaskar, S. V. Bhole, S. L. Patil. Comparative performance study of different algorithm sequence of thresholding and filtering applied on characters for noise reduction. Inter. J. of Math. Sci. Eng. App. 3(3) 2009: 11-20.

[90]. G. Kaushik, H. P. Sinha, L. Dewan. Biomedical signals analysis by DWT signal de-noising with neural networks. Research J. of Applied Sci. 9(5) 2013: 244-256.

[91]. R. Janani, Analysis of Wavelet Families for Baseline Wander Removal in ECG signals, International Journal of Advance Research in Computer Science and Management Studies 2(2) 2014: 169-176.

[92]. M. Misiti, Y. Misiti, G. Oppenheim, J. M. Poggi, Wavelet Toolbox™ User's Guide, The MathWorks, Inc. 3 Apple Hill Drive Natick, MA 01760-2098. 2012

[93]. T. Gandhi, B. K. Panigrahi, S. Anand. A comparative study of wavelet families for EEG signal classification. Neuro-computing 74 2011: 3051-3057.

[94]. M. E. Cohen, D. L. Hudson. Neural network models for bio-signal analysis. IEEE Annual Conf. on Eng. in Med. and Biol. Society (EMBS '06) New York, NY. 2006: 3537 – 3540.

[95]. U. R. Acharya, O. Faust, D. N. Ghista, S. V. Sree, A. P. C. Alvin, S. Chattopadhyay, T. C. Lim, E. Y. K. Ng, W. Yu. A systems approach to cardiac health diagnosis. J. of

Medical Imag. and Health Inform. 3 (2) 2013: 61-267.

[96]. J. Makhoul, Linear prediction: a tutorial review, Proc. IEEE 63 1975: 561–580.

[97]. R. Duda, P. Hart, D. Stork (Eds.), Pattern Recognition, Wiley- Inter-science, New York 2001.

[98]. E. Oja, A. Hyvarinen, J. Karhunen(Eds.), Independent Component Analysis, John Wiley & Sons. 2001.

[99]. D. L.Fugal, Conceptual Wavelets in Digital Signal Processing, Space & Signals Technical Publishing, USA. 2009.

[100]. M. Sheoran, S. Kumar, A. Kumar. Wavelet ICA based de-noising of electroencephalogram signal. Inter. J. of Inform. Comp. Tech. 4(12) 2014: 1205-1210.

[101]. J.G. Proakis, Digital Signal Processing: Principles Algorithms and Applications, third edition, Prentice Hall, New Jersy, USA. 1992.

[102]. R. J. Martis, U. R. Acharya, A. K. Ray, C. Chakraborty, Application of higher order cumulants to ECG signals for the cardiac health diagnosis, in: Annual International Conference of the IEEE Engineering in Medicine and Biology Society 2011: 1697–1700.

[103]. C.L. Nikias, J. M. Mendel, Signal processing with higher-order spectra, IEEE Signal Process. Mag. 10 1993: 10–37.

[104]. S. Pal, M. Mitra, Empirical mode decomposition based ECG enhancement and QRS detection, Comput. Biol. Med. 42, 83–92 (2012).

[105]. S.C. Mahesh, Suppression of noise in the ECG signal using digital IIR Filter, Proc. of the 8th WSEAS Intern. Conf. on Multi-media Sys. & Signal Process. Hangzhou, China 2008: 1-10.

[106]. S.M.M. Martens, M. Mischi, S.G. Oej, J. W. M. Bergmans. An improved adaptive power line interference canceller for electrocardiography. IEEE Trans. Bio. Med. Eng. 53, 2006: 2220-2231.

[107]. F. C. Chang, C.K. Chang, K. Y. Chi .Evaluation measures for adaptive PLI filters in ECG signal processing .IEEE Conf. on Comp. in Cardiology Durham, NC 2007: 529-532.

[108]. D. Dobromir, T. Neycheva, N. Mudrov. Digital lock-in techniques for adaptive power line interference extraction, Physiol. Meas. 29 2008: 803-816.

[109]. S.G. Tareen. Removal of power line interference and other single frequency tones from signals, M. Sc. Thesis, Department of Computer Science and Electronics, Malardalen University, Sweden 2008.

[110]. M.S. Chavan, R.A. Agarwal, M.D. Upalne. Design and implementation of digital FIR equi-ripple notch filter on ECG signal for removal of power line interference. WSEAS Trans. Signal Process. 4 2008: 1256-1266.

[111]. V. J. A. Alste, T.S. Schilder. Removal of baseline wanders and power line interference from the ECG by an efficient FIR filter with a reduced number of taps, IEEE Trans. on Bio. Med. Eng. 32 1985: 1052-1060.

[112]. C. B. Mbachu, G.N. Onoh, V.E. Idigo, O.S. Oguejiofor. Processing ECG signal with Kaiser window based FIR digital filters. Int. J. Eng. Sci. and Tech. 3 2011: 6775-6783.

[113]. M.R. Rangaraj. Biomedical Signal Analysis: A Case Study Approach. Wiley IEEE Press, Los Alamitos 2002.

[114]. M. P. S. Chawla, H.K. Verma, V. Kumar. Artifacts and noise removal in electrocardiograms using independent component analysis. Inter. J. of Cardio. 129 2008: 278-281.

[115]. H. Taigang, C. Gari, L. Tarassenko. Application of independent component analysis in removing artifacts from the electrocardiogram, Neural Comp. Appl. 15 2006 :105-116.

[116]. A. K. Barros, A. Mansour, N. Ohnishi. Removing artifacts from electrocardiographic signals using independent components analysis. Neural Comp. 22 1998: 173–186.

[117]. Z. Zhidong, M. Chan. A novel cancellation method of power line interference in ECG signal based on EMD and adaptive filter, Proc. of IEEE 11th Int. Conf. on Comm. Tech. Hangzhou, 2008: 517-520.

[118]. J. Mateo, C. Sanchez, A. Torres, R. Cervigon, J. J. Rieta. Neural network based canceller power line interference in ECG signal, IEEE Conf. on Comp. in Cardiology Bologna 2008: 1073-1076.

[119]. M.P.S. Chawla. PCA & ICA processing for removal of artifacts and noise in electrocardiograms: A survey and comparison, J. of Applied Soft Comp. 11 2011: 2216-2226.

[120]. M. Kania, M. Fereniec, R. Maniewski. Wavelet denoising for multi lead high resolution ECG signals. Meas. Sci. Review 7 2007: 30-33.

[121]. A.D. Ivan, S.M. Georgy. Tremor suppression in ECG. Biomed. Eng. Online 7 2008: 1-10.

[122]. P. Augustyniak. Adaptive wavelet discrimination of muscular noise in the ECG. IEEE Conf. on Comp. in Cardiology Valencia 2006: 481−484.

[123]. B.S. Raghavendra, D.D. Narayana. Wavelet enhanced CCA for minimization of ocular and muscle artifacts in EEG. Intern J. of Bio. and Life Sci. 8 2012: 179-184.

[124]. J. S. Paul, M.R. Reddy, V.J. Kumar. A transform domain SVD filter for suppression of muscle noise artifacts in exercise ECG's. IEEE Trans. on Biomed. Eng. 47 2000: 654-663.

[125]. I. Markovsky, A. Amann, S.V. Huffel. Application of filtering methods for removal of resuscitation artifacts from human ECG signals. System Identification Env. Modell. & Control System Design 2012: pp 273-291.

[126]. J. R. Laguna, P. Thakor, P. Caminal. Adaptive baseline wander removal in the ECG: comparative analysis with cubic spline technique, Proc. of IEEE Conf. on Comp. in Cardiology Durham, NC 1992: 143-146.

[127]. L. Sornmo. Time varying digital filtering of ECG baseline wander. J. of Med. & Biol. Eng and Comp. 31 1993: 503-508.

[128]. H. Norbert. A new class of digital filters designed for ECG noise reduction. Proc. of 9th Conf. on Med. Inform. & Technol., Silesian University of Technology, Poland, Akademicka 2006: 44-101.

[129]. U. Zahoor, A.O. Farooq. Baseline wandering removal from human electrocardiogram signal using projection pursuit gradient ascent algorithm, Inter J of Elect & Comp. Sci. 9 2009: 11-13.

[130]. K. Daqrouq. ECG baseline wandering reduction using discrete wavelet transforms. Asian J. of Inform Tech 4 2005: 989-995.

[131]. H. Nagendra, S. Mukherjee, K. Vinod. Application of wavelet techniques in ECG signal processing: an overview, Intern. J. of Eng. Sci. Tech. 3 2011: 7432-7443.

[132]. E.B. Lin, M. Haske, M. Smith, D. Sowards. Wavelet analysis of ECG signals, Multi-scale Signal Analysis and Modelling, Lecture Notes in Electrical Eng. Springer, New York, 2013: 233-256.

[133]. O. Sayadi, M.B. Shamsollahi, Multi-adaptive bionic wavelet transform: application to ECG de-noising and baseline wandering reduction, EURASIP J. Adv. in Signal Process., Article ID-41274, 2007: 1-11.

[134]. K.M. Chang, S.H. Liu. Gaussian noise filtering from ECG by wiener filter and ensemble empirical mode decomposition. J. of Signal Process. Sys. 64 2010: 1-16.

[135]. E.S. El-Dahshan, Genetic algorithm and wavelet hybrid scheme for ECG signal de-noising, Telecom. Sys. 46 209-215 (2011).

[136]. F. A. Afsar. A comparison of baseline removal algorithms for electrocardiogram based automated diagnosis of coronary heart disease, IEEE Intern. Conf. on Bio-inform. and Biomed. Eng. Beijing 2009: 1-4.

[137]. A.K. Manocha, M. Singh. Automatic delineation of ECG characteristics points using window search & multi resolution wavelet transform approach, Proc. of 4th Int. Conf. on Emerging Trends in Eng. & Tech., Kurukshetra, India 2013: 756-761.

[138]. L.N. Sharma, S. Dandapat, A. Mahanta. Kurtosis based noise estimation and multi-scale energy to de-noise ECG signal. J. of Sig. Image & Video Process. 7 2013: 235-245.

[139]. M. Singh, V. Kumar, S.C. Saxsena. Modified SPIHT wavelet compression for ECG signal, J. Med. Eng. Technol. 31 2007: 29-35.

[140]. M. Singh, V. Kumar, S.C. Saxena. Distortion measurement in ECG reconstructed signals. J. of Institute of Engineers, India: Electronics and Telecommunication division 91 2010: 26-30.

[141]. D. L. Donoho. De-noising by soft thresholding. IEEE Trans. on Inform. Theory 41 1995: 613-627.

[142]. A. K. Manocha, G. Kaushik, U. Singh. Performance calculation of wavelet transforms for removal of baseline wander from ECG, Intern. J. of Eng Sci. & Tech 4 2012: 2441-2445.

[143]. A. Kumar, M. Singh. Optimal selection of wavelet function and decomposition level for removal of ECG signal artifacts. J. of Medical Imaging and Health Informatics, 5 2015: 138-147.

[144]. M. M. Beena, S. Prabavathy, B. S. Priestly, J. A. Mohanalin. Robust rule based de-noising scheme using wavelets J. of Medical Imaging and Health Informatics 4 2014: 457-468.

[145]. M. Merri, M. Alberto, A. J. Moss. Dynamic analysis of ventricular representation Duration from 24 hour recording. IEEE Trans. on Biomed. Eng 40 1993:1219-1225.

[146]. N. V. Thakor, Y. Zho. Application of adaptive filtering to ECG analysis: noise cancellation and arrhythmia detection. IEEE Trans. on Biomed. Eng. 38 1991: 785-794.

[147]. K. Daqrouq, I. N. Qawasmi, QRS complex detection based on symlets wavelet function, Proc. of 5th Intern. Conf. on Systems, Signals Devices, SSD'08, Amman, Jordan, 2008: 20-23.

[148]. M. Alfaouri, K. Daqrouq. ECG signal de-noising by wavelet transform thresholding, American J. of Applied Sci. 5 2008: 276-281.

[149]. C. Saritha, V. Sukanya, Y. N. Murthy. ECG analysis using wavelets, Bulg. J. Phys. 35 2008: 68-77.

[150]. J. Pan, W.J. Tomkins. A real-time QRS detection algorithm. IEEE Trans. Biomed. Eng. 32 1985: 230-236.

[151]. O. Pahlm, L. Sornmo. Software QRS detection in ambulatory monitoring: a review. Med. Biol. Eng. Comput. 22 1984: 289-297.

[152]. F. Gritzali. Toward a generalized scheme for QRS detection in ECG waveforms, Signal Process. 15 1988:183-192.

[153]. A. Ghaffari, H. Golbayani, M. Ghasemi. A new mathematical based QRS detector using continuous wavelet transform Comp. Elect. Eng. 34 2008: 81-91.

[154]. B.U. Kohler, C. Hennig, R. Orglmeister. The principles of software QRS detection. IEEE Eng. Med. Biol. Mag. 21 2002: 42-57.

[155]. G.M. Friesen, T.C. Jannett, M.A. Jadallah, S.L. Yates, S.R. Quint, H.T. Nagle. A comparison of the noise sensitivity of nine QRS detection algorithms. IEEE Trans. Biomed. Eng. 37 1990: 85-98.

[156]. A. S. M. Koeleman, H. H. Ros, T. J. Van Den Akker. Beat to beat interval measurement in the electrocardiogram, Med. Biol. Eng. Comp. 23 1985: 213-219.

[157]. J.G.C. Kemmelings, A.C. Linnenbank, S.L.C. Muilwijk, A. Sippens-Groenewegen, A. Peper, C.A. Grimbergen. Automatic QRS onset and offset detection for body surface QRS integral mapping of ventricular tachycardia. IEEE Trans. Biomed. Eng. 41 1994: 830-836.

[158]. I. K. Daskalov, I.A. Dotsinsky, I.I. Christov. Developments in ECG acquisition, pre processing, parameter measurement and recording. IEEE Eng. Med. Biol. Mag. 17 1998: 50-58.

[159]. M. J. Vaessen. An approach to ECG delineation using wavelet analysis and hidden Markov models, Master Thesis, Department of General Sciences, Universiteit Maastricht 2006.

[160]. C. Lin C. Mailhes, J.Y. Tourneret. P and T wave delineation in ECG signals using a Bayesian approach and a partially collapsed Gibbs sampler. IEEE Trans. Biomed. Eng. 57 2010: 2840-49.

[161]. B. M. Evangelos, D. Biswas, A. Acharyya, T. Chen. A low complexity ECG feature extraction algorithm for mobile healthcare applications. IEEE Trans. Inform. Tech. Biomed. 20 2010: 1-11.

[162]. C. Li, C. Zheng, C. Tai. Detection of ECG characteristic points using wavelet transforms. IEEE Trans. Biomed. Eng. 42 1995: 21-28.

[163]. S. Banerjee, R. Gupta, M. Mitra. Delineation of ECG characteristic features using multi-resolution wavelet analysis method, Measurement, Elsevier, 45, 2010: 474-487.

[164]. J. S. Sahambi, S. Tandon, R. K. P. Bhatt, Using wavelet transform for ECG characterization, IEEE Eng. Med. Biol. 16 1997: 77–83.

[165]. J. P. Martnez, R. Almeida, S. Olmos, A.P. Rocha, P. Laguna. A wavelet based ECG delineator: evaluation on standard databases, IEEE Trans. on Biomed. Eng. 51 2004: 570-581.

[166]. S. C. Saxena, V. Kumar, S. T. Hamde. Feature extraction from ECG signals using wavelet transforms for disease diagnostics. Inter. J. of Systems Sci. 33(13) 2002: 1073-1085.

[167]. M. R. Homaeinezhad, M. E. M. Nejad, H. Naseri. A correlation analysis based detection and delineation of ECG characteristic events using template waveforms extracted by ensemble averaging of clustered heart cycles. Comp. Biol. and Medicine 44 2014: 66-75.

[168]. I. Saini, D. Singh, A. Khosla. K-Nearest neighbour-based algorithm for P and T-waves detection and delineation. J. of Medical Eng. and Tech. 38 2014: 115-124.

[169]. J. Dumont, A. I. Hernandez, G. Carrault. ECG beat delineation with an evolutionary optimization process, IEEE Trans. Biomed. Eng. 57 2010: 607–615.

[170]. S. S. Mehta, N.S. Lingayat. Application of support vector machine for the detection of P and T wave in 12 lead Electrocardiogram. Comp. Methods Programs Biomed. 93 2009: 46-60.

[171]. A. Karimipour, M. R. Homaeinezhad. Real time electrocardiogram P-QRS-T detection delineation algorithm based on quality supported analysis of characteristic templates. Comp. Biol. Med. 11 2014: 153-165.

[172]. A. Kumar, M Singh, Robust multi-resolution wavelet analysis and window search based approach for electrocardiogram features delineation, J. of Medical Imaging and Health

Informatics, Accepted manuscript for publication in Dec. 2015 issue.

[173]. A. Ghaffaria, M. R. Homaeinezhada, M. Akraminiaa, M. Ataroda, M. Daevaeihac, A robust wavelet based multi lead electrocardiogram delineation algorithm, Med. Eng. & Physics 31 2009: 1219–1227.

[174]. Z. Zidelmala, Amiroua A, Adnaneb M, Belouchranib. A QRS detection based on wavelet coefficients, Computer Methods and Prog. in Biomedicine 107 2012: 490-496.

[175]. I. I. Amr, M. Amin, P. El-Kafrawy, A. M. Sauber. Using statistical moment invariants and entropy in image retrieval. Inter. J. of Comp. Sci. and Inform. Security 7(1) 2010: 160-164.

[176]. S. Scheidt, Basic Electrocardiography: Abnormalities of Electrocardiographic Patterns, 6(36), Ciba Pharmaceutical Company, Summit, N.J 1984: 32.

[177]. E. Pietka. Feature extraction in computerized approach to the ECG analysis. Pattern Recog. 24 1991: 139-146.

[178]. Q. Z. Xie, Y.H. Hu, W. J. Tomkins. Neural network based adaptive matched filtering of QRS detection. IEEE Trans. Biomed. Eng. 39 1992: 317-329.

[179]. P. S. Hamilton, W. J. Tompkins. Quantitative investigation of QRS detection rules using the MIT/BIH arrhythmia database, IEEE Tran. Biomed. Eng. 33 1986: 1157-65.

[180]. F. Gritzali, G. Frangakis, G. Papakonstantinou. Detection of the P and T waves in an ECG. J. of Comp. and Biomed. Res. 22 1989: 83-91.

[181]. G. B. Moody, R. G. Mark. Development and evaluation of a 2-lead ECG analysis program. Proc. of Comp. in Cardiology Conf. 1982: 39–44.

[182]. L. Y. Di Marco, L. Chiari. A wavelet based ECG delineation algorithm for 32-bit integer online processing, Biomed. Eng. Online. 10 2011: 1-19.

[183]. N. Maglaveras, T. Stamkopoulos, C. Pappas, M. Strintzis. ECG processing techniques based on neural networks and bidirectional associative memories, J. Med. Eng. Technol. 22 1998: 106–111.

[184]. A. Taddei, G. Constantino, R. Silipo, M. Emdin, C. Marchesi. A system for the detection of ischemic episodes in ambulatory ECG, Proc. of Computers in Cardiology Conf., Los Alamitos, CA: IEEE Comput. Soc. Press 1995: 705–708.

[185]. C. Papaloukas, D. I. Fotiadis, A. Likas, L. K. Michalis. An expert system for ischemia detection based on parametric modelling and artificial neural networks, Proc. Eur. Med. Biol. Eng. Conf. 2002: 742–743.

[186]. Y. Goletsis, C. Papaloukas, D. I. Fotiadis, A. Likas, L. K. Michalis. A multi-criteria decision based approach for ischemia detection in long duration ECGs Proc. of IEEE EMBS 4th Int. Conf. Information Tech. App. in Biomedicine (ITAB 2003) 2003: 230–233.

[187]. C. Papaloukas, D. I. Fotiadis, A. Likas, A. P. Liavas, L. K. Michalis. A knowledge-based technique for automated detection of ischemic episodes in long duration electrocardiograms Med. Biol. Eng. Comput. 39 2001: 105–112.

[188]. B. Rotman, B. Eber, J. Duslag. Comparison of different methods of ST measurement for evaluation of myocardial ischaemia in Holter monitoring. Eur Heart J. 9 1988: 78-84.

[189]. L. O. Resende, E. S. Resende, A. O. Andrade. Assessment of the ST segment deviation area as a potential physiological marker of the acute myocardial infarction, Proc. of 8th IEEE Annual inert. Conf. on Eng. in Medicine and Biology Society. 2012; 669-72.